

Isotropic tensor fields in amorphous solids: Correlation functions of displacement and strain tensor fields

J.P. Wittmer^{1,*} and J. Baschnagel¹

¹*Institut Charles Sadron, Université de Strasbourg & CNRS,
23 rue du Loess, 67034 Strasbourg Cedex, France*

(Dated: June 18, 2024)

Generalizing recent work on isotropic tensor fields in isotropic and achiral condensed matter systems from two to arbitrary dimensions we address both mathematical aspects assuming perfectly isotropic systems and applications focusing on correlation functions of displacement and strain field components in amorphous solids. Various general points are exemplified using simulated poly-disperse Lennard-Jones particles in two dimensions. It is shown that the strain components in reciprocal space have essentially a complex circularly-symmetric Gaussian distribution albeit weak non-Gaussianity effects become visible for large wavenumbers q where also anisotropy effects become relevant. The dynamical strain correlation functions are strongly non-monotonic with respect to q with a minimum roughly at the breakdown of the continuum limit.

I. INTRODUCTION

The characterization of structural properties of condensed matter systems [1–8] often boils down to the experimental determination of “correlation functions” (CFs) $c(\mathbf{q}) = \langle f(\mathbf{q})f(-\mathbf{q}) \rangle$ of fields $f(\mathbf{q}) = \mathcal{F}[f(\mathbf{r})]$ measured in reciprocal space as a function of the wavevector \mathbf{q} [1, 2]. ($\mathcal{F}[\dots]$ stands here for the “Fourier transformation” (FT) and $\langle \dots \rangle$ denotes a convenient average specified below.) Due to the (partial) translational invariance of many systems it is also useful in theoretical work [1, 3, 5, 7, 9] and computational studies [10] to focus on the characterization of CFs in reciprocal space, at least as a first step. The CFs $c(\mathbf{r}) = \mathcal{F}^{-1}[c(\mathbf{q})]$ in real space, as shown in Fig. 1, may then finally be obtained by inverse FT. As already emphasized elsewhere [11–18], it is now of importance whether the measured field $f(\mathbf{q})$ is a *scalar field* (order $o = 0$) or a component of a “*tensor field*” (TF) of order $o > 0$ [19–21]. Let us first focus on CFs $c(\mathbf{r})$ of scalar fields in real space as sketched in the second panel of Fig. 1. For *isotropic* systems such a CF only depends on the magnitudes $r = |\mathbf{r}|$ or $q = |\mathbf{q}|$ of the field vectors \mathbf{r} or \mathbf{q} in real or reciprocal space. If a dependency on the normalized directions $\hat{\mathbf{r}} = \mathbf{r}/r$ or $\hat{\mathbf{q}} = \mathbf{q}/q$ of the field vectors is observed [22], this demonstrates *anisotropy*. Moreover, an observed anisotropic pattern in the material reference frame (dashed line) does not depend on the orientation of the coordinate system. This is in general different if CFs of components of TFs are probed, simply since the components of TFs depend explicitly on the coordinate system. This implies that components of mathematically and physically legitimate “isotropic tensor fields” (ITFs) may depend on the coordinate systems, however, subject to a generic mathematical structure summarized in Sec. II A. As an example further discussed in Sec. IV D, panel (c) of Fig. 1 shows

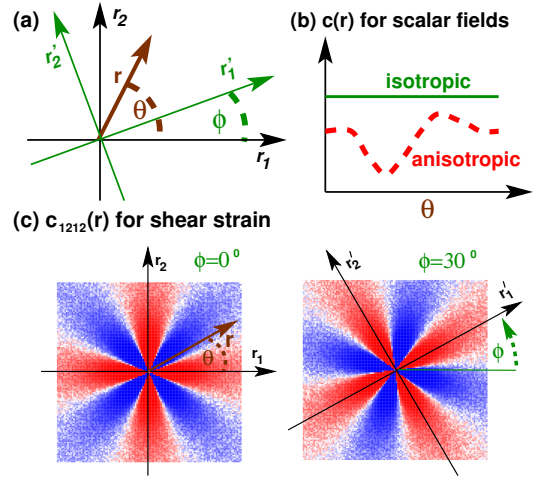


FIG. 1: Some useful notions: (a) We consider tensor fields (TFs) and their correlation functions (CFs) under orthogonal transformations as the shown rotation of a coordinate system by an angle ϕ . θ denotes the angle of the field vector \mathbf{r} in the 12-plane of unrotated coordinates. (b) CFs $c(\mathbf{r})$ of scalar fields do not depend on the coordinate system. For isotropic systems $c(\mathbf{r})$ only depends on the magnitude $r = |\mathbf{r}|$ of the field vector \mathbf{r} but not on its direction (angle θ). (c) CF $c_{1212}(\mathbf{r})$ of shear strain field $\varepsilon_{12}(\mathbf{r})$ for an isotropic elastic body revealing an octupolar pattern. The CF is positive along the axes and negative along the bisection lines of the respective axes. The pattern rotates with the coordinate frame.

the CF $c_{1212}(\mathbf{r})$ of the shear strain component $\varepsilon_{12}(\mathbf{r})$ for an isotropic linear elastic body [23] in two dimensions [18] revealing an octupolar pattern [24] which, moreover, turns if the coordinate frame is rotated by an angle ϕ . Importantly, the fourth-order strain CFs $c_{\alpha\beta\gamma\delta}(\mathbf{r})$ of ideal isotropic elastic bodies in d dimensions can be theoretically shown to decay as $1/r^d$ for sufficiently large r . As stressed in Refs. [11, 12, 17, 18], the observation of such angle-dependences or long-range power-law decays of CFs of TFs can thus *a priori* not be used as an indication of Eshelby-like plastic rearrangements [25, 26].

*Electronic address: joachim.wittmer@ics-cnrs.unistra.fr

We generalize here recent work [15–18] on ITFs and their invariants in isotropic and achiral condensed matter systems from $d = 2$ to arbitrary dimensions d and address both mathematical aspects assuming perfectly isotropic systems and various applications of CFs and linear “response fields” (RFs) of TF components in real or simulated systems where the isotropy assumption may not hold on all scales. Focusing on displacement and strain fields in amorphous solid bodies it is emphasized that in any dimension $d > 1$ CFs of TF components must for mathematical reasons have angle dependencies distinct from those of true frame-invariant anisotropies. Second-order CFs of first-order TFs are thus described by *two* “invariant correlation functions” (ICFs) while fourth-order CFs of second-order TFs require in general (under mild assumptions) *five* ICFs. We emphasize here that only *two independent* ICFs are required for the static and dynamical CFs of displacement and strain fields, cf. Sec. IV and Sec. V, and that these ICFs are related to the two invariant material functions $L(q, t)$ and $G(q, t)$ of the generalized elasticity TF $E_{\alpha\beta\gamma\delta}(\mathbf{q}, t)$ characterizing the longitudinal and transverse (shear) displacement field relaxation in so-called “Natural Rotated Coordinates” (NRC) with respect to the wavevector \mathbf{q} [17]. As discussed in Sec. IIB and Sec. IVF, possible (true) anisotropies must be described and quantified, just as for any symmetry breaking, in terms of invariants of the symmetry group assumed to be broken. For $d = 2$ a more compact representation in terms of only *four* ICFs for fourth-order ITFs will be given using a general transformation which should be useful for the characterization of CFs of second-order TFs in (effectively) two-dimensional systems. Such systems have been considered in recent experimental work [27–29] and a huge number of numerical studies. Following Refs. [17, 18, 30] we shall in fact also exemplify theoretical predictions and numerical procedures in $d = 2$ using computational results obtained by means Monte Carlo (MC) simulations [10] of “polydisperse Lennard-Jones” (pLJ) particles.

We begin in Sec. II with a summary of some properties of ITFs and a discussion of possibilities to pinpoint true anisotropies. Some well-known technical notions are reminded in Sec. III where we summarize in turn the computational model used in this study (cf. Sec. IIIA), the averaging procedures (cf. Sec. IIIB), the macroscopic elastic moduli (cf. Sec. IIIC), some consequences of the assumed stationarity of all sampled time-series (cf. Sec. IIID), the definitions of “response fields” (RFs), “source fields” (SFs) and “Green and growth function fields” (GFs) in Sec. IIIE and finally in Sec. IIIF the linear relation between GFs and CFs from the “Fluctuation-Dissipation-Theorem” (FDT) [1, 7, 9]. We turn then in Sec. IV to static CFs of strain TFs in amorphous solids and in Sec. V to more general time-dependent strain CFs. Our work is summarized in Sec. VI. We provide additional information on FTs and “Laplace-Carson transformations” (LTs) in Appendix A, on ITFs for isotropic and achiral systems in Appendix B, on inverse FTs of

such ITFs in Appendix C, on the linear response of displacement fields in Appendix D and on the large-time behavior of strain ICFs in Appendix E.

II. ISOTROPIC TENSOR FIELDS

A. Summary of properties of isotropic TFs

We summarize here various properties of ITFs. More details can be found in Appendix II. Using the standard indicial notation [21] and Cartesian coordinates with orthonormal basis [20] it is assumed that all second-order TFs are symmetric and that the minor and major index symmetries [21] hold for all fourth-order TFs. Moreover, it is supposed that all second- and fourth-order ITFs are *even* with respect to the field vector as required for CFs of *achiral* systems. Most importantly, it is assumed that the TFs are *isotropic*, i.e. the isotropy condition [17, 20]

$$T_{\alpha_1 \dots \alpha_o}^*(\mathbf{q}) = T_{\alpha_1 \dots \alpha_o}(\mathbf{q}^*) \quad (1)$$

holds for *any* orthogonal transformation (marked by “ \star ”) of the coordinate system. As further discussed in Appendix B4, these assumptions imply for second- and fourth-order ITFs that

$$T_{\alpha\beta}(\mathbf{q}) = k_1(q) \delta_{\alpha\beta} + k_2(q) \hat{q}_\alpha \hat{q}_\beta \quad (2)$$

$$\begin{aligned} T_{\alpha\beta\gamma\delta}(\mathbf{q}) &= i_1(q) \delta_{\alpha\beta} \delta_{\gamma\delta} \quad (3) \\ &+ i_2(q) (\delta_{\alpha\gamma} \delta_{\beta\delta} + \delta_{\alpha\delta} \delta_{\beta\gamma}) \\ &+ i_3(q) (\hat{q}_\alpha \hat{q}_\beta \delta_{\gamma\delta} + \hat{q}_\gamma \hat{q}_\delta \delta_{\alpha\beta}) \\ &+ i_4(q) \hat{q}_\alpha \hat{q}_\beta \hat{q}_\gamma \hat{q}_\delta \\ &+ i_5(q) (\hat{q}_\alpha \hat{q}_\gamma \delta_{\beta\delta} + \hat{q}_\alpha \hat{q}_\delta \delta_{\beta\gamma} + \\ &\quad \hat{q}_\beta \hat{q}_\gamma \delta_{\alpha\delta} + \hat{q}_\beta \hat{q}_\delta \delta_{\alpha\gamma}) \end{aligned}$$

for $d \geq 2$ in terms of two invariant scalars $k_n(q)$ for the second-order fields and five invariants $i_n(q)$ for the fourth-order fields. For two-dimensional systems it is possible to rewrite Eq. (3) more compactly by means of the simple transformation

$$\begin{aligned} i_1(q) &\rightarrow i_1(q) - 2i_5(q), \quad (4) \\ i_2(q) &\rightarrow i_2(q) + i_5(q), \\ i_3(q) &\rightarrow i_3(q) + 2i_5(q), \\ i_4(q) &\rightarrow i_4(q) \text{ and} \\ i_5(q) &\rightarrow 0 \end{aligned}$$

in terms of only four invariants $i_{n \leq 4}(q)$. See Appendix B4e for details. Following Refs. [15, 17, 18] let us rotate the coordinate system such that the 1-axis points into the direction of \mathbf{q} , i.e. $q_\alpha^\circ = q \delta_{1\alpha}$ with $q = |\mathbf{q}|$. We mark coordinates in these “Natural Rotated Coordi-

nates" (NRC) by "o" and define

$$\begin{aligned}
k_L(q) &\equiv T_{11}^\circ(\mathbf{q}), i_L(q) \equiv T_{1111}^\circ(\mathbf{q}), \\
k_N(q) &\equiv T_{22}^\circ(\mathbf{q}), i_N(q) \equiv T_{2222}^\circ(\mathbf{q}), \\
i_M(q) &\equiv T_{1122}^\circ(\mathbf{q}), \\
i_G(q) &\equiv T_{1212}^\circ(\mathbf{q}) \text{ and} \\
i_P(q) &\equiv T_{2233}^\circ(\mathbf{q})
\end{aligned} \tag{5}$$

for second- and fourth-order ITFs in NRC. Since the system is isotropic these functions depend on the scalar q but not on $\hat{\mathbf{q}}$. In other words, they are *invariant* under rotation and they do not change either if one of the coordinate axes is inverted. These functions (marked by capital indices) thus provide an alternative set of invariants. Both sets of invariants are related by

$$\begin{aligned}
k_L(q) &= k_1(q) + k_2(q), k_N(q) = k_1(q), \\
i_L(q) &= i_1(q) + 2i_2(q) + 2i_3(q) + i_4(q) + 4i_5(q), \\
i_G(q) &= i_2(q) + i_5(q), \\
i_M(q) &= i_1(q) + i_3(q), \\
i_N(q) &= i_1(q) + 2i_2(q) \text{ and} \\
i_P(q) &= i_1(q).
\end{aligned} \tag{6}$$

Using the product theorem of ITFs (cf. Appendix B3) one may construct ITFs by taking outer products of ITFs of lower order. Let us introduce the linear operator

$$\begin{aligned}
T_{\alpha\beta\gamma\delta}(\mathbf{q}) &= \mathcal{O}^{2+}[T_{\alpha\beta}(\mathbf{q})] \text{ with} \\
\mathcal{O}^{2+}[T_{\alpha\beta}(\mathbf{q})] &\equiv \frac{1}{4} [\hat{q}_\alpha \hat{q}_\delta T_{\beta\gamma}(\mathbf{q}) + \hat{q}_\alpha \hat{q}_\gamma T_{\beta\delta}(\mathbf{q}) \\
&\quad + \hat{q}_\beta \hat{q}_\delta T_{\alpha\gamma}(\mathbf{q}) + \hat{q}_\beta \hat{q}_\gamma T_{\alpha\delta}(\mathbf{q})]
\end{aligned} \tag{7}$$

constructing a fourth-order ITF from a given second-order ITF $T_{\alpha\beta}(\mathbf{q})$. The invariants of $T_{\alpha\beta}(\mathbf{q})$ and $T_{\alpha\beta\gamma\delta}(\mathbf{q})$ in NRC are related by

$$\begin{aligned}
i_L(q) &= k_L(q) \text{ and } i_G(q) = k_N(q)/4 \text{ while} \\
i_M(q) &= i_N(q) = i_P(q) = i_T(q) = 0.
\end{aligned} \tag{8}$$

Similarly, it is possible to construct from a higher order ITF by contraction with another ITF a lower order ITF. We shall thus use below the linear operator

$$T_{\alpha\beta}(\mathbf{q}) \equiv \mathcal{O}^{2-}[T_{\alpha\beta\gamma\delta}(\mathbf{q})] \equiv \hat{q}_\gamma \hat{q}_\delta T_{\alpha\gamma\beta\delta}(\mathbf{q}), \tag{9}$$

generating a second-order ITF by taking twice the inner product of a fourth-order ITF $T_{\alpha\beta\gamma\delta}(\mathbf{q})$ with \hat{q}_α . As shown in Appendix B8f, the invariants of $T_{\alpha\beta}(\mathbf{q})$ are

$$k_L(q) = i_L(q) \text{ and } k_N(q) = i_G(q). \tag{10}$$

We also note that assuming $A_{\alpha\beta}(\mathbf{q})$ to be an ITF one may (under mild conditions) define an associated inverse ITF $B_{\alpha\beta}(\mathbf{q})$ by

$$A_{\alpha\gamma}(\mathbf{q})B_{\gamma\beta}(\mathbf{q}) = \delta_{\alpha\beta}. \tag{11}$$

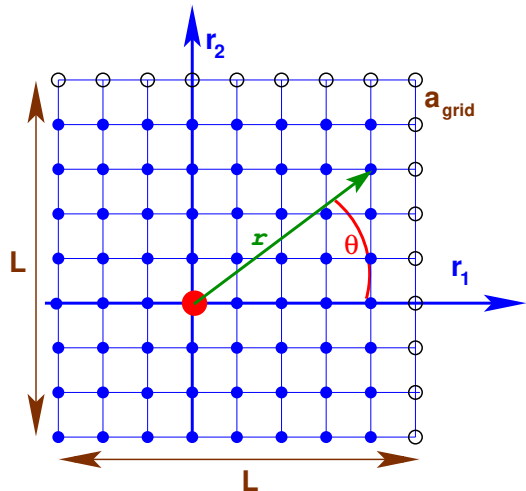


FIG. 2: Two-dimensional ($d = 2$) square lattice for fields in real space with a_{grid} being the lattice constant and $n_L = L/a_{\text{grid}}$ the number of grid points in one spatial dimension. The filled circles indicate microcells of the principal box, the open circles some periodic images. The spatial position \mathbf{r} of a microcell is either given by the r_1 - and r_2 -coordinates (in the principal box) or by the distance $r = |\mathbf{r}|$ from the origin (large circle) and the angle θ .

With $a_L(q)$ and $a_N(q)$ denoting the two *finite* invariants of $A_{\alpha\beta}(\mathbf{q})$ in NRC and $b_L(q)$ and $b_N(q)$ the corresponding invariants of $B_{\alpha\beta}(\mathbf{q})$ this implies

$$b_L(q) = 1/a_L(q) \text{ and } b_N(q) = 1/a_N(q). \tag{12}$$

We have formulated above all properties in reciprocal space. TFs in real and reciprocal space are related by

$$T_{\alpha\dots}(\mathbf{q}) = \mathcal{F}[T_{\alpha\dots}(\mathbf{r})] \tag{13}$$

as further discussed in Appendix C. Importantly, the FT of any ITF must also be an ITF, i.e.

$$T_{\alpha\dots}^*(\mathbf{r}) = T_{\alpha\dots}(\mathbf{r}^*) \stackrel{\mathcal{F}}{\Leftrightarrow} T_{\alpha\dots}^*(\mathbf{q}) = T_{\alpha\dots}(\mathbf{q}^*) \tag{14}$$

for the isotropy conditions in, respectively, real and in reciprocal space. If an ITF of a certain order and index symmetry is given in reciprocal space, the same holds in real space and the components and the invariants of each TF in real and reciprocal space are related by Eq. (13).

B. Numerical test of isotropy hypothesis

We have assumed above that the stated symmetries hold for *all* field vectors \mathbf{r} or \mathbf{q} . Obviously, this cannot be the case for experimentally or numerically obtained TFs. Deviations do in practice occur at least in the low- q (large- r) and the large- q (small- r) limits. As shown in Fig. 2, low- q deviations commonly arise due to anisotropic boundary conditions [31], e.g., the use of a standard square periodic simulation box in computer

simulations [10], large- q deviations simply due to the grid symmetry and the finite grid lattice constant a_{grid} in real space used for the data sampling [17]. Moreover, due to the finite size ξ_{mon} of the particles and the ensuing packing constraints at high densities no real condensed matter system can be perfectly isotropic for large q . We remind that inhomogeneity necessarily implies anisotropy, i.e. the failure of Eq. (1) [20]. Let us assume that the system is homogeneous for small wavenumbers $q \ll 1/\xi_{\text{hom}}$ with ξ_{hom} being set by the typical size of the local heterogeneities. This implies that Eq. (1) can only hold for

$$\frac{1}{L} \ll q \ll \frac{1}{\xi_{\text{iso}}} \leq \frac{1}{\xi_{\text{hom}}} \quad (15)$$

with L being the linear system size in Fig. 2 and ξ_{iso} characterizing the size of local anisotropies.

To test the isotropy hypothesis and to quantify possible anisotropic effects one needs to measure true invariants. For TFs sampled using ordinary coordinates in reciprocal space for a given q -range one has in principle

- to measure a sufficiently large number of components of the TF,
- to fit the invariants $k_n(q)$ or $i_n(q)$ according to the generic mathematical structure of ITFs and
- to decide according to a scalar χ^2 -test [32] whether the “isotropy hypothesis” holds.

A related alternative procedure is to do this analysis entirely in NRC. Let us illustrate this for a second-order TF $T_{\alpha\beta}(\mathbf{q})$ in $d = 2$. Instead of the two invariants $k_1(q)$ and $k_2(q)$ in ordinary space, cf. Eq. (2), one measures in NRC the components $T_{11}^\circ(\mathbf{q})$ and $T_{22}^\circ(\mathbf{q})$ parallel (longitudinal) and perpendicular (normal) to \mathbf{q} . For an idealized perfectly isotropic system these components only depend on the magnitude q of the wavevector and not on its direction $\hat{\mathbf{q}}$. In practice, even for reasonable isotropic systems some $\hat{\mathbf{q}}$ -dependence is always present due to, e.g., thermal fluctuations. It is thus justified to compute $k_L(q)$ and $k_N(q)$, cf. Eq. (5), using

$$\begin{aligned} k_L(q) &= k_1(q) + k_2(q) = \langle T_{11}^\circ(\mathbf{q}) \rangle_{\hat{\mathbf{q}}} \text{ and} \\ k_N(q) &= k_1(q) = \langle T_{22}^\circ(\mathbf{q}) \rangle_{\hat{\mathbf{q}}} \end{aligned} \quad (16)$$

by averaging over all wavevectors in some q -bin (of small width). Possible anisotropies may be measured using the invariant moments

$$\begin{aligned} \delta k_L(q) &\equiv \langle (T_{11}^\circ(\mathbf{q}) - k_L(q))^m \rangle_{\hat{\mathbf{q}}}^{1/m} \text{ and} \\ \delta k_N(q) &\equiv \langle (T_{22}^\circ(\mathbf{q}) - k_N(q))^m \rangle_{\hat{\mathbf{q}}}^{1/m} \end{aligned} \quad (17)$$

(with $m = 2, 3, \dots$) which must vanish for perfectly isotropic systems. An example is given in Sec. IV F.

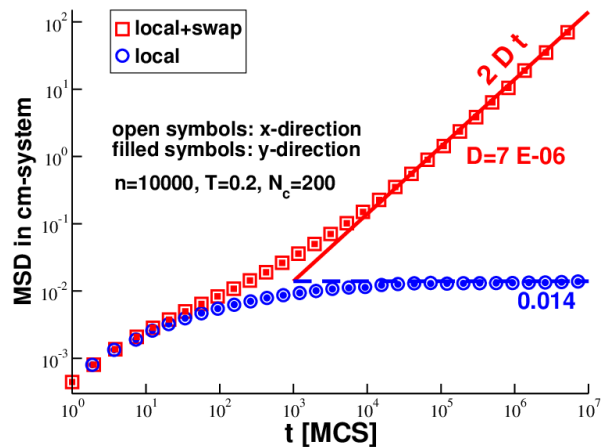


FIG. 3: Double-logarithmic representation of the MSD in x - and y -direction for pLJ particles with $n = 10000$ and $T = 0.2$. The MC time t in units of MC steps (MCS) counts the average number of local move attempts per monomer. Free diffusion with a finite diffusion constant D is observed if swap MC moves are included (squares). This allows to efficiently equilibrate the systems at the given temperature. If the swap MC moves are switched off (circles), the MSD rapidly level off and glassy behavior is observed. As expected for isotropic systems the MSD in both spatial directions are identical.

III. SOME TECHNICAL ISSUES

A. Polydisperse Lennard-Jones particles

Quite generally, computer simulations are of interest where a slow but realistic dynamical algorithm is mixed with a fast albeit artificial algorithm allowing to efficiently sample the phase space [10, 33]. This can be achieved for polydisperse glass-forming colloids by combining “molecular dynamics” (MD) simulations or local MC hopping moves [10, 33] with “swap MC moves” [34] exchanging the diameters of two randomly chosen particles [17, 30]. As in previous studies [17, 18, 30], we present numerical results obtained for two-dimensional “polydisperse Lennard-Jones” (pLJ) particles quenched and tempered with switched on swap MC moves. As can be seen from Fig. 3 presenting the standard particle “mean-square displacements” (MSD), due to the additional swap MC moves free particle diffusion over large distances is observed and all systems can be considered to be well equilibrated. More information on computational details can be found in Refs. [17, 18]. Lennard-Jones units [10] are used throughout this work. All production runs are finally performed by switching off the swap MC moves. The MSD then rapidly level off as can be seen from the circles in Fig. 3. As expected for an amorphous solid, the particles are only able to move over distances of about 1/10 of the typical particle size (“Lindemann criterion” [4]). Due to the use of an MC algorithm, not only the particle trajectories but also collective relaxation modes reveal an overdamped dynamics (without momen-

tum conservation) characterized by an effective friction coefficient ζ which we shall determine in Sec. V F below. All data are sampled at a temperature $T = 0.2$ which is much lower than the glass transition temperature $T_g \approx 0.26$ [30]. We consider systems containing up to $n = 160000$ particles. Compared to Ref. [18] we have thus increased n by a factor 4. As described in Sec. III C, the macroscopic elastic properties are determined by the two Lamé coefficients $\lambda \approx 38$ and $\mu \approx 14$ [30]. We store and manipulate the various microscopic fields using periodic square lattices. This is shown in Fig. 2 for fields in real space. A lattice constant $a_{\text{grid}} \approx 0.1$ is used.

B. Different types of averages

As a final and last averaging step we always take the *c-average* $\langle \dots \rangle_c$ over all independent configurations c (equilibrated using swap MC moves). It is assumed that this ensemble is isotropic and achiral and that the number N_c of configurations of this ensemble is as large as possible. In practice we have prepared and sampled at least $N_c = 100$ independent configurations. For $n = 10000$ we have $N_c = 200$.

The *k-average* $a(c) \equiv \langle \hat{a}_{ck} \rangle_k$ for some observable \hat{a}_{ck} depending on the state k for the given independent configuration c corresponds ideally to the standard thermodynamic average over all allowed states k [1]. For non-ergodic systems this average generally depends on c . Naturally, in practice only a finite number N_k is sampled. Since this is done by analyzing the N_k stored “frames” k of each configuration c , we are limited to $N_k = 10000$ for $n = 10000$ and $N_k = 1000$ for larger n .

We store for each n and c *four* time-series with N_k frames k with equidistant time intervals $\delta\tau = 1, 10, 100$ and 1000 MCS. The total production time of each time-series is thus $\Delta\tau_{\text{max}} = N_k\delta\tau$, e.g., $\Delta\tau_{\text{max}} = 10^6$ MCS for $n > 10000$ and $\delta\tau = 1000$ MCS. Storing these different time-series allows us to check for possible effects of system size, aging and production time and also to determine dynamical properties. This is often done in this work by analyzing *t-averages*

$$\bar{a}(\Delta\tau) \equiv \frac{1}{\Delta\tau} \int_0^{\Delta\tau} dt \hat{a}(t) \approx \frac{1}{N_t} \sum_{i=1}^{N_t} \hat{a}(t = i\delta\tau) \quad (18)$$

of instantaneous $\hat{a}(t)$ over “preaveraging times” $\Delta\tau = N_t\delta\tau \leq \Delta\tau_{\text{max}}$ with $\delta\tau$ being the discrete time increment of the $N_t \leq N_k$ equidistant measurements. Such “*t-averages*” generally depend on both $\Delta\tau$ and c .

C. Macroscopic elastic moduli

The well-known macroscopic elastic modulus tensor $E_{\alpha\beta\gamma\delta}$ [23] is for isotropic systems completely described by *two* invariants. Consistently with Eq. (B9),

$$E_{\alpha\beta\gamma\delta} = \lambda\delta_{\alpha\beta}\delta_{\gamma\delta} + \mu(\delta_{\alpha\gamma}\delta_{\beta\delta} + \delta_{\alpha\delta}\delta_{\beta\gamma}) \quad (19)$$

using the Lamé moduli λ and μ [21, 23]. We have determined $\lambda \approx 38$ and $\mu \approx 14$ for our pLJ particle systems at $T = 0.2$ using the stress-fluctuation formalism described elsewhere [30, 35]. Alternatively, we may describe the elastic response by means of the creep compliance tensor $J_{\alpha\beta\gamma\delta}$ defined by

$$J_{\alpha\beta\gamma\delta} E_{\gamma\delta\alpha'\beta'} = \frac{1}{2} (\delta_{\alpha\alpha'}\delta_{\beta\beta'} + \delta_{\alpha\beta'}\delta_{\alpha'\beta}). \quad (20)$$

For isotropic bodies [21, 23]

$$J_{\alpha\beta\gamma\delta} = \frac{1+\nu}{2E} (\delta_{\alpha\gamma}\delta_{\beta\delta} + \delta_{\alpha\delta}\delta_{\beta\gamma}) - \frac{\nu}{E} \delta_{\alpha\beta}\delta_{\gamma\delta} \quad (21)$$

with E being the Young modulus and ν Poisson’s ratio. Consistently with Eq. (20) the two sets of invariants (λ, μ) and (E, ν) are related in d dimensions by

$$\begin{aligned} \nu &= \frac{\lambda}{2\mu + \lambda(d-1)} \text{ and} \\ E &= \lambda + 2\mu - (d-1)\lambda\nu. \end{aligned} \quad (22)$$

Using the known values for λ and μ for our pLJ particle systems at $T = 0.2$ (obtained by means of the stress-fluctuation formalism) this implies $E \approx 45$ and $\nu \approx 0.6$. These values have been crosschecked using the corresponding strain-fluctuation relations. We note finally that all these moduli have first been obtained for each independent configuration c and only finally *c-averaged*. The dispersion of values for different c is, however, negligible for the system sizes with $n \geq 10000$ we focus on.

D. Correlation functions

All instantaneous fluctuating TFs [22] are assumed in this work to be *stationary stochastic* TFs (including time-reversal symmetry). Let us focus first on one independent configuration c and on a vector field $\hat{\rho}_\alpha(\mathbf{r}, t)$. The time-dependent CFs of this TF are defined by

$$c_{\alpha\beta}(\mathbf{q}, t) \equiv \langle \hat{\rho}_\alpha(\mathbf{q}, t) \hat{\rho}_\beta(-\mathbf{q}, t = 0) \rangle \quad (23)$$

in reciprocal space with t being the “time lag” [10]. $\langle \dots \rangle$ stands here and in the next two subsections for the standard thermal average for the given configuration. Taking advantage of the assumed stationarity, the statistics is commonly improved by means of a “gliding average” [10] over all pairs of time t' and t'' with $t = |t'' - t'|$. It is also useful to introduce the associated MSD [30]

$$\begin{aligned} h_{\alpha\beta}(\mathbf{q}, t) &\equiv \frac{1}{2} \langle (\hat{\rho}_\alpha(\mathbf{q}, t) - \hat{\rho}_\alpha(\mathbf{q}, t = 0)) \\ &\quad (\hat{\rho}_\beta(-\mathbf{q}, t) - \hat{\rho}_\beta(-\mathbf{q}, t = 0)) \rangle \\ &= c_{\alpha\beta}(\mathbf{q}, t = 0) - c_{\alpha\beta}(\mathbf{q}, t). \end{aligned} \quad (24)$$

We have used in the last step that achirality, stationarity and time-reversal symmetry imply

$$c_{\alpha\beta}(\mathbf{q}, t) = c_{\alpha\beta}(-\mathbf{q}, -t) = c_{\beta\alpha}(\mathbf{q}, t), \quad (25)$$

i.e. second-order CFs are symmetric. For large times t the fields at $t = 0$ and t decorrelate and we get

$$c_{\alpha\beta}(\mathbf{q}, t) \rightarrow \langle \hat{\rho}_\alpha(\mathbf{q}) \rangle \langle \hat{\rho}_\beta(-\mathbf{q}) \rangle \text{ and} \quad (26)$$

$$h_{\alpha\beta}(\mathbf{q}, t) \rightarrow c_{\alpha\beta}(\mathbf{q}, 0) - \langle \hat{\rho}_\alpha(\mathbf{q}) \rangle \langle \hat{\rho}_\beta(-\mathbf{q}) \rangle \quad (27)$$

for $t \rightarrow \infty$. For the special cases where $\langle \hat{\rho}_\alpha(\mathbf{q}, t) \rangle = 0$ this implies $c_{\alpha\beta}(\mathbf{q}, t) \rightarrow 0$ and $h_{\alpha\beta}(\mathbf{q}, t) \rightarrow c_{\alpha\beta}(\mathbf{q}, 0)$. For non-ergodic systems the above functions depend also explicitly on the configuration c . The ensemble average is obtained by c -averaging, i.e., $c_{\alpha\beta}(\mathbf{q}, t) \equiv \langle c_{\alpha\beta}(\mathbf{q}, t, c) \rangle_c$. Only this final averaging step over an isotropic ensemble may guarantee that $c_{\alpha\beta}(\mathbf{q}, t)$ and $h_{\alpha\beta}(\mathbf{q}, t)$ are ITFs. Similarly, we shall also consider below fourth-order TFs $c_{\alpha\beta\gamma\delta}(\mathbf{q}, t)$ and $h_{\alpha\beta\gamma\delta}(\mathbf{q}, t)$ characterizing the correlations of second-order instantaneous TFs $\hat{\rho}_{\alpha\beta}(\mathbf{q}, t, c)$.

In many cases instantaneous stochastic TFs are strongly fluctuating. It is thus useful to systematically project out irrelevant fluctuations by preaveraging the field by means of a t -average as defined by Eq. (18). Let us focus on t -averaged second-order TFs $\bar{\rho}_{\alpha\beta}(\mathbf{q}, \Delta\tau)$. The corresponding fourth-order CFs are defined by

$$\bar{c}_{\alpha\beta\gamma\delta}(\mathbf{q}, \Delta\tau) = \langle \bar{c}_{\alpha\beta\gamma\delta}(\mathbf{q}, \Delta\tau, c) \rangle_c \text{ with} \quad (28)$$

$$\bar{c}_{\alpha\beta\gamma\delta}(\mathbf{q}, \Delta\tau, c) = \bar{\rho}_{\alpha\beta}(\mathbf{q}, \Delta\tau, c) \bar{\rho}_{\gamma\delta}(-\mathbf{q}, \Delta\tau, c)$$

Dropping the TF indices and the \mathbf{q} -argument of the CFs let us write more compactly $c(t)$ for the standard CF with time lag t and $\bar{c}(\Delta\tau)$ for the CF of the t -averaged stochastic TF. As shown elsewhere [30] assuming a *stationary* stochastic process, the $\Delta\tau$ -dependence of $\bar{c}(\Delta\tau)$ can be traced back via

$$\bar{c}(\Delta\tau) = \frac{2}{\Delta\tau^2} \int_0^{\Delta\tau} dt (\Delta\tau - t) c(t) \quad (29)$$

to the time-dependent corresponding CF $c(t)$. Note that Eq. (29) is closely related to the general equivalence [3, 10, 30] for transport coefficients of Einstein relations, corresponding to $\bar{c}(\Delta\tau)$, and Green-Kubo relations, corresponding here to $c(t)$. Using $\bar{c}(\Delta\tau)$ has the advantage that the integral Eq. (29) filters irrelevant high frequencies, i.e. $\bar{c}(\Delta\tau)$ is a natural smoothing function of $c(t)$. Note that Eq. (29) implies that $c(t)$ is constant *iff* $\bar{c}(\Delta\tau)$ is constant and both constants are equal. This even holds if $c(t)$ and $\bar{c}(\Delta\tau)$ are only constant for a finite but sufficiently large time window [30]. Assuming a Maxwell mode $c(t) = \hat{c}_p \exp(-t/\tau_p)$ Eq. (29) implies [30]

$$\bar{c}(\Delta\tau) = \hat{c}_p D(\Delta\tau/\tau_p) \text{ with} \quad (30)$$

$$D(x) = 2[\exp(-x) - 1 + x]/x^2$$

being the ‘‘Debye function’’ well known in polymer science [7, 8]. Note that $D(x) \rightarrow 2/x$ for $x \gg 1$. For systems with overdamped dynamics the relaxation dynamics can be efficiently described by a linear superposition of a small number of such Maxwell modes [6, 8].

E. Green and growth function fields

TFs may be characterized by measuring within linear response the ‘‘response field’’ (RF) due to a small external ‘‘source field’’ (SF) perturbing the system. As an example let us consider again a fluctuating vector field $\hat{\rho}_\alpha(\mathbf{q}, t)$ in reciprocal space. We assume that at $t = 0$ a tiny SF $S_\alpha(\mathbf{q})H(t)$ is switched with $H(t)$ denoting the Heaviside function, i.e. the SF depends on the wavevector \mathbf{q} but is constant with respect to time for all $t \geq 0$. To leading order this yields a first-order RF

$$R_\alpha(\mathbf{q}, t) \equiv \langle \hat{\rho}_\alpha(\mathbf{q}, t) \rangle - \langle \hat{\rho}_\alpha(\mathbf{q}, t < 0) \rangle \\ = \mathbf{G}_{\alpha\beta}(\mathbf{q}, t) S_\beta(\mathbf{q}) H(t) \quad (31)$$

with $\mathbf{G}_{\alpha\beta}(\mathbf{q}, t)$ being a second-order TF depending in general also on t . Due to the ‘‘convolution theorem’’ of FTs, cf. Eq. (A12), this becomes

$$R_\alpha(\mathbf{r}, t) = \frac{1}{V} \int d\mathbf{r}' \mathbf{G}_{\alpha\beta}(\mathbf{r} - \mathbf{r}', t) S_\beta(\mathbf{r}') H(t) \quad (32)$$

in real space. We call $\mathbf{G}_{\alpha\beta}(\mathbf{q}, t)$ a ‘‘Green function field’’ since a localized SF $S_\alpha(\mathbf{r}) \propto \delta(\mathbf{r})$ becomes a \mathbf{q} -independent tensor in reciprocal space as further discussed in Appendix B 8c. As stated above, it is assumed that the system is not driven by an instantaneous $\delta(t)$ -pulse but rather by a perturbation constant in time. While $\mathbf{G}_{\alpha\beta}(\mathbf{q}, t)$ is thus a Green function with respect to space it is strictly speaking not a Green function with respect to time but a ‘‘growth function’’ [7], i.e. the time integral of the $\delta(t)$ -response. Hence, ‘‘GF’’ denotes below ‘‘Green function field’’ if the spatial aspects matter and ‘‘growth function field’’ otherwise.

We emphasize that for an isotropic system the GF must be an ITF, i.e.

$$\mathbf{G}_{\alpha\beta}(\mathbf{q}, t) = k_1(q, t) \delta_{\alpha\beta} + k_2(q, t) \hat{q}_\alpha \hat{q}_\beta \quad (33)$$

must hold with $k_1(q, t)$ and $k_2(q, t)$ being two time-dependent invariants. While the GF is an ITF, this does in general not apply for the SF, even for a perfectly isotropic system. This may happen especially if the SF for the perturbation is generated not by an external perturbation but by an intrinsic instantaneous fluctuation of the system, e.g., due to a local plastic reorganization of an elastic body such as the change of connectivity matrix of a polymer network [8]. While on average for isotropic systems such intrinsic fluctuating SFs must also be isotropic, this does in general not hold for an individual event. Hence, although the GF is an ITF, SFs and RFs are in general not. It is thus important to carefully distinguish between the three types of TFs [17, 18].

F. Fluctuation dissipation theorem for TFs

It is crucial that CFs, as defined in Sec. III D with all external perturbations being switched off, and GFs, as

defined in Sec. III E, may be linearly related according to the ‘‘Fluctuation Dissipation Theorem’’ (FDT) [1, 7, 9]. This implies that the perturbed TF and the SF must be thermodynamically conjugate, i.e. their inner product yields a contribution to the (scalar) Hamiltonian. Details depend now on whether the fluctuating TF is thermodynamically an *extensive* field and the perturbation TF an *intensive* field or the opposite. Only the former case is relevant for the present study for which [7, 18]

$$\mathbf{G}_{\alpha\beta}(\mathbf{q}, t) = \beta V h_{\alpha\beta}(\mathbf{q}, t) H(t) \quad (34)$$

holds. The RF $R_{\alpha\beta}(\mathbf{q}, t)$ thus reveals a continuous growth behavior starting continuously at $R_{\alpha\beta}(\mathbf{q}, 0) = 0$ [7]. Let us assume that we can *by construction* impose $\langle \hat{\rho}_\alpha(\mathbf{q}, t) \rangle = 0$ as shown in Sec. IV B for the displacement TFs. Using Eq. (27) we thus get

$$\mathbf{G}_{\alpha\beta}(\mathbf{q}, t) \rightarrow \beta V c_{\alpha\beta}(\mathbf{q}, t = 0) \text{ for } t \rightarrow \infty. \quad (35)$$

Dropping the time argument, we may write the FDT relation for the static limit concisely as

$$\mathbf{G}_{\alpha\beta}(\mathbf{q}) = \beta V c_{\alpha\beta}(\mathbf{q}) = \beta V \langle \hat{\rho}_\alpha(\mathbf{q}) \hat{\rho}_\beta(-\mathbf{q}) \rangle. \quad (36)$$

We will use Eq. (36) in Appendix D to compute the (static) linear response of displacement fields under externally applied force fields and Eq. (34) to establish in Sec. V the relation between the the time-dependent CFs of displacement and strain fields with the longitudinal and transverse material functions $L(q, t)$ and $G(q, t)$.

IV. FLUCTUATIONS OF DISPLACEMENTS AND STRAINS FIELDS IN ELASTIC BODIES

A. Introduction

We consider now the static correlations of displacement and strain fields $u_\alpha(\mathbf{q})$ and $\varepsilon_{\alpha\beta}(\mathbf{q})$ in *linear elastic* bodies of finite compression modulus. We shall first solve the problems for arbitrary dimensions d in reciprocal space and only move back to real space at the end using the inverse FTs stated in Appendix C 4. The CFs of the displacements $u_\alpha(\mathbf{q})$ are discussed in Sec. IV C. This allows us to define two important *static* material functions, the longitudinal and shear moduli $L(q)$ and $G(q)$. We turn then in Sec. IV D to the (‘‘small’’) strain TF $\varepsilon_{\alpha\beta}(\mathbf{q})$ and verify in Sec. IV E that its components in NRC are for sufficiently small q circularly-symmetric complex Gaussian variables. The anisotropy of k -averaged strain CFs is finally characterized in Sec. IV F.

B. Operational definitions

The displacement field $u_\alpha(\mathbf{q})$ in reciprocal space (for a given configuration c and a given state k or time t) may in principle be defined by integrating the measured velocity field $v_\alpha(\mathbf{q}, t) = \dot{u}_\alpha(\mathbf{q}, t)$ starting from any reference

time $t = 0$. In order to avoid the arbitrary integration constant, it is imposed that

$$\langle u_\alpha(\mathbf{q}, c, k) \rangle_k = 0 \text{ for all } \mathbf{q} \text{ and } c, \quad (37)$$

i.e. any measured $u_\alpha(\mathbf{q}, c, k)$ is shifted by its k -average. This means physically and in numerical practice that we use in real space as a reference position \tilde{r}_α^a for the displacement vector $u_\alpha^a = r_\alpha^a - \tilde{r}_\alpha^a$ of each particle a at time t the k -averaged monomer position

$$\tilde{r}_\alpha^a \equiv \langle r_\alpha^a(k) \rangle_k, \text{ i.e. } \langle u_\alpha^a(k) \rangle_k \equiv 0, \quad (38)$$

with $r_\alpha^a(k)$ denoting the coordinates of particle a of configuration c and state k [18]. We remind that the displacement field in real space may be defined by [36]

$$u_\alpha(\mathbf{r}) \equiv \frac{1}{n/V} \sum_a u_\alpha^a \delta(\mathbf{r} - \tilde{r}_\alpha^a). \quad (39)$$

It follows from Eq. (38) that the k -average indeed vanishes. The linear strain TF is defined by [23]

$$\varepsilon_{\alpha\beta}(\mathbf{q}) \equiv \frac{i}{2} [u_\alpha(\mathbf{q}) q_\beta + u_\beta(\mathbf{q}) q_\alpha] \quad (40)$$

as a symmetric second-order TF associated to $u_\alpha(\mathbf{q})$. Due to Eq. (40) the CFs of displacement and strain fields are closely related. By construction Eq. (37) and Eq. (40) imply that the k -averaged strain field must also vanish. That a displacement or strain TF is an instantaneously taken phase function is often emphasized by carrets, i.e. we write $\hat{u}_\alpha(\mathbf{q})$ and $\hat{\varepsilon}_{\alpha\beta}(\mathbf{q})$.

C. Displacement correlations

1. Reciprocal space

The CFs $c_{\alpha\beta}(\mathbf{q})$ of the instantaneous displacement TF $\hat{u}_\alpha(\mathbf{q})$ in reciprocal space are defined by [22]

$$c_{\alpha\beta}(\mathbf{q}) \equiv \langle c_{\alpha\beta}(\mathbf{q}, c) \rangle_c \text{ with} \quad (41)$$

$$c_{\alpha\beta}(\mathbf{q}, c) \equiv \langle c_{\alpha\beta}(\mathbf{q}, c, k) \rangle_k \text{ and}$$

$$c_{\alpha\beta}(\mathbf{q}, c, k) \equiv \hat{u}_\alpha(\mathbf{q}, c, k) \hat{u}_\beta(-\mathbf{q}, c, k) \quad (42)$$

assuming by construction $\langle \hat{u}_\alpha(\mathbf{q}, c, k) \rangle_k = 0$. In agreement with Eq. (2) we may write

$$c_{\alpha\beta}(\mathbf{q}) = k_1(q) \delta_{\alpha\beta} + k_2(q) \hat{q}_\alpha \hat{q}_\beta. \quad (43)$$

Using the first relation of Eq. (6) we express $k_1(q)$ and $k_2(q)$ in terms of the corresponding invariants in NRC

$$k_L(q) = k_1(q) + k_2(q) = \langle c_{11}^\circ(\mathbf{q}) \rangle_{\hat{\mathbf{q}}} \text{ and} \quad (44)$$

$$k_N(q) = k_1(q) = \langle c_{22}^\circ(\mathbf{q}) \rangle_{\hat{\mathbf{q}}} = \dots = \langle c_{dd}^\circ(\mathbf{q}) \rangle_{\hat{\mathbf{q}}}.$$

While for mathematically idealized isotropic systems $c_{\alpha\beta}^\circ(\mathbf{q})$ must only dependent on the wavenumber q and not on the wavevector direction $\hat{\mathbf{q}}$, this is generally only

approximatively true for real experiments or computer simulations for often merely statistical reasons. It is then justified to additionally take the average $\langle \dots \rangle_{\hat{\mathbf{q}}}$ over all measured directions $\hat{\mathbf{q}}$ [17, 18]. This procedure allows in principle an appropriate phenomenological characterization of displacement fields in, say, dense active matter and other systems where the equipartition theorem of statistical physics [1] may not be applicable to relate the CFs to thermodynamic linear response moduli. We shall assume here, however, that the displacements $\hat{u}_\alpha^\circ(\mathbf{q})$ in NRC are Gaussian variables following Maxwell-Boltzmann statistics. For details see the standard textbooks [1]. Within this harmonic approximation all contributions to the free energy from different wavevectors and modes factorize and the partition function for a given \mathbf{q} becomes an integral over all $u_\alpha(\mathbf{q})$ with a Gibbs weight $\exp[-\beta V \delta f(\mathbf{q})]$ set by the free energy density

$$\begin{aligned} \delta f(\mathbf{q}) &\equiv \frac{1}{2} \hat{u}_\alpha(\mathbf{q}) q^2 E_{\alpha\beta}(\mathbf{q}) \hat{u}_\beta(-\mathbf{q}) \\ &= \frac{1}{2} \hat{u}_\alpha^\circ(\mathbf{q}) q^2 E_{\alpha\beta}^\circ(\mathbf{q}) \hat{u}_\beta^\circ(-\mathbf{q}) \end{aligned} \quad (45)$$

where we have used in the second step that $\delta f(\mathbf{q})$ is a scalar. Here, $E_{\alpha\beta}(\mathbf{q})$ denotes a second-order symmetric ITF with invariants given by

$$\begin{aligned} k_L^E(q) &= k_1^E(q) + k_2^E(q) \equiv L(q) \text{ and} \\ k_N^E(q) &= k_1^E(q) \equiv G(q) \end{aligned} \quad (46)$$

where we have introduced the q -dependent longitudinal modulus $L(q)$ and the q -dependent shear modulus $G(q)$. Performing then the Gaussian integrals leads to

$$q^2 k_L(q) = \frac{1}{\beta V L(q)} \text{ and } q^2 k_N(q) = \frac{1}{\beta V G(q)} \quad (47)$$

in agreement with Ref. [1]. Let us define by

$$E_{\alpha\gamma}(\mathbf{q}) K_{\gamma\beta}(\mathbf{q}) = \delta_{\alpha\beta} \quad (48)$$

a second-order TF $K_{\alpha\beta}(\mathbf{q})$ as the inverse with respect to $E_{\alpha\beta}(\mathbf{q})$. Using Eq. (12) the invariants of $K_{\alpha\beta}(\mathbf{q})$ are

$$k_L^K(q) = \frac{1}{L(q)} \text{ and } k_N^K(q) = \frac{1}{G(q)}. \quad (49)$$

Following Ref. [1] we thus rewrite Eq. (47) compactly as

$$q^2 c_{\alpha\beta}(\mathbf{q}) = K_{\alpha\beta}(\mathbf{q}) / \beta V \quad (50)$$

in ordinary coordinates. We note finally that following Ref. [1] $E_{\alpha\beta}(\mathbf{q})$ may alternatively be defined by the contraction $E_{\alpha\beta}(\mathbf{q}) \equiv \mathcal{O}^2[E_{\alpha\beta\gamma\delta}(\mathbf{q})]$ of the fourth-order static elasticity TF $E_{\alpha\beta\gamma\delta}(\mathbf{q})$ being also an ITF. This will be elaborated in Sec. VB within a more general context.

2. Computational results

The relations Eq. (47) may be used to determine $L(q)$ and $G(q)$ from the fluctuations of displacement TFs.

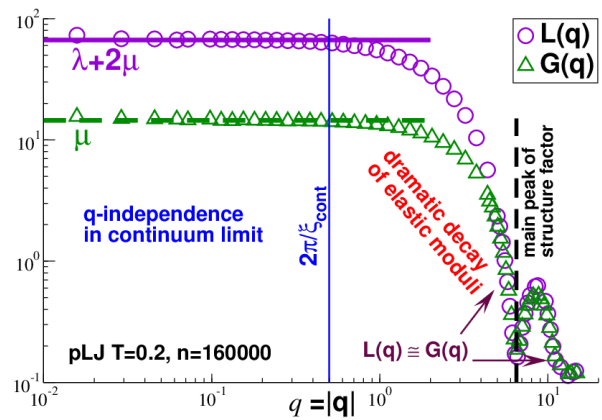


FIG. 4: Static microscopic elastic moduli $L(q)$ and $G(q)$ in reciprocal space obtained by rescaling according to Eq. (47) the measured ICFs $k_L(q)$ and $k_N(q)$ of the displacement TFs of pLJ particles at $T = 0.2$ for $n = 160000$ particles. The horizontal lines indicate the macroscopic elastic moduli $\lambda + 2\mu$ and μ . $L(q)$ and $G(q)$ are essentially constant below $q \approx 0.5$ (thin vertical line) but are seen to strongly decrease for larger q with a first minimum at the position of the main peak of the coherent structure factor at $q \approx 6.5$ (dashed vertical line). $L(q)$ and $G(q)$ become similar for $q > 4$.

This is demonstrated in Fig. 4 for our pLJ particle model with $n = 160000$. As can be seen, $L(q)$ and $G(q)$ are essentially constant for wavenumbers below $q \approx 0.5$ (thin vertical line). Using the known macroscopic Lamé coefficients $\lambda \approx 38$ and $\mu \approx 14$, we find as expected

$$L(q) \rightarrow \lambda + 2\mu \text{ and } G(q) \rightarrow \mu \text{ for } q \ll 2\pi/\xi_{\text{cont}}. \quad (51)$$

Depending somewhat on the criterion, the length scale ξ_{cont} characterizing the breakdown of the elastic continuum assumption is thus about $\xi_{\text{cont}} \approx 10$ for the presented pLJ particle system. (The trivial prefactor 2π used here for the determination of ξ_{cont} is often suppressed elsewhere for clarity.) See Refs. [28, 29] for related experimental work using Eq. (47) to extract the shear modulus $\mu(T)$ as a function of temperature T from the low- q limit of $G(q, T)$ using the recorded positions of effectively two-dimensional colloidal systems. Both generalized static moduli are seen to dramatically decay over two orders of magnitude for larger q and the minimum of both moduli at $q \approx 6.5$ (dashed vertical line) coincides perfectly with the main peak of the coherent structure factor presented elsewhere [30]. Note also that $L(q)$ and $G(q)$ are surprisingly similar for the largest q .

3. Back to real space

According to Eq. (14) the inverse FT $c_{\alpha\beta}(\mathbf{r}) = \mathcal{F}[c_{\alpha\beta}(\mathbf{q})]$ must also be an ITF, i.e.

$$c_{\alpha\beta}(\mathbf{r}) = \tilde{k}_1(r) \delta_{\alpha\beta} + \tilde{k}_2(r) \hat{r}_\alpha \hat{r}_\beta \quad (52)$$

where the two invariants $\tilde{k}_1(r)$ and $\tilde{k}_2(r)$ are in principle given by $k_1(q) = k_N(q)$ and $k_2(q) = k_L(q) - k_N(q)$. Fortunately, both generalized moduli become constant in the continuum limit as seen in Fig. 4. This suggests for sufficiently large systems the approximation $L(q) \approx \lambda + 2\mu$ and $G(q) \approx \mu$ for all q . We use then Eq. (C52), Eq. (C53) and Table VIII for the exponent $\eta = 2$ and introduce the convenient constants [18]

$$J_1 \equiv \frac{1}{\mu} - \frac{1}{\lambda + 2\mu} = \frac{\lambda + \mu}{\mu(\lambda + 2\mu)} \text{ and } J_2 \equiv \frac{2}{\lambda + 2\mu} \quad (53)$$

having the same units as inverse moduli. Within this approximation we finally obtain

$$\beta\tilde{k}_1(r) = \frac{J_1 + J_2}{8\pi r} \text{ and } \beta\tilde{k}_2(r) = \frac{J_1}{8\pi r} \quad (54)$$

for $d = 3$ and a logarithmic behavior for $d = 2$. We show in Appendix D how the CFs obtained here determine the displacement RFs if an external force density is applied.

D. Correlations of strain fields

1. Reciprocal space

The CFs of the instantaneous strain TF, cf. Eq. (40), are given in reciprocal space by

$$\begin{aligned} c_{\alpha\beta\gamma\delta}(\mathbf{q}) &\equiv \langle c_{\alpha\beta\gamma\delta}(\mathbf{q}, c) \rangle_c \text{ with} & (55) \\ c_{\alpha\beta\gamma\delta}(\mathbf{q}, c) &\equiv \langle c_{\alpha\beta\gamma\delta}(\mathbf{q}, c, k) \rangle_k \text{ and} \\ c_{\alpha\beta\gamma\delta}(\mathbf{q}, c, k) &\equiv \hat{\varepsilon}_{\alpha\beta}(\mathbf{q}, c, k) \hat{\varepsilon}_{\gamma\delta}(-\mathbf{q}, c, k) \end{aligned}$$

similarly as the CFs of the displacement TFs by Eq. (41). For an achiral and isotropic system this TF must take the generic form given by Eq. (3). In fact, only two of the in general five invariants matter as may be seen by expressing the strain CFs using Eq. (40) by the CF $c_{\alpha\beta}(\mathbf{q})$ of the displacement fields. As readily seen,

$$c_{\alpha\beta\gamma\delta}(\mathbf{q}) = q^2 \mathcal{O}^{2+}[c_{\alpha\beta}(\mathbf{q})] \quad (56)$$

as in Eq. (7). Using Eq. (8) we get in NRC the two ICFs

$$\begin{aligned} c_L(q) &= q^2 k_L(q) = \frac{1}{\beta V L(q)} \text{ and} \\ 4c_G(q) &= q^2 k_N(q) = \frac{1}{\beta V G(q)} \end{aligned} \quad (57)$$

and $c_4(q) = k_2(q)$ and $4c_5(q) = k_1(q)$ in ordinary coordinates while all other invariants vanish. Note also that using $q_\alpha^\circ = q\delta_{\alpha 1}$ and Eq. (40) it is seen that only

$$\begin{aligned} \hat{\varepsilon}_{11}^\circ(\mathbf{q}) &= iq\hat{u}_1^\circ(\mathbf{q}) \text{ and} \\ \hat{\varepsilon}_{1\beta}^\circ(\mathbf{q}) &= \hat{\varepsilon}_{\beta 1}^\circ(\mathbf{q}) = \frac{iq}{2}\hat{u}_\beta^\circ(\mathbf{q}) \text{ for } \beta \neq 1 \end{aligned} \quad (58)$$

can be finite while $\hat{\varepsilon}_{\alpha\beta}^\circ(\mathbf{q}) = 0$ for all other strain components. Only the longitudinal and shear ICFs in NRC

$$\begin{aligned} c_L(q) &= \langle c_{1111}^\circ(\mathbf{q}) \rangle_{\hat{\mathbf{q}}} \text{ and} \\ c_G(q) &= \langle c_{1212}^\circ(\mathbf{q}) \rangle_{\hat{\mathbf{q}}} = \dots = \langle c_{1d1d}^\circ(\mathbf{q}) \rangle_{\hat{\mathbf{q}}} \end{aligned} \quad (59)$$

can thus be finite. This implies using Eq. (6) that only two invariants in ordinary space can be finite:

$$c_4(q) = c_L(q) - 4c_G(q) \text{ and } c_5(q) = c_G(q). \quad (60)$$

2. Back to real space

As we have seen, all ICFs in reciprocal space become constant for small q . Hence, $\beta V c_4(q) \simeq -J_1$ and $4\beta V c_5(q) \rightarrow J_1 + J_2/2$ for $q\xi_{\text{cont}} \ll 1$ using the constants J_1 and J_2 of Eq. (53). Let us thus define the two amplitudes $\hat{c}_4 = -J_1/\beta$ and $\hat{c}_5 = (J_1 + J_2/2)/4\beta$ of dimension volume. The inverse FT $c_{\alpha\beta\gamma\delta}(\mathbf{r})$ is then obtained using Table VIII for $\eta = 0$ in terms of the five invariants $\tilde{c}_n(r)$ in real space. For $d = 3$ we get

$$\begin{aligned} 8\pi r^3 \tilde{c}_1(r) &\simeq \hat{c}_4, \\ 8\pi r^3 \tilde{c}_2(r) &\simeq \hat{c}_4 + 4\hat{c}_5, \\ 8\pi r^3 \tilde{c}_3(r) &\simeq -3\hat{c}_4, \\ 8\pi r^3 \tilde{c}_4(r) &\simeq 15\hat{c}_4 \text{ and} \\ 8\pi r^3 \tilde{c}_5(r) &\simeq -3\hat{c}_4 - 6\hat{c}_5 \end{aligned} \quad (61)$$

where “ \simeq ” marks that this is the asymptotic limit for large r and sufficiently large systems. For $d = 2$ one may also use Table VII where the “compact representation” is used. This leads to

$$\begin{aligned} 4\pi r^2 \tilde{c}_1(r) &\simeq 5\hat{c}_4 + 8\hat{c}_5, \\ 4\pi r^2 \tilde{c}_2(r) &\simeq -\hat{c}_4, \\ 4\pi r^2 \tilde{c}_3(r) &\simeq -6\hat{c}_4 - 8\hat{c}_5, \\ 4\pi r^2 \tilde{c}_4(r) &\simeq 8\hat{c}_4 \text{ and} \\ \tilde{c}_5(r) &= 0. \end{aligned} \quad (62)$$

Note that this result is consistent with Ref. [18]. Importantly, all invariants $\tilde{c}_n(r)$ for $d = 3$ decay asymptotically as $1/r^3$ and all for $d = 2$ as $1/r^2$. More generally, the strain CFs of isotropic elastic bodies in real space thus decay in any dimension d analytically as $c_{\alpha\beta\gamma\delta}(\mathbf{r}) \simeq 1/r^d$.

3. Numerical results

The latter relations for $d = 2$ are put to the test for our two-dimensional pLJ particle system in Fig. 5. We present data obtained for $n = 160000$ beads at $T = 0.2$. Following Ref. [18] we first compute the $c_{\alpha\beta\gamma\delta}(\mathbf{q})$ in reciprocal space using a discrete square grid and perform then numerically an inverse FT to obtain $c_{\alpha\beta\gamma\delta}(\mathbf{r})$. The shear-strain CF $c_{1212}(\mathbf{r})$ has already been presented in the last panel of Fig. 1. It follows from Eq. (62) that

$$\beta c_{1212}(\mathbf{r}) \simeq \frac{J_1}{4\pi r^2} \cos(4\theta) \text{ for } r \gg 1. \quad (63)$$

The same large- r limit holds also for $\beta c_{1122}(\mathbf{r})$ and for $-\beta(c_{1111}(\mathbf{r}) + c_{2222}(\mathbf{r}))/2$. Moreover,

$$\beta(c_{1111}(\mathbf{r}) - c_{2222}(\mathbf{r}))/2 \simeq -\frac{J_2}{4\pi r^2} \cos(2\theta) \quad (64)$$

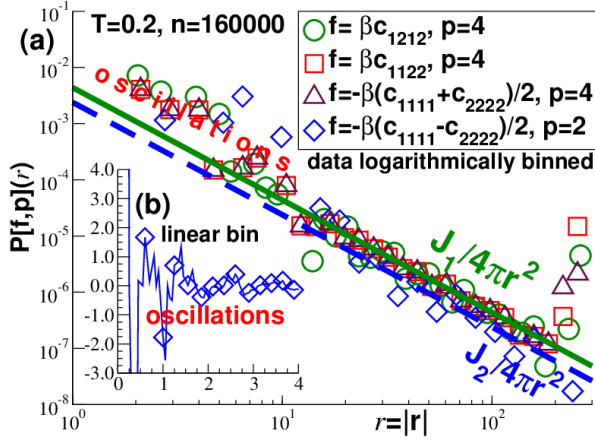


FIG. 5: r -dependence of strain CFs $c_{\alpha\beta\gamma\delta}(\mathbf{r})$ obtained for pLJ particles in $d = 2$ for $n = 160000$ and $T = 0.2$. The expected θ -dependence is projected out using Eq. (65) for $f(r, \theta)$ and p as indicated in the legend. (a) Double-logarithmic representation for logarithmically binned data. The two power-law slopes indicate the expected asymptotic behavior using the constants $J_1 \approx 0.07$ and $J_2 \approx 0.03$, cf. Eq. (53), known from the Lamé moduli λ and μ . (b) Linear representation for $f = -\beta(c_{1111}(\mathbf{r}) - c_{2222}(\mathbf{r}))/2$ and $p = 2$ emphasizing the generic oscillatory behavior for $r \ll 10$.

for $r \gg 1$. Note that if the coordinate system is turned by an angle ϕ , as shown in the first panel of Fig. 1, the above CFs turn with the coordinate system. To obtain a precise test of the expected r -dependences we project out in Fig. 5 the angular dependences using

$$P[f, p](r) \equiv 2 \times \frac{1}{2\pi} \int_0^{2\pi} d\theta f(r, \theta) \cos(p\theta) \quad (65)$$

for any function $f(r, \theta)$ of the polar coordinates r and θ using (here) $p = 2$ and $p = 4$. For convenience the prefactor of the integral is chosen such that $P[\cos(2\theta), 2] = P[\cos(4\theta), 4] = 1$. Panel (a) of Fig. 5 presents logarithmically averaged data using a double-logarithmic representation. In agreement with Eq. (63) the indicated first three cases collapse for $p = 4$ and $r \gtrsim 20$ on $J_1/4\pi r^2$ (bold solid line). This confirms the octupolar symmetry [24] of these (rescaled) CFs. Confirming Eq. (64) the last indicated case with $f(\mathbf{r}) = -\beta(c_{1111}(\mathbf{r}) - c_{2222}(\mathbf{r}))/2$ collapses onto $J_2/4\pi r^2$ (dashed line). $p = 2$ is used here in agreement with the predicted quadrupolar symmetry. We note that the logarithmic average used in panel (a) suppresses oscillatory behavior for $r \ll 10$ which ultimately stems from the packing of the discrete particles. This is emphasized in panel (b) using a linear representation for $f(\mathbf{r}) = -\beta(c_{1111}(\mathbf{r}) - c_{2222}(\mathbf{r}))/2$. Similar results are obtained for other particle numbers n [18].

E. Strain distributions in NRC

We have assumed above in Sec. IV C that the displacements $\hat{u}_\alpha^c(\mathbf{q})$ in NRC are distributed according to a

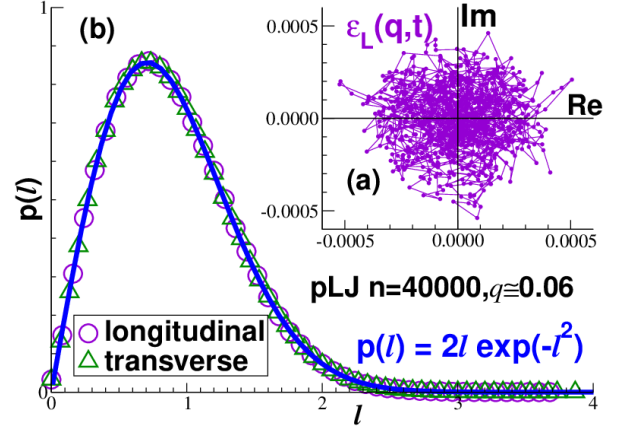


FIG. 6: Distribution of strain components $\varepsilon_L(\mathbf{q})$ and $\varepsilon_N(\mathbf{q})$ in NRC for $n = 40000$ pLJ particles: (a) Trajectory of $\varepsilon_L(\mathbf{q}, t)$ in reciprocal space for one configuration and one wavevector with $q \ll 1$. (b) Normalized distribution of the real-valued length l defined by Eq. (68) for $\varepsilon_L(\mathbf{q})$ and $\varepsilon_N(\mathbf{q})$. The distribution confirms the expected Rayleigh distribution Eq. (72).

complex circularly-symmetric Gaussian distribution [37]. The same also applies due to Eq. (58) to the strain components $\hat{\varepsilon}_{\alpha\beta}^c(\mathbf{q})$ in NRC being merely rescaled displacement components. We show here that this is indeed the case for our model system. Let us introduce the convenient notation

$$\begin{aligned} \varepsilon_L(\mathbf{q}) &\equiv \hat{\varepsilon}_{11}^c(\mathbf{q}) = i q \hat{u}_1^c(\mathbf{q}) \quad \text{and} \quad (66) \\ \varepsilon_N(\mathbf{q}) &\equiv \hat{\varepsilon}_{12}^c(\mathbf{q}) = \frac{i q}{2} \hat{u}_2^c(\mathbf{q}) \end{aligned}$$

for the longitudinal and normal (transverse) components in NRC. A scatter plot of $\varepsilon_L(\mathbf{q})$ in the complex plane for one configuration and one wavevector \mathbf{q} is shown in panel (a) of Fig. 6. The data appears to be indeed distributed symmetrically around the origin of the complex plane. The goal is now to numerically characterize this complex distribution. $\langle \dots \rangle$ stands in this subsection for the combined c - and k -average $\langle \langle \dots \rangle_k \rangle_c$.

Let us rescale for later convenience $\varepsilon_L(\mathbf{q})$ and $\varepsilon_N(\mathbf{q})$ by the square root of their typical squared averages

$$e(\mathbf{q}) \Rightarrow e(\mathbf{q}) \equiv \frac{\varepsilon(\mathbf{q})}{\langle \varepsilon(\mathbf{q}) \varepsilon(-\mathbf{q}) \rangle^{1/2}} \quad (67)$$

for both components “L” and “N”. Due to the Wiener-Khinchin theorem, cf. Eq. (A11), both averages are real and positive and, moreover, equivalent to the ICFs or the elastic moduli $L(q)$ and $G(q)$, cf. Eq. (47). Let us write

$$e(\mathbf{q}) = e'(\mathbf{q}) + i e''(\mathbf{q}) = l(\mathbf{q}) e^{i\phi(\mathbf{q})} \quad (68)$$

with e' and e'' being the real and the imaginary parts of e , $l \geq 0$ its real-valued length and ϕ its phase angle. (l and ϕ are the polar coordinates of $e(\mathbf{q})$.) Hence,

$$l^2(\mathbf{q}) = e(\mathbf{q}) e(-\mathbf{q}) = (e')^2 + (e'')^2. \quad (69)$$

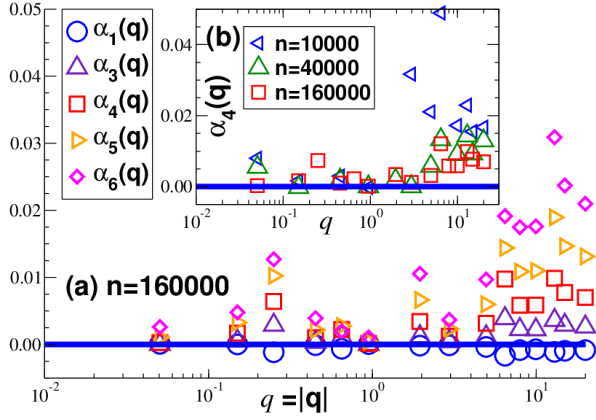


FIG. 7: Non-Gaussianity parameters $\alpha_m(q)$ for the rescaled length l of the longitudinal strain components $\varepsilon_L(\mathbf{q})$ in NRC obtained for our pLJ model at $T = 0.2$: (a) $\alpha_m(q)$ for $m = 1, 3, 4, 5$ and 6 for $n = 160000$. (b) comparison of $\alpha_4(q)$ for three system sizes. As seen, $\alpha_m(q)$ is tiny for all m, q and n but increases with m and q and decreases with n .

Due to the above rescaling $\langle l^2(\mathbf{q}) \rangle = 1$ for both strain components. Panel (b) of Fig. 6 shows the normalized distributions $p(l)$ of the lengths l of the reduced longitudinal (circles) and normal (squares) displacements. As emphasized by the bold solid line, a Rayleigh distribution [38, 39] with $p(l) = 2l \exp(-l^2)$ is observed. We also note that plotting $p(l)/2l$ as a function of l^2 in half-logarithmic coordinates yields a purely exponential decay (not shown). The observed distribution can be explained by reworking Maxwell’s argument [40] for the velocity distribution of an ideal gas for the (effectively two-dimensional) complex plane. This assumes that the two components e' and e'' are decorrelated, equivalent and isotropically distributed. This implies a random phase angle ϕ of uniform distribution and the factorization

$$p_2(e', e'') de' de'' = p_1(e') de' \times p_1(e'') de'' \quad (70)$$

of the probability for observing both e' and e'' with $p_1(x)$ being the same distribution for each component. Moreover, isotropy implies that $p_2(e', e'')$ must be a function of the scalar l^2 . Following Maxwell this functional equation is solved by the normalized Gaussian distribution

$$p_2(e', e'') de' de'' = \frac{1}{\pi} \exp(-l^2) de' de'' \quad (71)$$

with $l^2 = (e')^2 + (e'')^2$. Such a probability density of a complex random variable $e(\mathbf{q})$ is called a “complex circularly-symmetric Gaussian probability density function” [37]. The probability $p(l)$ for observing a length l is then the Rayleigh distribution [39]

$$p(l) = 2\pi l \times p_2(e', e'') = 2l \exp(-l^2) \quad (72)$$

with $l = l(\mathbf{q})$ being either the length of the rescaled longitudinal or normal strain component.

We have thus demonstrated in panel (b) of Fig. 6 for one small wavevector that the distribution is a circularly-centered complex Gaussian. Whether this still holds for larger wavevectors is best tested by computing moments $\langle l^m \rangle$ as a function of q . It is convenient to rescale these measured moments such that they must vanish for a perfect Rayleigh distribution. We thus compute for both strain components the non-Gaussianity parameters

$$\begin{aligned} \alpha_1(q) &\equiv \frac{2}{\sqrt{\pi}} \langle l^1 \rangle - 1, \\ \alpha_3(q) &\equiv \frac{4}{3\sqrt{\pi}} \langle l^3 \rangle - 1, \\ \alpha_4(q) &\equiv \frac{1}{2} \langle l^4 \rangle - 1, \\ \alpha_5(q) &\equiv \frac{8}{15\sqrt{\pi}} \langle l^5 \rangle - 1 \text{ and} \\ \alpha_6(q) &\equiv \frac{1}{6} \langle l^6 \rangle - 1 \end{aligned} \quad (73)$$

where we note that $\alpha_2(q) \equiv 0$ by definition. The results obtained for the longitudinal strain components are given in Fig. 7. Panel (a) presents for our largest system with $n = 160000$ particles the moments $m = 1, 3, 4, 5$ and 6 . Not surprisingly, the observed values systematically increase with m . A comparison of $\alpha_4(q)$ for different system sizes is seen in panel (b). We also note an increase with q , especially for the largest q . Importantly, $|\alpha_m(q)| \ll 0.1$ for all measured m, q and n . Similar results have been observed for the transverse strain components.

F. Various variances and test of anisotropy

1. Introduction

As estimated in Sec. IV C 2, the length ξ_{cont} characterizing the breakdown of the continuum assumption is about $\xi_{\text{cont}} \approx 10$ for the pLJ particle system. Moreover, it can be shown [17] that the standard monomer structure factor, which measures the density fluctuations, only becomes constant for similar q as the moduli $L(q)$ and $G(q)$. The length ξ_{hom} , characterizing the range of inhomogeneities due to the local packing of the polydisperse LJ particles, is thus similar to ξ_{cont} . According to Sec. II B the length scale ξ_{iso} , above which isotropic behavior is expected, is bounded from below by ξ_{hom} , cf. Eq. (15). This argument suggests that all three length scales ξ_{cont} , ξ_{iso} and ξ_{hom} are of similar order for the presented computer model. We attempt here to characterize ξ_{iso} *directly* following Sec. II B by characterizing the anisotropies of the lateral and transverse strain ICFs. Naturally, the order of the averaging procedure is important here since c -averaged CFs (assuming an arbitrarily large ensemble with $N_c \rightarrow \infty$) must by construction be perfectly isotropic as confirmed in Sec. IV F 4. What is meant by ξ_{iso} is the (finally c -averaged) length characterizing the isotropy of each configuration c . As defined by

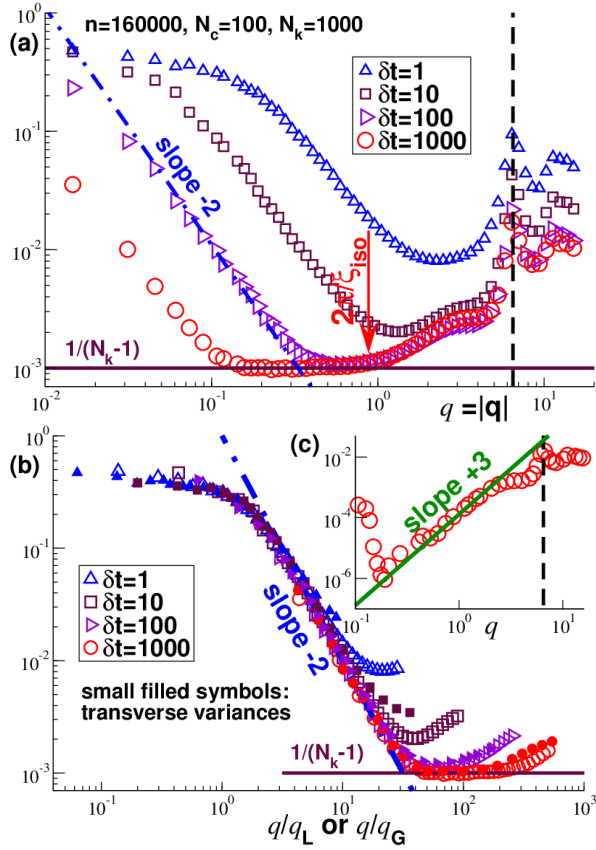


FIG. 8: c -variances of rescaled k -averaged ICFs for pLJ particles with $n = 160000$: (a) Data for longitudinal ICFs $d_L(\mathbf{q}, c)$ for different $\delta\tau$. The power law with exponent -2 (dash-dotted line) is a dynamical effect due to relaxation times $\tau_L(q) \propto 1/q^2$, the intermediate regime (bold horizontal line) is expected for uncorrelated Gaussian fluctuations. (b) Data collapse using q/q_L for longitudinal ICFs (open symbols) and q/q_G for transverse ICFs (filled symbols). (c) Longitudinal variances for $\delta\tau = 1000$ after subtracting $1/(N_k - 1)$.

the second relation of Eq. (55), we focus in this subsection on the k -averaged strain CFs $c_{\alpha\beta\gamma\delta}(\mathbf{q}, c)$ and their longitudinal and transverse ICFs $c_L(\mathbf{q}, c)$ and $c_G(\mathbf{q}, c)$ in NRC. (The argument \mathbf{q} is used to indicate that we first do not average over $\hat{\mathbf{q}}$.) As in the preceding Sec. IVE it is convenient to normalize the ICFs by their c - and $\hat{\mathbf{q}}$ -averaged means $c_L(q)$ and $c_G(q)$ presented in Fig. 4. These rescaled ICFs are denoted by $d_L(\mathbf{q}, c)$ and $d_G(\mathbf{q}, c)$.

2. q -averaged c -variance of ICFs

Let us first compute for $d_L(\mathbf{q}, c)$ and $d_G(\mathbf{q}, c)$ the c -averaged (empirical) variances

$$\left\langle \left\langle d(\mathbf{q}, c)^2 \right\rangle_c - \left\langle d(\mathbf{q}, c) \right\rangle_c^2 \right\rangle_{\hat{\mathbf{q}}} \quad (74)$$

for each wavevector \mathbf{q} taking in a final step the $\hat{\mathbf{q}}$ -average over all $\|\mathbf{q}\|$ in a bin around q . The data for the longitudinal ICFs are shown in panel (a) of Fig. 8 for a broad

range of time-increments $\delta\tau$ between always $N_k = 1000$ stored frames. The thin solid and dashed lines presented in Fig. 9 show the corresponding variances for both the longitudinal and the transverse ICFs for $\delta\tau = 1000$. As can be seen from both representations, non-monotonic behavior with three different q -regimes is observed. Let us begin with the most simple intermediate regime for $0.1 \ll q \ll 1$ where the variances approach $1/(N_k - 1)$ for large $\delta\tau$. We recall from Fig. 7 that the instantaneous strains are Gaussian variables for $q \ll 1$. This implies that also the k -averaged ICFs $d_L(\mathbf{q}, c)$ and $d_G(\mathbf{q}, c)$ must also be Gaussian and this with a variance given by the number of *independent* contributions k . The horizontal lines thus correspond to the empirical standard deviation if the relaxation times $\tau_L(q)$ and $\tau_G(q)$ for the corresponding longitudinal and transverse relaxation modes are smaller than $\delta\tau$. One expects that the relaxation times strongly increase in the hydrodynamic limit with increasing wavelength and the contributions k to the ICFs $d_L(\mathbf{q}, c)$ and $d_G(\mathbf{q}, c)$ must thus become increasingly correlated. As will be shown in Sec. VF, the longitudinal and transverse relaxation processes are characterized in the continuum limit by the relaxation times

$$\tau_L(q) \simeq \zeta/q^2(\lambda + 2\mu) \quad \text{and} \quad \tau_G(q) \simeq \zeta/q^2\mu \quad (75)$$

diverging quadratically with the probed wavelength. ($\zeta \approx 750$ will be determined in Sec. VF.) This explains the strong power law decay with apparent exponent -2 indicated by dot-dashed lines. As suggested by Eq. (75), the small- q data should thus collapse by rescaling the horizontal axis as $q \rightarrow q/q_L$ and $q \rightarrow q/q_G$ for, respectively, the longitudinal and transverse variances with

$$q_L^2 \equiv \frac{\zeta}{(\lambda + 2\mu)\Delta\tau} \quad \text{and} \quad q_G^2 \equiv \frac{\zeta}{\mu\Delta\tau}. \quad (76)$$

The expected scaling is confirmed in panel (b) of Fig. 8.

More importantly, deviations from the plateau for uncorrelated frames (horizontal lines) are also seen for large wavenumbers $q \gg 1$. Since we know already from Fig. 7 that non-Gaussianity becomes relevant in this limit, this is not unexpected. This last regime must in fact become more striking if numerical data were available with both larger N_k and $\delta\tau \gg \tau_{L,G}(q)$ making the first two N_k - and $\delta\tau$ -dependent regimes decay more rapidly. This can be also seen by simply subtracting the trivial limit $1/(N_k - 1)$ from the measured variances as shown in panel (c) of Fig. 8. This subtraction makes manifest the strong increase of the reduced variances with increasing q . The solid line indicates an empirical power law.

3. c -averaged q -variance of ICFs

That non-Gaussian and anisotropic behavior are related in the large- q limit may be better understood from the second type of variances indicated by the open sym-

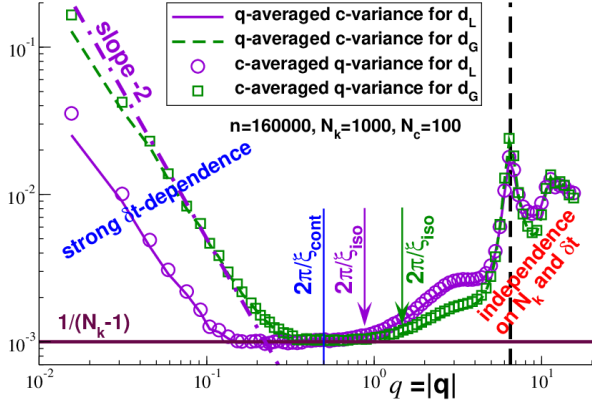


FIG. 9: Comparison of two types of variances for the longitudinal and transverse ICFs $d_L(\mathbf{q}, c)$ and $d_G(\mathbf{q}, c)$ for pLJ particles with $n = 160000$, $N_k = 1000$ and $\delta\tau = 1000$. The thin solid and dashed lines represent the finally $\hat{\mathbf{q}}$ -averaged c -variances, the open symbols the fluctuations with \mathbf{q} for a given q -bin being finally c -averaged. Similar non-monotonic behavior is obtained for both properties.

bols in Fig. 9. We sample here

$$\left\langle \langle d(\mathbf{q}, c)^2 \rangle_{\hat{\mathbf{q}}} - \langle d(\mathbf{q}, c) \rangle_{\hat{\mathbf{q}}}^2 \right\rangle_c, \quad (77)$$

i.e. the (empirical) variances of the rescaled ICFs $d_L(\mathbf{q}, c)$ and $d_G(\mathbf{q}, c)$ are computed for all \mathbf{q} in a given q -bin in a first step which is followed by a final c -average. As can be seen, the data are very similar to the $\hat{\mathbf{q}}$ -averaged c -variances discussed above. Importantly, this shows that the deviations from $1/N_k$ seen for $q \gg 1$ are due to anisotropic correlations. Such anisotropic behavior is, of course, expected due to the packing of the particles. Consistently, the data become rapidly N_k - and $\delta\tau$ -independent in this q -limit. As shown by the vertical arrows we may use the observed deviations from the bold horizontal line to estimate ξ_{iso} . The anisotropic effects are apparently slightly different for longitudinal and transverse correlations, rising faster in the former case.

4. q -variance of c -averaged ICFs

As already emphasized above, one expects that anisotropic effects become irrelevant for the variance

$$\langle d(\mathbf{q})^2 \rangle_{\hat{\mathbf{q}}} - \langle d(\mathbf{q}) \rangle_{\hat{\mathbf{q}}}^2 \text{ with } d(\mathbf{q}) = \langle d(\mathbf{q}, c) \rangle_c \quad (78)$$

being the first c -averaged ICFs for each wavevector \mathbf{q} . This point is made in Fig. 10. To get rid of the dynamical effect in the small- q limit we divide these variances by the $\hat{\mathbf{q}}$ -averaged c -variances shown by the thin solid and dashed lines in Fig. 10. Since all c are by construction independent this ratio must decay a $1/(N_c - 1)$. This is confirmed in Fig. 10 for data obtained for two N_c by rescaling the vertical axis by $N_c - 1$. Interestingly, the anisotropic behavior for $q \gg 1$ remains visible for the

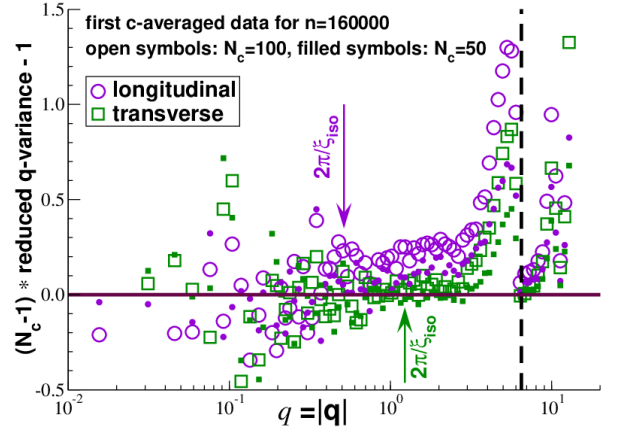


FIG. 10: Reduced dimensionless q -variances of c -averaged ICFs $d_L(\mathbf{q})$ and $d_G(\mathbf{q})$ for pLJ systems. Data collapse for $N_c = 100$ (open symbols) and $N_c = 50$ (filled symbols) is observed upon multiplying the vertical axis with $N_c - 1$. Estimations of ξ_{iso} for both ICFs are indicated by arrows.

rescaled data (albeit with more scatter since a very small signal has been amplified). This can be used to cross-check the values of ξ_{iso} for the two ICFs (vertical arrows).

V. TIME-DEPENDENT CORRELATIONS

A. Introduction

We present finally applications of the mathematical formalism for ITFs focusing on the time-dependent GFs and CFs of the displacement and strain fields. We formulate first in Sec. VB the Boltzmann linear superposition relations for the first-order displacement and force density TFs. We show then in Sec. VC how the GFs and CFs of displacement fields are related to the two longitudinal and transverse material functions $L(q, t)$ and $G(q, t)$. The corresponding relations for strain GFs and CFs are formulated and numerically tested in the subsequent subsections. We use here $g_L(q, s)$ and $g_G(q, s)$ for the two relevant invariants of the fourth-order GFs and $c_L(q, s)$ and $c_G(q, s)$ for the corresponding ICFs.

B. Boltzmann superposition relations

Boltzmann superposition relations are generally formulated in terms of second-order stress and strain fields being linearly related by means of fourth-order TFs [1, 8, 15]. Using the convolution relations Eq. (A12) and Eq. (A19) these relations are best stated in Fourier-Laplace space, e.g., the stress increment $\sigma_{\alpha\beta}(\mathbf{q}, t)$ caused by a strain $\varepsilon_{\alpha\beta}(\mathbf{q}, t)$ may be compactly written as [15]

$$\sigma_{\alpha\beta}(\mathbf{q}, s) = E_{\alpha\beta\gamma\delta}(\mathbf{q}, s)\varepsilon_{\gamma\delta}(\mathbf{q}, s) \quad (79)$$

with $E_{\alpha\beta\gamma\delta}(\mathbf{q}, s)$ being the generalized elasticity TF characterizing the viscoelastic material properties. It is as-

sumed here that the stress and strain increments both vanish in the time domain for $t < 0$. We denote by

$$L(q, s) \equiv E_{1111}^{\circ}(\mathbf{q}, s) \text{ and } G(q, s) \equiv E_{1212}^{\circ}(\mathbf{q}, s) \quad (80)$$

the only two invariants in NRC of $E_{\alpha\beta\gamma\delta}(\mathbf{q}, s)$ relevant in the present work. We need in Sec. VC the corresponding relation for the displacement fields caused by a force density. We demonstrate here that

$$u_{\alpha}(\mathbf{q}, s) = q^{-2} K_{\alpha\beta}(\mathbf{q}, s) g_{\beta}(\mathbf{q}, s) \quad (81)$$

with $K_{\alpha\beta}(\mathbf{q}, s) = \mathcal{L}[K_{\alpha\beta}(\mathbf{q}, t)]$ being the s -dependent generalization of the static creep compliance $K_{\alpha\beta}(\mathbf{q}, s = 0)$ introduced above in Sec. IV C 1. Using that the second-order ICFs $E_{\alpha\beta}(\mathbf{q}, s)$ and $K_{\alpha\beta}(\mathbf{q}, s)$ are defined to be inverse with respect to each other, i.e.

$$E_{\alpha\gamma}(\mathbf{q}, s) K_{\gamma\beta}(\mathbf{q}, s) = \delta_{\alpha\beta}, \quad (82)$$

we get by tracing Eq. (81) with $E_{\alpha\beta}(\mathbf{q}, s)$ the corresponding Boltzmann superposition relation

$$g_{\alpha}(\mathbf{q}, s) = q^2 E_{\alpha\beta}(\mathbf{q}, s) u_{\beta}(\mathbf{q}, s) \quad (83)$$

expressing the force TF by the displacement TF. Both relations are equivalent as may be seen by tracing the latter relation with $K_{\alpha\beta}(\mathbf{q}, s)$. Interestingly, Eq. (83) can be directly obtained from the more familiar stress-strain relation Eq. (79) if we define $E_{\alpha\beta}(\mathbf{q}, s)$ as the contraction

$$E_{\alpha\beta}(\mathbf{q}, s) \equiv \mathcal{O}^{2-}[E_{\alpha\beta\gamma\delta}(\mathbf{q}, s)]. \quad (84)$$

Let us also remind that the displacement and strain fields are related by Eq. (40) and that the force density field is given by the contraction

$$g_{\alpha}(\mathbf{q}, s) \equiv -iq_{\beta} \sigma_{\alpha\beta}(\mathbf{q}, s) \quad (85)$$

of the stress field. Applying the linear operator \mathcal{O}^{2-} to Eq. (79) then yields Eq. (83) and thus in turn Eq. (81). Using finally Eq. (10) and Eq. (12) the invariants of $E_{\alpha\beta}(\mathbf{q}, s)$ and $K_{\alpha\beta}(\mathbf{q}, s)$ are thus given in NRC by

$$\begin{aligned} k_{\text{L}}^{\text{E}}(q, s) &= 1/k_{\text{L}}^{\text{K}}(q, s) = L(q, s) \text{ and} \\ k_{\text{N}}^{\text{E}}(q, s) &= 1/k_{\text{N}}^{\text{K}}(q, s) = G(q, s) \end{aligned} \quad (86)$$

with the superscript indicating the respective ITF.

C. Invariants of CFs of displacement fields

Let us consider an isotropic elastic body at equilibrium for $t < 0$ perturbed by an external force density $g_{\alpha}^{\text{ex}}(\mathbf{q}, t) = g_{\alpha}^{\text{ex}}(\mathbf{q})H(t)$ being switched on at $t = 0$ and kept constant for all $t \geq 0$. Within linear response this will generate a time-dependent displacement field

$$u_{\alpha}(\mathbf{q}, t) = \mathbf{G}_{\alpha\beta}(\mathbf{q}, t) g_{\beta}^{\text{ex}}(\mathbf{q}) H(t). \quad (87)$$

$\mathbf{G}_{\alpha\beta}(\mathbf{q}, t)$ must be a second-order ITF for $q\xi_{\text{iso}} \ll 1$ characterized by two invariants $k_{\text{L}}(q, t)$ and $k_{\text{N}}(q, t)$ in NRC.

We show here that these invariants are given by the two material functions $L(q, s)$ and $G(q, s)$ defined by Eq. (80).

Let us first emphasize that there is a profound difference between applied macroscopic ($\mathbf{q} = \mathbf{0}$) and microscopic (finite \mathbf{q}) forces. While in the former case the total inner force $g_{\alpha}(t) = g_{\alpha}^{\text{ex}}(t)$ is imposed and under direct experimental control, this is different for the inner force density $g_{\alpha}(\mathbf{q}, t)$ at finite \mathbf{q} due to the internal degrees of freedom of the system. These allow the system to respond by means of generated forces. For an overdamped fluid the external force density is simply diminished by the frictional force generated by the internal motion, i.e. the effective inner force density driving the system is

$$g_{\alpha}(\mathbf{q}, t) = g_{\alpha}^{\text{ex}}(\mathbf{q}) + g_{\alpha}^{\text{f}}(\mathbf{q}, t) \text{ with} \quad (88)$$

$$g_{\alpha}^{\text{f}}(\mathbf{q}, t) = -\zeta v_{\alpha}(\mathbf{q}, t) \quad (89)$$

and $v_{\alpha}(\mathbf{q}, t)$ being the velocity field in reciprocal space. The friction is caused by the motion generated at $t > 0$ [41]. (For momentum conserving dynamics ζ must be replaced by $\rho \frac{d}{dt}$ with ρ being the mass density [15].) Using that $v_{\alpha}(q, s) = s u_{\alpha}(\mathbf{q}, s)$ we may rewrite the generated force density in Fourier-Laplace space as

$$g_{\alpha}^{\text{f}}(\mathbf{q}, s) = -\frac{q^2}{w(q, s)} u_{\alpha}(\mathbf{q}, s) \text{ with } w(q, s) \equiv \frac{q^2}{\zeta s} \quad (90)$$

standing for a convenient scalar. As a next step we insert now Eq. (88) and Eq. (90) into the Boltzmann relation Eq. (81). This leads to the recursion relation

$$\begin{aligned} u_{\alpha}(\mathbf{q}, s) &= q^{-2} K_{\alpha\beta}(\mathbf{q}, s) g_{\beta}^{\text{ex}}(\mathbf{q}) \\ &\quad - w(q, s)^{-1} K_{\alpha\beta}(\mathbf{q}, s) u_{\beta}(\mathbf{q}, s) \end{aligned} \quad (91)$$

for the displacement field. To obtain the invariants $k_{\text{L}}(q, s)$ and $k_{\text{N}}(q, s)$ one compares the invariants of Eq. (87) and Eq. (91) in NRC. Using Eq. (86) we get

$$\begin{aligned} q^2 k_{\text{L}}(q, s) &= \frac{w(q, s)}{1 + w(q, s)L(q, s)} \text{ and} \\ q^2 k_{\text{N}}(q, s) &= \frac{w(q, s)}{1 + w(q, s)G(q, s)}. \end{aligned} \quad (92)$$

Interestingly, instead of Eq. (91) we could have also analyzed in NRC the equivalent recursion relation

$$\begin{aligned} \mathbf{G}_{\alpha\beta}(\mathbf{q}, s) &= q^{-2} K_{\alpha\beta}(\mathbf{q}, s) \\ &\quad - w(q, s)^{-1} K_{\alpha\gamma}(\mathbf{q}, s) \mathbf{G}_{\gamma\beta}(\mathbf{q}, s) \end{aligned} \quad (93)$$

entirely written in terms of linear ITF operators. (Note that the latter relation reduces to Eq. (91) upon contracting with $g_{\beta}^{\text{ex}}(\mathbf{q}, s)$.) This leads in NRC to

$$k_{\text{L}} = \frac{1}{q^2 L} - \frac{k_{\text{L}}}{wL} \text{ and } k_{\text{N}} = \frac{1}{q^2 G} - \frac{k_{\text{N}}}{wG}$$

(all arguments omitted) which is equivalent (all functions and arguments assumed to be finite) to Eq. (92). We use then in a final step Eq. (34) to relate the GFs via

$$\mathbf{G}_{\alpha\beta}(\mathbf{q}, t) = \beta V [c_{\alpha\beta}(\mathbf{q}, t = 0) - c_{\alpha\beta}(\mathbf{q}, t)] \quad (94)$$

to the time-dependent displacement CFs $c_{\alpha\beta}(\mathbf{q}, t)$ defined by Eq. (23). Using Eq. (92) one readily obtains the ICFs in Fourier-Laplace for $c_{\alpha\beta}(\mathbf{q}, t)$. We shall state this below for the essentially equivalent strain CFs.

D. Corresponding invariants for strain fields

The linear strain increment $\varepsilon_{\alpha\beta}(\mathbf{q}, t)$ in reciprocal space caused by a weak constant external stress $\sigma_{\alpha\beta}^{\text{ex}}(\mathbf{q})$ applied at $t = 0$ is given by

$$\varepsilon_{\alpha\beta}(\mathbf{q}, t) = \mathbf{G}_{\alpha\beta\gamma\delta}(\mathbf{q}, t)\sigma_{\gamma\delta}^{\text{ex}}(\mathbf{q})H(t) \text{ with} \quad (95)$$

$$\mathbf{G}_{\alpha\beta\gamma\delta}(\mathbf{q}, t) = q^2 \mathcal{O}^{2+}[\mathbf{G}_{\alpha\beta}(\mathbf{q}, t)] \quad (96)$$

being the outer product of the displacement GFs $\mathbf{G}_{\alpha\beta}(\mathbf{q}, t)$ discussed in the preceding paragraph. To show this we have used Eq. (87) and Eq. (40) and that the imposed external force density is a contraction

$$g_{\alpha}^{\text{ex}}(\mathbf{q}, s) \equiv -iq_{\beta}\sigma_{\alpha\beta}^{\text{ex}}(\mathbf{q}, s) \quad (97)$$

of the externally imposed stress $\sigma_{\alpha\beta}^{\text{ex}}(\mathbf{q})$. Using Eq. (8) the only two finite invariants of $\mathbf{G}_{\alpha\beta\gamma\delta}(\mathbf{q}, s)$ are thus

$$\begin{aligned} g_{\text{L}}(q, s) &= q^2 k_{\text{L}}(q, s) = \frac{w(q, s)}{1 + w(q, s)L(q, s)} \text{ and} \\ 4g_{\text{G}}(q, s) &= q^2 k_{\text{N}}(q, s) = \frac{w(q, s)}{1 + w(q, s)G(q, s)} \end{aligned} \quad (98)$$

with $k_{\text{L}}(q, s)$ and $k_{\text{N}}(q, s)$ being given by Eq. (92). While for large s (small t) both $g_{\text{L}}(q, s)$ and $g_{\text{G}}(q, s)$ vanish, i.e. the GFs of the strain TF are continuous at $t = 0$, they naturally approach for small s (large t)

$$g_{\text{L}}(q, s) \rightarrow \frac{1}{L(q)} \text{ and } 4g_{\text{L}}(q, s) \rightarrow \frac{1}{G(q)} \quad (99)$$

with $L(q, s) \rightarrow L(q)$ and $G(q, s) \rightarrow G(q)$ for $s \rightarrow 0$.

According to the FDT relation Eq. (34) the strain GFs derived above are related to the time-dependent CFs of instantaneous strain TFs by

$$\mathbf{G}_{\alpha\beta\gamma\delta}(\mathbf{q}, t) = \beta V [c_{\alpha\beta\gamma\delta}(\mathbf{q}, t = 0) - c_{\alpha\beta\gamma\delta}(\mathbf{q}, t)]. \quad (100)$$

This leads in Fourier-Laplace space to

$$\beta V c_{\alpha\beta\gamma\delta}(\mathbf{q}, s) = \beta V c_{\alpha\beta\gamma\delta}(\mathbf{q}, t = 0) - \mathbf{G}_{\alpha\beta\gamma\delta}(\mathbf{q}, s). \quad (101)$$

Consistently with Eq. (57) and Eq. (98) the invariants $c_{\text{L}}(q, s)$ and $c_{\text{G}}(q, s)$ of the fourth-order CF TF thus are

$$\begin{aligned} \beta V c_{\text{L}}(q, s) &= \frac{1}{L(q)} - \frac{w(q, s)}{1 + w(q, s)L(q, s)} \text{ and} \\ \beta V 4c_{\text{G}}(q, s) &= \frac{1}{G(q)} - \frac{w(q, s)}{1 + w(q, s)G(q, s)}. \end{aligned} \quad (102)$$

The special limit for $s \rightarrow \infty$ ($t \rightarrow 0$) has already been considered in Sec. IV C 1. In the opposite small- s (large- t) limit $w(q, s)$ becomes very large and thus cancels out and both ICFs thus vanish as expected.

E. Large-time limit

The leading corrections for the small- s (large- t) limit can be readily obtained supposing that $L(q, s) \simeq L(q)$ and $G(q, s) \simeq G(q)$, i.e. the time-dependence of the material function is *assumed* to be negligible. It is convenient to introduce by

$$\tau_{\text{L}}(q) = \zeta/q^2 L(q) \text{ and } \tau_{\text{G}}(q) = \zeta/q^2 G(q) \quad (103)$$

two time scales characterizing the overdamped strain relaxation under the above ansatz. This definition reduces in the continuum limit to Eq. (75). It follows then from Eq. (102) that

$$\begin{aligned} \beta V c_{\text{L}}(q, s) &\simeq \frac{1}{L(q)} \frac{s}{s + 1/\tau_{\text{L}}(q)} \text{ and} \\ \beta V 4c_{\text{G}}(q, s) &\simeq \frac{1}{G(q)} \frac{s}{s + 1/\tau_{\text{G}}(q)} \end{aligned} \quad (104)$$

for $s \rightarrow 0$. Using Eq. (A16) an exponential decay

$$\begin{aligned} L(q)\beta V c_{\text{L}}(q, t) &\simeq \exp(-t/\tau_{\text{L}}(q)) \text{ and} \\ G(q)\beta V 4c_{\text{G}}(q, t) &\simeq \exp(-t/\tau_{\text{G}}(q)) \end{aligned} \quad (105)$$

is obtained for large t as expected for overdamped motion. Instead of the standard time-dependent CFs we shall investigate below the CFs of the t -averaged strain fields as defined in Sec. III D, i.e. we switch from a Green-Kubo representation to an Einstein representation. Using Eq. (30) the above results can be reformulated as

$$\begin{aligned} L(q)\beta V \bar{c}_{\text{L}}(q, \Delta\tau) &\simeq D(\Delta\tau/\tau_{\text{L}}(q)) \text{ and} \\ G(q)\beta V 4\bar{c}_{\text{G}}(q, \Delta\tau) &\simeq D(\Delta\tau/\tau_{\text{G}}(q)) \end{aligned} \quad (106)$$

with $\bar{c}_{\text{L}}(q, \Delta\tau)$ and $\bar{c}_{\text{G}}(q, \Delta\tau)$ being the ICFs of the CFs of the t -averaged strain, cf. Eq. (28), and $D(x)$ denoting Debye's function, cf. Eq. (30). We have assumed above that the material functions can be assumed to be time-independent. This approximation is sufficient for the continuum limit considered below. As shown in Appendix E more care is needed in general.

F. Simulation results

Using our pLJ model system we have computed the ICFs $\bar{c}_{\text{L}}(q)$ and $\bar{c}_{\text{G}}(q)$ for t -averaged longitudinal and transverse strain fields in NRC. Results obtained for $\beta V \bar{c}_{\text{L}}(q, \Delta\tau)$ are plotted in Fig. 11 as a function of q for different preaveraging times $\Delta\tau$ and for two system sizes. Panel (a) focuses on data for $q \leq 1$ obtained for $n = 160000$ and $\Delta\tau_{\text{max}} = 10^6$, panel (b) on the large- q and large- $\Delta\tau$ behavior for the smaller systems with $n = 10000$ and $\Delta\tau_{\text{max}} = 10^7$. Since the total time series is used to construct the displacement/strain fields (cf. Sec. IV B) the t -averaged strain fields trivially vanish for $\Delta\tau \rightarrow \Delta\tau_{\text{max}}$ and therefore the corresponding CFs. Only data with $\Delta\tau \ll \Delta\tau_{\text{max}}$ is thus useful. Note that

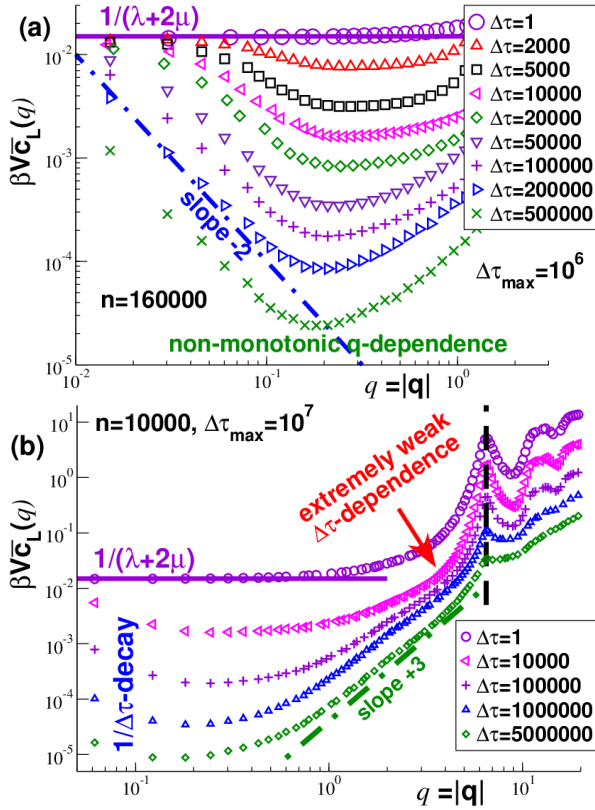


FIG. 11: Longitudinal ICF $\beta V \bar{c}_L(q, \Delta\tau)$ for pLJ systems for a broad range of preaveraging times $\Delta\tau \ll \Delta\tau_{\max}$: (a) $n = 160000$ with $\Delta\tau_{\max} = 10^6$ focusing on $q \leq 1$ showing that $\beta V \bar{c}_L(q, \Delta\tau) \rightarrow 1/L(q)$ for $\Delta\tau \rightarrow 1$ and that all data decay systematically with increasing $\Delta\tau$ for all q but are non-monotonic for constant $\Delta\tau$ with respect to q . (b) $n = 10000$ for $\Delta\tau_{\max} = 10^7$ focusing on large $\Delta\tau$ and q demonstrating a strong increase with q (dashed-dotted line) and a weak dependency on $\Delta\tau$ especially for q slightly below the maximum of the structure factor (dashed vertical line).

data for $\Delta\tau = 1$ (circles) corresponds to the CF of the instantaneous longitudinal strain already shown in Fig. 4 and used for the determination of the static longitudinal modulus $L(q)$. From this upper limit the ICFs are seen to monotonically decrease with $\Delta\tau$ and this for all q . As can be better seen from panel (a), the data are *strongly non-monotonic* with respect to q decreasing first in the continuum limit to a minimum roughly located at $q \approx 2\pi/\xi_{\text{cont}}$ (shifting to lower q with increasing $\Delta\tau$).

The $1/q^2$ -decay seen in panel (a) of Fig. 11 (dash-dotted line) is expected in the continuum limit from Eq. (106) for reduced times $x = \Delta\tau/\tau_L(q) \gg 1$. Focusing on the data for $q \ll 1/\xi_{\text{cont}}$ and large $\Delta\tau$ we present in Fig. 12 a scaling plot suggested by Sec. VE and using $L(q) \simeq \lambda + 2\mu$. We focus again on the longitudinal ICFs computed for different $\Delta\tau$. Following the first relation given in Eq. (106) we plot $y = (\lambda + 2\mu)\beta V \bar{c}_L(q, \Delta\tau)$ as a function of the scaling variable $x = \Delta\tau/\tau_L(q) = (q/q_L(\Delta\tau))^2$ with the $\Delta\tau$ -dependent characteristic wavevector $q_L(\Delta\tau) = (\zeta/\Delta\tau(\lambda + 2\mu))^{1/2}$.

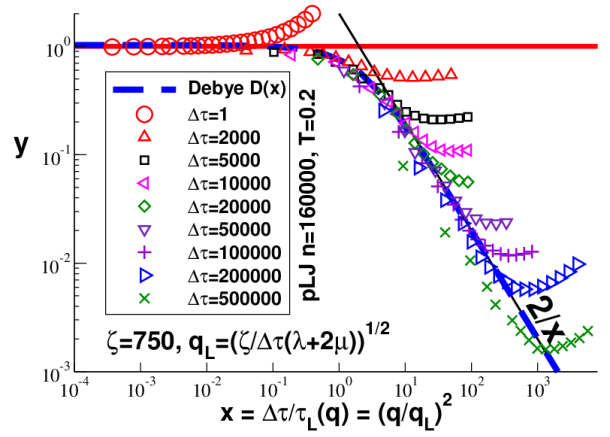


FIG. 12: Rescaled longitudinal ICF $y = (\lambda + 2\mu)\beta V \bar{c}_L(q, \Delta\tau)$ for $n = 160000$ as a function of $x = \Delta\tau/\tau_L(q) = (q/q_L(\Delta\tau))^2$ as suggested by Eq. (106) for sufficiently small q and large $\Delta\tau$. The bold dashed line indicates the Debye function $D(x)$, the thin solid line the asymptotic power law $D(x) \simeq 2/x$ for $x \gg 1$. The same friction constant $\zeta \approx 750$ is used for all $\Delta\tau$.

The bold dashed line indicates the Debye function $D(x)$, the thin solid line its large- x limit $D(x) \simeq 2/x$. Note that in the latter limit the ICFs asymptotically decay as $1/\Delta\tau q^2$. Since $\lambda \approx 38$ and $\mu \approx 14$ are known, there is only one fitting parameter, namely the effective friction coefficient $\zeta = 750$. This value was determined by horizontally shifting the data sets for $10^4 \leq \Delta\tau \leq 10^5$ onto the Debye function. Naturally, data for $q \gg 1/\xi_{\text{cont}}$ deviates from $D(x)$ as expected from the unscaled data in Fig. 11. Note also that the data for $\Delta\tau = 500000$ are slightly too small. This deviation can be explained from the fact that all data for $\Delta\tau \simeq \Delta\tau_{\max}$ must vanish due to the numerical construction of the strain field, cf. Eq. (37). Similar behavior has been observed for $\bar{c}_G(q, \Delta\tau)$ using the *same* friction coefficient (not shown).

We note finally that it is unfortunately not possible for our pLJ systems to determine the terminal relaxation times for $q \gg 1/\xi_{\text{cont}}$ since we are unable to reach the final $1/\Delta\tau$ -decay of the ICFs for the available $\Delta\tau_{\max}$. This can be better seen from the data presented in panel (b) of Fig. 11 for $n = 10000$ and $\Delta\tau_{\max} = 10^7$ MSD. As emphasized by the arrow, much larger production times $\Delta\tau_{\max}$ are warranted to get $\tau_{L,G}(q)$. More details on the large- q strain relaxation are given in Appendix E.

VI. CONCLUSION

We have addressed in the presented work various aspects of ITFs relevant for isotropic and achiral condensed matter systems, focusing especially on CFs of strain TFs in amorphous solids. Several predictions and numerical procedures have been illustrated using computational results obtained by means of a pLJ particle model in $d = 2$. We have emphasized that

- a generic mathematical structure in terms of a finite number of invariants is expected,
- theoretical and numerical studies should focus on these invariants and this especially in reciprocal space where the results can be formulated in a d -independent manner,
- generic ITFs contain in general terms depending on the direction of the field vector, e.g., in reciprocal space on the components \hat{q}_α of the wavevector, and for this reason components of ITFs may superficially appear to be “anisotropic” (cf. Fig. 1),
- the generic structure is relevant for all q for properly c -averaged CFs (cf. Fig. 10),
- any true anisotropy of an individual independent configurations c should be characterized in terms of proper invariants (cf. Sec. II B and Sec. IV F).

We have given in Sec. II A a short summary of the most salient features needed for the description of ITFs reminded in more detail in Appendix B. Under the additional mild assumptions stated in Sec. II A, the most general fourth-order ITFs are given by *five* invariants, cf. Eq. (3). Using the transformation Eq. (4) one may reduce for $d = 2$ the number of independent invariants of fourth-order ITFs from five to four. This allows to simplify the general results for $d \geq 2$ for two-dimensional systems. We emphasized the advantages to analyze ITFs using NRC by means of an alternative set of equivalent invariants, cf. Eq. (6). Using the general formalism of ITFs it is shown in Appendix C for $d = 2$ and $d = 3$ how the invariants in real space may be obtained from those in reciprocal space.

We have investigated in Sec. IV static correlations of displacement and strain fields in linear elastic bodies taking also advantage of well-known relations from statistical physics, cf. Eq. (45) [1]. The static elastic moduli $L(q)$ and $G(q)$ of the pLJ particle system used in this study have been determined and we argued, cf. Fig. 4 and Fig. 9, that the three length scales ξ_{cont} , ξ_{iso} and ξ_{hom} are of the same order. We have explicitly checked in Sec. IV E for our pLJ glasses that the strain components in NRC are complex circularly-symmetric Gaussian variables. This holds especially for $q < 1$ while small deviations are visible for larger q , cf. Fig. 7. As we have seen in Sec. IV F, it is possible by k -averaging instantaneous strain ICFs to project out strong predominately Gaussian fluctuations for each configuration c and to obtain thus a better characterization of the anisotropic behavior which becomes relevant above $q \approx 1$. Moreover, in the latter limit the number of independent modes was found to decrease as shown by the increase of the two types of empirical variances presented in Fig. 9.

Assuming overdamped dynamics we have derived in Sec. V the general relations between the time-dependent CFs of displacement and strain fields with the material functions $L(q, t)$ and $G(q, t)$ being two invariants in NRC

of the fourth-order elasticity TF $E_{\alpha\beta\gamma\delta}(\mathbf{q}, t)$. Obviously, Eq. (102) can be read in two directions: One may either use the known or assumed material functions to obtain the CFs or, as shown in Ref. [16], one may obtain the material functions from the measured CFs being fitted by a generalized Maxwell model. By analyzing the ICFs $\bar{c}_L(q)$ and $\bar{c}_G(q)$ of t -averaged strain fields in NRC for a broad range of preaveraging times $\Delta\tau$ we have confirmed that the terminal relaxation times decay as $\tau_{L,G}(q) \propto 1/q^2$ for our overdamped systems in the continuum limit (cf. Fig. 12). The determination of $\tau_{L,G}(q)$ was unfortunately not possible beyond the continuum limit due to the strong slowing-down shown in the second panel of Fig. 11. Additional details on this limit are given in Appendix E.

We have illustrated various theoretical aspects by means of numerical results obtained for an extremely simplified coarse-grained computer model of structural colloidal glasses using pLJ particles in strictly *two* dimensions and sampled using an overdamped MC dynamics. Note that the arguments presented in Sec. V can readily be reformulated for momentum-conserving MD simulations. One merely has to replace the friction coefficient ζ by ρs with ρ being the mass density. The scalar $w(q, s)$, defined by Eq. (90), then becomes $w(q, s) = q^2/\rho s^2$ consistently with related recent studies for the stress CFs [15, 16]. Moreover, the choice of $d = 2$ was largely due to historical reasons but also because for a particle number $n \ll 10^6$ larger linear system sizes $L \propto n^{1/d}$ can be simulated and thus smaller wavenumbers q sampled than for $d = 3$. This allowed us to probe the continuum limit as shown by Fig. 4. Since our theoretical results are relevant for Euclidean spaces of arbitrary d , this suggests the use of the presented methodology focusing on ICFs in NRC also for more realistic three-dimensional systems. Our work makes predictions for strain CFs and associated RFs for many experimental systems, e.g., we predict long-range correlations for instantaneous strain TFs decaying as $1/r^d$ in any viscoelastic system with a broad intermediate elastic plateau regime. Such strong viscoelastic hydrodynamic effects should thus also be relevant, e.g., for three-dimensional bulks of entangled polymer melts for times below the reptation time [8].

Acknowledgments. We are indebted to A.N. Semenov (Strasbourg) and H. Xu (Metz) for helpful discussions.

Data availability statement. Data sets are available from the corresponding author on reasonable request.

Appendix A: Useful general transformations

We investigate in this work tensors depending on time t and TFs depending additionally on the spatial position \mathbf{r} . Due to the various convolution and correlation relations it is useful to move to Fourier space with \mathbf{q} being the wavevector and to Laplace space with s being the Laplace variable. We define the “Fourier transformation” (FT) $f(\mathbf{q}) = \mathcal{F}[f(\mathbf{r})]$ and the “Laplace transformation” (LT)

$f(s) = \mathcal{L}[f(t)]$ such that the original functions and their transformations have the *same* units. This may make it easier to dimensionally check the relations. For notational simplicity the function names remain unchanged by the transform. Which space is meant is indicated by the argument. Some well-known properties of these transformations are summarized here for convenience.

1. Fourier transformations

We consider real-valued functions $f(\mathbf{r})$ of a d -dimensional spatial “position vector” \mathbf{r} . Following Refs. [16–18] we define the FT from “real space” (variable \mathbf{r}) to “reciprocal space” (variable \mathbf{q}) by

$$f(\mathbf{q}) \equiv \frac{1}{V} \int d\mathbf{r} f(\mathbf{r}) \exp(-i\mathbf{q} \cdot \mathbf{r}) \quad (\text{A1})$$

with V being the d -dimensional volume of the system [42, 43]. The inverse FT is then given by

$$f(\mathbf{r}) = \mathcal{F}^{-1}[f(\mathbf{q})] = \frac{V}{(2\pi)^d} \int d\mathbf{q} f(\mathbf{q}) \exp(i\mathbf{q} \cdot \mathbf{r}). \quad (\text{A2})$$

We note the FTs

$$\partial_\alpha f(\mathbf{r}) \stackrel{\mathcal{F}}{\Leftrightarrow} i q_\alpha f(\mathbf{q}), \quad (\text{A3})$$

$$1 \stackrel{\mathcal{F}}{\Leftrightarrow} \frac{(2\pi)^d}{V} \delta(\mathbf{q}) \text{ and} \quad (\text{A4})$$

$$V \delta(\mathbf{r}) \stackrel{\mathcal{F}}{\Leftrightarrow} 1 \quad (\text{A5})$$

with $\partial_\alpha \equiv \partial/\partial r_\alpha$ for the partial derivative in the α -direction in real space and $\delta(\mathbf{r})$ being Dirac’s delta function [42]. It follows from Eq. (A3) and Eq. (A5) that

$$\partial_\alpha V \delta(\mathbf{r}) \stackrel{\mathcal{F}}{\Leftrightarrow} i q_\alpha. \quad (\text{A6})$$

Using $\mathcal{F}[f(\mathbf{r} - \mathbf{v})] = f(\mathbf{q}) \exp(-i\mathbf{q} \cdot \mathbf{v})$ for a constant vector \mathbf{v} we have

$$V \delta(\mathbf{r} - \mathbf{v}) \stackrel{\mathcal{F}}{\Leftrightarrow} \exp[-i\mathbf{q} \cdot \mathbf{v}]. \quad (\text{A7})$$

This implies consistently with Eq. (A6) for a “dipole distribution” of Dirac functions that

$$V \mathcal{F}[\delta(\mathbf{r} + \mathbf{v}/2) - \delta(\mathbf{r} - \mathbf{v}/2)] \simeq i\mathbf{q} \cdot \mathbf{v} \text{ for } |\mathbf{q} \cdot \mathbf{v}| \ll 1. \quad (\text{A8})$$

Let us next consider the “correlation function” (CF)

$$c(\mathbf{r}) = \frac{1}{V} \int d\mathbf{r}' g(\mathbf{r} + \mathbf{r}') h(\mathbf{r}') \quad (\text{A9})$$

with real-valued fields $g(\mathbf{r})$ and $h(\mathbf{r})$. According to the “correlation theorem” [32] we get in reciprocal space

$$c(\mathbf{q}) = \mathcal{F}[c(\mathbf{r})] = g(\mathbf{q}) h(-\mathbf{q}) \quad (\text{A10})$$

with $g(\mathbf{q}) = \mathcal{F}[g(\mathbf{r})]$, $h(\mathbf{q}) = \mathcal{F}[h(\mathbf{r})]$. For “auto-correlation functions” (ACFs), i.e. for $g(\mathbf{r}) = h(\mathbf{r})$, this simplifies to (“Wiener-Khinchin theorem”)

$$c(\mathbf{q}) = g(\mathbf{q}) g(-\mathbf{q}) = |g(\mathbf{q})|^2. \quad (\text{A11})$$

The Fourier transformed ACFs are thus real and ≥ 0 for all \mathbf{q} . Moreover, all CFs $c(\mathbf{r})$, Eq. (A9), considered in this work are even in real space, $c(\mathbf{r}) = c(-\mathbf{r})$, and thus also in reciprocal space, $c(\mathbf{q}) = c(-\mathbf{q})$. Any CF $c(\mathbf{q})$ considered in this work is thus a real function. We remind finally that according to the “convolution theorem” of FTs [32, 42]

$$\frac{1}{V} \int d\mathbf{r}' g(\mathbf{r} - \mathbf{r}') h(\mathbf{r}') \stackrel{\mathcal{F}}{\Leftrightarrow} g(\mathbf{q}) h(\mathbf{q}). \quad (\text{A12})$$

2. Laplace-Carson transformations

Following Refs. [16–18] we use the “Laplace-Carson transform” [44]

$$f(s) = \mathcal{L}[f(t)] = s \lim_{\epsilon \rightarrow 0} \int_{t=-\epsilon}^{\infty} dt f(t) \exp(-st). \quad (\text{A13})$$

Due the prefactor s the original function $f(t)$ and its transform $f(s)$ have the same dimension. We note the useful transforms [45]

$$aH(t) \stackrel{\mathcal{L}}{\Leftrightarrow} a \quad (\text{A14})$$

$$a\delta(t) \stackrel{\mathcal{L}}{\Leftrightarrow} as \text{ and} \quad (\text{A15})$$

$$\exp(-t/\tau) \stackrel{\mathcal{L}}{\Leftrightarrow} \frac{s}{s + 1/\tau} \quad (\text{A16})$$

with a and τ being some finite constants, $H(t)$ the Heaviside function (unit step) and $\delta(t) = \dot{H}(t)$ Dirac’s delta function [45]. Following Newton a dot marks a derivative with respect to time. We also consider functions $f(t) = f_{\text{sing}}(t) + f_{\text{reg}}(t)$ being the sum of a (cusp or impulsive) singularity $f_{\text{sing}}(t)$ and a regular (smooth) function $f_{\text{reg}}(t)$. For instance, we may apply a step function $f_{\text{sing}}(t) = aH(t)$ at $t = 0$. Using Eq. (A15) the LT of the time-derivative $\dot{f}(t)$ then becomes

$$\mathcal{L}[\dot{f}(t)] = s(a + f_{\text{reg}}(s) - f_{\text{reg}}(t = 0^+)). \quad (\text{A17})$$

Let us finally also remind the LTs for the integrals

$$\int_0^t f(t') dt' \stackrel{\mathcal{L}}{\Leftrightarrow} f(s)/s \text{ and} \quad (\text{A18})$$

$$\int_0^t g(t-t') h(t') dt' \stackrel{\mathcal{L}}{\Leftrightarrow} \frac{g(s)h(s)}{s} \quad (\text{A19})$$

and the initial and final value theorems

$$\lim_{s \rightarrow \infty} f(s) = \lim_{t \rightarrow 0} f(t) \text{ and } \lim_{s \rightarrow 0} f(s) = \lim_{t \rightarrow \infty} f(t) \quad (\text{A20})$$

for reasonably behaved functions relating, respectively, the large- s limit to the small- t limit and the small- s limit to the large- t limit [46].

Appendix B: More on isotropic tensor fields

1. Assumed symmetries

All second-order TFs considered in this work are defined to be symmetric,

$$T_{\alpha\beta}(\mathbf{q}) = T_{\beta\alpha}(\mathbf{q}), \quad (\text{B1})$$

and the standard major and minor index symmetries [21] for fourth-order TFs are *assumed* to hold, i.e.

$$T_{\alpha\beta\gamma\delta}(\mathbf{q}) = T_{\gamma\delta\alpha\beta}(\mathbf{q}) = T_{\beta\alpha\gamma\delta}(\mathbf{q}) = T_{\alpha\beta\delta\gamma}(\mathbf{q}). \quad (\text{B2})$$

Most importantly, it is assumed that the TFs are *isotropic*, i.e. the isotropy condition [17, 20]

$$T_{\alpha_1 \dots \alpha_o}^*(\mathbf{q}) = T_{\alpha_1 \dots \alpha_o}(\mathbf{q}^*) \quad (\text{B3})$$

holds for *any* orthogonal transformation of the coordinate system. Please note that the fields on the left hand side are evaluated with the original coordinates while the fields on the right hand are evaluated with the transformed coordinates, i.e. the left hand fields are computed at the original vector $\mathbf{q} = (q_1, \dots, q_d)$ while the right hand fields are computed at the “actively transformed” vector $\mathbf{q}^* = (q_1^*, \dots, q_d^*)$. We remind that isotropy, Eq. (B3), necessarily implies homogeneity as seen by proof by contradiction [20]. We thus do not need to assume homogeneity explicitly. This work focuses on *achiral* systems with complete “mirror symmetry” down to molecular level. As already pointed out in Sec. A 1, CFs thus must be *even*. We thus assume

$$T_{\alpha\beta}(\mathbf{q}) = T_{\alpha\beta}(-\mathbf{q}) \text{ and } T_{\alpha\beta\gamma\delta}(\mathbf{q}) = T_{\alpha\beta\gamma\delta}(-\mathbf{q}). \quad (\text{B4})$$

for TFs of even order corresponding to CFs.

2. Macroscopic isotropic tensors

It is important to distinguish “macroscopic tensors” $T_{\alpha\beta\dots}$ (without argument [46]) and the more general TFs $T_{\alpha\beta\dots}(\mathbf{q})$. (TFs may reduce to macroscopic tensors for $\mathbf{q} \rightarrow \mathbf{0}$ assuming this limit to exist.) For tensors the general isotropy condition Eq. (B3) becomes

$$T_{\alpha_1 \dots \alpha_o}^* = T_{\alpha_1 \dots \alpha_o}, \quad (\text{B5})$$

i.e. all tensor components are unchanged under any orthogonal transform. Macroscopic isotropic tensors of different order are discussed, e.g., in Sec. 2.5.6 of Ref. [21]. With k_1 , i_1 and i_2 being invariant scalars we have

$$T_\alpha = 0, \quad (\text{B6})$$

$$T_{\alpha\beta} = k_1 \delta_{\alpha\beta}, \quad (\text{B7})$$

$$T_{\alpha\beta\gamma} = 0 \text{ and } \quad (\text{B8})$$

$$T_{\alpha\beta\gamma\delta} = i_1 \delta_{\alpha\beta} \delta_{\gamma\delta} + i_2 (\delta_{\alpha\gamma} \delta_{\beta\delta} + \delta_{\alpha\delta} \delta_{\beta\gamma}) \quad (\text{B9})$$

with $\delta_{\alpha\beta}$ denoting the Kronecker symbol. Please note that all symmetries stated in Sec. B 1 hold. This implies that only *two* coefficients are needed for a fourth-order isotropic tensor. Importantly,

$$T_{12} = T_{1112} = T_{1222} = T_{1234} = T_{1344} = 0 \quad (\text{B10})$$

and also all components of tensors of odd order do vanish, cf. Eq. (B6) and Eq. (B8). These are consequences of a general property of macroscopic isotropic tensors [17]: the sign of tensor components change for a reflection of one axis if the number of indices equal to the inverted axis is *odd*. Consistency with Eq. (B5) implies then that

$$\text{components of macroscopic isotropic tensors} \\ \text{with an odd number of equal indices vanish.} \quad (\text{B11})$$

As emphasized below (cf. Sec. B 4 b and Sec. B 5), this is different for the more general ITFs.

3. Constructing isotropic tensor fields

Let us consider the TF $\mathbf{C}(\mathbf{q}) = \mathbf{A}(\mathbf{q}) \otimes \mathbf{B}(\mathbf{q})$ being the product of two ITFs $\mathbf{A}(\mathbf{q})$ and $\mathbf{B}(\mathbf{q})$ and \otimes standing either for an outer product, e.g. $C_{\alpha\beta\gamma\delta}(\mathbf{q}) = A_{\alpha\beta}(\mathbf{q})B_{\gamma\delta}(\mathbf{q})$, or an inner product, e.g. $C_{\alpha\beta\gamma\delta}(\mathbf{q}) = A_{\alpha\beta\gamma\nu}(\mathbf{q})B_{\nu\delta}(\mathbf{q})$. Hence,

$$\begin{aligned} \mathbf{C}^*(\mathbf{q}) &= (\mathbf{A}(\mathbf{q}) \otimes \mathbf{B}(\mathbf{q}))^* = \mathbf{A}^*(\mathbf{q}) \otimes \mathbf{B}^*(\mathbf{q}) \\ &= \mathbf{A}(\mathbf{q}^*) \otimes \mathbf{B}(\mathbf{q}^*) = \mathbf{C}(\mathbf{q}^*) \end{aligned} \quad (\text{B12})$$

using in the second step a general property of TF products and in the third step Eq. (B3) for $\mathbf{A}(\mathbf{q})$ and $\mathbf{B}(\mathbf{q})$ where \mathbf{q}^* stands for the “actively” transformed field position. We have thus demonstrated that $\mathbf{C}(\mathbf{q})$ is also an ITF (“product theorem for ITFs”). Similarly, one can show that the sum of two ITFs must also be an ITF (“addition theorem for ITFs”).

The above relation Eq. (B12) can also be used to state a “quotient theorem for ITFs” similar to the well-known general quotient theorem for TFs [19]: If $\mathbf{C}(\mathbf{q})$ and, say, $\mathbf{A}(\mathbf{q})$ are known to be ITFs, Eq. (B12) implies under mild and obvious conditions that $\mathbf{B}(\mathbf{q})$ must also be an ITF. Similarly, $C(\mathbf{q}) = A(\mathbf{q}) + B(\mathbf{q})$ for ITFs $C(\mathbf{q})$ and $A(\mathbf{q})$ implies that $B(\mathbf{q})$ must also be an ITF.

We note that the Kronecker symbol $\delta_{\alpha\beta}$ [20] and also each component q_α of the field vector are isotropic according to Eq. (B3), i.e. $(\delta_{\alpha\beta})^* = \delta_{\alpha\beta}$ and $(q_\alpha)^* = q_\alpha^*$. The above theorems allow quite generally the construction of ITFs from known ITFs. For instance, assuming $l(q)$, $k(q)$, $j(q)$ and $i(q)$ to be scalar invariants any product of these terms, e.g.,

$$l(q)q_\alpha, k(q)q_\alpha q_\beta, j(q)q_\alpha \delta_{\beta\gamma} \text{ or } i(q)q_\alpha q_\beta q_\gamma q_\delta, \quad (\text{B13})$$

must be an ITF and the same applies to sums of such terms. Albeit being legitimate ITFs, such sums may thus depend on the direction of the wavevector \mathbf{q} and on the orientation of the coordinate system.

4. Generic structure of isotropic tensor fields

a. General isotropic tensor fields

Let us state the most general ITFs for $1 \leq o \leq 4$ and any dimension $d > 1$ compatible with the assumed symmetries (cf. Appendix B 1). With $l_n(q)$, $k_n(q)$, $j_n(q)$ and $i_n(q)$ being invariant scalar functions we have

$$T_\alpha(\mathbf{q}) = l_1(q) q_\alpha, \quad (\text{B14})$$

$$T_{\alpha\beta}(\mathbf{q}) = k_1(q) \delta_{\alpha\beta} + k_2(q) q_\alpha q_\beta, \quad (\text{B15})$$

$$T_{\alpha\beta\gamma}(\mathbf{q}) = j_1(q) q_\alpha \delta_{\beta\gamma} + j_2(q) q_\beta \delta_{\alpha\gamma} + j_3(q) q_\gamma \delta_{\alpha\beta} + j_4(q) q_\alpha q_\beta q_\gamma, \quad (\text{B16})$$

$$T_{\alpha\beta\gamma\delta}(\mathbf{q}) = i_1(q) \delta_{\alpha\beta} \delta_{\gamma\delta} + i_2(q) (\delta_{\alpha\gamma} \delta_{\beta\delta} + \delta_{\alpha\delta} \delta_{\beta\gamma}) + i_3(q) (q_\alpha q_\beta \delta_{\gamma\delta} + q_\gamma q_\delta \delta_{\alpha\beta}) + i_4(q) q_\alpha q_\beta q_\gamma q_\delta + i_5(q) (q_\alpha q_\gamma \delta_{\beta\delta} + q_\alpha q_\delta \delta_{\beta\gamma} + q_\beta q_\gamma \delta_{\alpha\delta} + q_\beta q_\delta \delta_{\alpha\gamma}) \quad (\text{B17})$$

with $q_\alpha \equiv \mathbf{q} \cdot \mathbf{e}_\alpha$. One way to obtain these results is to construct ITFs using all possible ‘‘multilinear forms’’ [20, 21] of order o for additive terms of scalars of inner and triple products [20] and to eliminate then in a second step all terms not compatible with the additional symmetries formulated in Appendix B 1 [17]. See Refs. [11, 17, 20, 47] for details. We only check here that the stated relations are reasonable:

- all relations reduce (continuously) for $\mathbf{q} \rightarrow \mathbf{0}$ to the isotropic tensors stated in Appendix B 2;
- all relations are ITFs according to Eq. (B3) and are, more specifically, characterized by additive terms of the generic form Eq. (B13);
- all symmetries stated in Appendix B 1 for the second- and fourth-order TFs are satisfied;
- all ITFs of even (odd) order are even (odd) with respect to \mathbf{q} . Hence, ITFs of odd order vanish for $\mathbf{q} \rightarrow \mathbf{0}$ consistently with Appendix B 2.

b. Finite components with odd number of equal indices

We have noted in Appendix B 2 that all components of isotropic tensors with an odd number of equal indices do vanish. Apparently, this does not hold for ITFs since ITFs of odd order may be finite, cf. Eq. (B14) or Eq. (B16). The reader may also verify that while the isotropic tensor component $T_{1112} = 0$ vanishes the component $T_{1112}(\mathbf{q})$ is finite in general. The reason for this is that the condition Eq. (B3) for ITFs is less restrictive than Eq. (B5). As shown in Ref. [17], there are fortunately convenient coordinates, called ‘‘Natural Rotated Coordinates’’ (NRC), where the nice symmetry

Eq. (B10) for isotropic tensors can be also used for TFs of even order. We return to this in Appendix B 5.

c. Reformulation for finite wavevectors

For dimensional reasons it is useful to rewrite for finite wavevectors ($\mathbf{q} \neq \mathbf{0}$) the above ITFs in terms of the components $\hat{q}_\alpha = \hat{\mathbf{q}} \cdot \mathbf{e}_\alpha$ of the normalized wavevector $\hat{\mathbf{q}}$. It is thus convenient to bring in factors of q and to redefine $l_1(q) \rightarrow l_1(q)/q$, $k_2(q) \rightarrow k_2(q)/q^2$, $j_1(q) \rightarrow j_1(q)/q$, $j_2(q) \rightarrow j_2(q)/q$, $j_3(q) \rightarrow j_3(q)/q$, $j_4(q) \rightarrow j_4(q)/q^3$, $i_3(q) \rightarrow i_3(q)/q^2$, $i_4(q) \rightarrow i_4(q)/q^4$ and $i_5(q) \rightarrow i_5(q)/q^2$. We thus obtain, e.g.,

$$T_{\alpha\beta}(\mathbf{q}) = k_1(q) \delta_{\alpha\beta} + k_2(q) \hat{q}_\alpha \hat{q}_\beta \quad (\text{B18})$$

$$T_{\alpha\beta\gamma\delta}(\mathbf{q}) = i_1(q) \delta_{\alpha\beta} \delta_{\gamma\delta} + i_2(q) (\delta_{\alpha\gamma} \delta_{\beta\delta} + \delta_{\alpha\delta} \delta_{\beta\gamma}) + i_3(q) (\hat{q}_\alpha \hat{q}_\beta \delta_{\gamma\delta} + \hat{q}_\gamma \hat{q}_\delta \delta_{\alpha\beta}) + i_4(q) \hat{q}_\alpha \hat{q}_\beta \hat{q}_\gamma \hat{q}_\delta + i_5(q) (\hat{q}_\alpha \hat{q}_\gamma \delta_{\beta\delta} + \hat{q}_\alpha \hat{q}_\delta \delta_{\beta\gamma} + \hat{q}_\beta \hat{q}_\gamma \delta_{\alpha\delta} + \hat{q}_\beta \hat{q}_\delta \delta_{\alpha\gamma}) \quad (\text{B19})$$

for the second- and fourth-order ITFs. Now *all* invariants of each ITF of order o have the *same* physical units.

d. Full index permutation symmetry

We shall occasionally find useful to demand for third- and fourth-order ITFs that they remain invariant for any permutation of the indices, i.e.

$$T_{\alpha\beta\gamma}(\mathbf{q}) = T_{\beta\gamma\alpha}(\mathbf{q}) = T_{\gamma\alpha\beta}(\mathbf{q}) = \dots \quad \text{and} \quad (\text{B20})$$

$$T_{\alpha\beta\gamma\delta}(\mathbf{q}) = T_{\beta\gamma\delta\alpha}(\mathbf{q}) = T_{\alpha\gamma\beta\delta}(\mathbf{q}) = \dots \quad (\text{B21})$$

in addition to the major and minor index symmetry already stated in Eq. (B2). In this case we have

$$j_1(q) = j_2(q) = j_3(q) \quad \text{and} \quad (\text{B22})$$

$$i_1(q) = i_2(q) \quad \text{and} \quad i_3(q) = i_5(q), \quad (\text{B23})$$

i.e. only two invariants remain for third-order ITFs and only three for the fourth-order ITFs.

e. Fourth-order ITFs for two-dimensional fields

For two-dimensional systems it is possible and useful to rewrite Eq. (B19) more compactly in terms of the first four invariants $i_1(q)$, $i_2(q)$, $i_3(q)$ and $i_4(q)$. One way to see this is to rewrite the last parenthesis of Eq. (B19) as

$$\begin{aligned} \hat{q}_\alpha \hat{q}_\gamma \delta_{\beta\delta} + \hat{q}_\alpha \hat{q}_\delta \delta_{\beta\gamma} + \dots &= -2 [\delta_{\alpha\beta} \delta_{\gamma\delta}] \\ &+ [\delta_{\alpha\gamma} \delta_{\beta\delta} + \delta_{\alpha\delta} \delta_{\beta\gamma}] \\ &+ 2 [\hat{q}_\alpha \hat{q}_\beta \delta_{\gamma\delta} + \hat{q}_\gamma \hat{q}_\delta \delta_{\alpha\beta}] \end{aligned} \quad (\text{B24})$$

as may be verified using that $\hat{q}_1^2 + \hat{q}_2^2 = 1$ in $d = 2$ and comparing all possible cases for $(\alpha, \beta, \gamma, \delta)$, e.g., $(1, 1, 1, 1)$, $(2, 2, 2, 2)$, $(1, 1, 2, 2)$, $(1, 2, 1, 2)$ or $(1, 1, 2, 2)$. Hence, if one has obtained by means of a numerical or theoretical argument a representation of fourth-order ITFs with a finite value for the invariant $i_5(q)$, this result may be rewritten by means of the transformation Eq. (4) given in Sec. II A in terms of only four finite invariants.

5. NRC for two-dimensional systems

That *four* invariants for fourth-order ITFs are sufficient in $d = 2$ can also be seen using NRC. Following Refs. [15, 17, 18] let us rotate the coordinate system such that the 1-axis points into the direction of \mathbf{q} , i.e.

$$q_\alpha^\circ = q\delta_{1\alpha} \text{ with } q = |\mathbf{q}|. \quad (\text{B25})$$

We mark coordinates in NRC by “ \circ ”. Let us define

$$\begin{aligned} k_L(q) &\equiv T_{11}^\circ(\mathbf{q}), i_L(q) \equiv T_{1111}^\circ(\mathbf{q}), \\ k_N(q) &\equiv T_{22}^\circ(\mathbf{q}), i_N(q) \equiv T_{2222}^\circ(\mathbf{q}), \\ i_M(q) &\equiv T_{1122}^\circ(\mathbf{q}) \text{ and} \\ i_G(q) &\equiv T_{1212}^\circ(\mathbf{q}) \end{aligned} \quad (\text{B26})$$

for second- and fourth-order ITFs in NRC. Since the system is isotropic these functions depend on the scalar q but not on $\hat{\mathbf{q}}$. In other words, they are *invariant* under rotation and they do not change either if one of the coordinate axes is inverted. $k_L(q)$ and $i_L(q)$ are called “longitudinal invariants”, $k_N(q)$ and $i_N(q)$ “normal invariants”, $i_M(q)$ “mixed invariant” and $i_G(q)$ “transverse” (or “shear”) invariant. All other components $T_{\alpha\beta}^\circ(\mathbf{q})$ and $T_{\alpha\beta\gamma\delta}^\circ(\mathbf{q})$ are either by Eq. (B1) or Eq. (B2) identical to these invariants or must vanish for an *odd number of equal indices*, as demonstrated in Ref. [17], behaving thus in NRC as isotropic tensors, cf. Eq. (B10). The $2^d = 4$ components of $T_{\alpha\beta}^\circ(\mathbf{q})$ in $d = 2$ are thus completely determined by the *two* invariants $k_L(q)$ and $k_N(q)$ and the $4^d = 16$ components $T_{\alpha\beta\gamma\delta}^\circ(\mathbf{q})$ by the *four* invariants $i_L(q)$, $i_G(q)$, $i_M(q)$ and $i_N(q)$. These functions (marked by capital indices) thus provide an alternative set of invariants.

The fields $T_{\alpha\beta}(\mathbf{q})$ and $T_{\alpha\beta\gamma\delta}(\mathbf{q})$ in the original frame may then be obtained by an inverse rotation. Both sets of invariants are thus related by

$$\begin{aligned} k_L(q) &= k_1(q) + k_2(q), k_N(q) = k_1(q), \\ i_L(q) &= i_1(q) + 2i_2(q) + 2i_3(q) + i_4(q), \\ i_G(q) &= i_2(q), \\ i_M(q) &= i_1(q) + i_3(q) \text{ and} \\ i_N(q) &= i_1(q) + 2i_2(q). \end{aligned} \quad (\text{B27})$$

This is equivalent to the inverse relations

$$\begin{aligned} k_1(q) &= k_N(q), k_2(q) = k_L(q) - k_N(q), \\ i_1(q) &= i_N(q) - 2i_G(q), \\ i_2(q) &= i_G(q), \\ i_3(q) &= i_M(q) - i_N(q) + 2i_G(q), \\ i_4(q) &= i_L(q) + i_N(q) - 2i_M(q) - 4i_G(q) \text{ and} \\ i_5(q) &= 0. \end{aligned} \quad (\text{B28})$$

The last line stresses the “compact representation” for invariants of fourth-order ITF in $d = 2$.

6. NRC in general dimensions

We can extend the above identification of the two sets of invariants for two-dimensional systems to higher dimensions. Let us first consider $d = 3$. As above we turn the 1-axis into the direction of the wavevector \mathbf{q} . This rotation is, of course, now not unique. However, any rotation around \mathbf{q} is equivalent due to isotropy. This implies, e.g., that $T_{2222}^\circ(\mathbf{q}) = T_{3333}^\circ(\mathbf{q})$ or $T_{1122}^\circ(\mathbf{q}) = T_{1133}^\circ(\mathbf{q})$. We use again the same invariants as in Eq. (B26). While the two invariants $k_L(q)$ and $k_N(q)$ for second-order ITFs are sufficient for $d = 3$, the four invariants $i_L(q)$, $i_G(q)$, $i_M(q)$ and $i_N(q)$ for fourth-order ITFs must be supplemented by *one* additional invariant. Hence, either

$$i_P(q) \equiv T_{2233}^\circ(\mathbf{q}) \text{ or } i_T(q) \equiv T_{2323}^\circ(\mathbf{q}). \quad (\text{B29})$$

Both functions are clearly also invariants; since only five invariants $i_n(q)$ are needed for Eq. (B19), both cannot be *independent*. In any case, as in $d = 2$ this completely determines $T_{\alpha\beta}^\circ(\mathbf{q})$ and $T_{\alpha\beta\gamma\delta}^\circ(\mathbf{q})$ and we may rotate back to the original coordinate frame. If we choose, without restricting the generality of the argument, a wavevector $\mathbf{q} = \mathbf{e}_1$, one obtains for the invariants of the fourth-order ITF, cf. Eq. (B19), that Eq. (6) stated in Sec. II A holds. Upon inversion this implies

$$\begin{aligned} i_1(q) &= i_P(q), \\ i_2(q) &= i_T(q) = (i_N(q) - i_P(q))/2, \\ i_3(q) &= i_M(q) - i_P(q), \\ i_4(q) &= i_L(q) + i_N(q) - 2i_M(q) - 4i_G(q) \text{ and} \\ i_5(q) &= i_G(q) - (i_N(q) - i_P(q))/2 = i_G(q) - i_T(q). \end{aligned} \quad (\text{B30})$$

The above five invariants (in either ordinary coordinates or NRC) are in fact also sufficient for higher dimensions d since by symmetry

$$\begin{aligned} k_N(q) &= T_{22}^\circ(\mathbf{q}) = \dots = T_{dd}^\circ(\mathbf{q}), \\ i_G(q) &= T_{1212}^\circ(\mathbf{q}) = \dots = T_{1d1d}^\circ(\mathbf{q}), \\ i_M(q) &= T_{1122}^\circ(\mathbf{q}) = \dots = T_{11dd}^\circ(\mathbf{q}), \\ i_N(q) &= T_{2222}^\circ(\mathbf{q}) = \dots = T_{dddd}^\circ(\mathbf{q}), \\ i_P(q) &= T_{2233}^\circ(\mathbf{q}) = T_{2244}^\circ(\mathbf{q}) = T_{3344}^\circ(\mathbf{q}) = \dots \text{ and} \\ i_T(q) &= T_{2323}^\circ(\mathbf{q}) = T_{2424}^\circ(\mathbf{q}) = T_{3535}^\circ(\mathbf{q}) = \dots \end{aligned} \quad (\text{B31})$$

where in any case $i_T(q) = (i_N(q) - i_P(q))/2$ must hold.

7. Invariants of outer products

As already noted in Sec. B 3, by taking outer products of ITFs one may construct ITFs of higher order. One minor technical difficulty is that we assumed for the generic ITFs in Sec. B 4 the index symmetries stated in Sec. B 1. The standard procedure is to sum properly *symmetrized* outer products. The invariants of the new ITFs are then given by those of the “generator fields”. We consider as an example the fourth-order TF

$$T_{\alpha\beta\gamma\delta}(\mathbf{q}) = \frac{1}{4} [\hat{q}_\alpha \hat{q}_\delta T_{\beta\gamma}(\mathbf{q}) + \hat{q}_\alpha \hat{q}_\gamma T_{\beta\delta}(\mathbf{q}) + \hat{q}_\beta \hat{q}_\delta T_{\alpha\gamma}(\mathbf{q}) + \hat{q}_\beta \hat{q}_\gamma T_{\alpha\delta}(\mathbf{q})] \quad (\text{B32})$$

constructed using the normalized components \hat{q}_α of the field vector and a second-order generator field $T_{\alpha\beta}(\mathbf{q})$. We often use the compact notation \mathcal{O}^{2+} for the linear operator which produces according to Eq. (B32) a fourth-order TF starting from a symmetric second-order generator TF. By construction $T_{\alpha\beta\gamma\delta}(\mathbf{q})$ has the same dimension as $T_{\alpha\beta}(\mathbf{q})$, it is also achiral and the major and minor index symmetries hold, cf. Eq. (B2). Concerning the *a priori* five invariants $i_n(q)$ of $T_{\alpha\beta\gamma\delta}(\mathbf{q})$ in ordinary coordinates one verifies that

$$\begin{aligned} i_1(q) &= i_2(q) = i_3(q) = 0 \text{ while} \\ i_4(q) &= k_2(q) \text{ and } i_5(q) = k_1(q)/4 \end{aligned} \quad (\text{B33})$$

may be finite. Using Eq. (6) this corresponds in NRC to the invariants

$$\begin{aligned} i_L(q) &= k_L(q) \text{ and } i_G(q) = k_N(q)/4 \text{ while} \\ i_M(q) &= i_N(q) = i_P(q) = i_T(q) = 0. \end{aligned} \quad (\text{B34})$$

Let us consider the component

$$T_{1212}(\mathbf{q}) = i_4(q) \hat{q}_1^2 \hat{q}_2^2 + i_5(q) (\hat{q}_1^2 + \hat{q}_2^2). \quad (\text{B35})$$

Focusing on the 12-plane for $\hat{q}_3 = 0$ and using the polar angle θ with $\hat{q}_1 = \cos(\theta)$ and $\hat{q}_2 = \sin(\theta)$ this may be rewritten as

$$T_{1212}(\mathbf{q}) = \frac{k_1(q)}{4} + \frac{k_2(q)}{8} - \frac{k_2(q)}{8} \cos(4\theta). \quad (\text{B36})$$

We thus obtain again an octupolar pattern as in Fig. 1.

8. Various inner products

a. Introduction

It follows also from the product theorem, cf. Eq. (B12), that ITFs may be obtained by contracting ITFs of higher order by taking inner products with a second isotropic tensor or ITF. Such contractions are useful for the calculation of FTs of TFs presented in Sec. C 3. An inner product of experimental relevance is the linear response

of a system due to an applied small and localized perturbation characterized in reciprocal space by a constant tensor (cf. Sec. B 8 c). This “source” tensor may be either *isotropic* (cf. Sec. B 8 d) or *anisotropic* (cf. Sec. B 8 e). We discuss finally two important cases of contracting ITFs with components of the wavevector (cf. Sec. B 8 f).

b. Contraction with Kronecker tensor

The contraction of a TF by summing over a pair of equal indices, say $T_{\alpha\beta\gamma\gamma}(\mathbf{q})$ for the fourth-order TF $T_{\alpha\beta\gamma\delta}(\mathbf{q})$, is equivalent, of course, to the inner product $T_{\alpha\beta\gamma\delta}(\mathbf{q})\delta_{\gamma\delta}$ of the TF with the Kronecker tensor. Using that $\delta_{\gamma\gamma} = d$ and $\hat{q}_\gamma^2 = 1$ yields the second-order ITF

$$\begin{aligned} T_{\alpha\beta}(\mathbf{q}) &\equiv T_{\alpha\beta\gamma\gamma}(\mathbf{q}) = k_1(q)\delta_{\alpha\beta} + k_2(q)\hat{q}_\alpha\hat{q}_\beta \\ \text{with } k_1(q) &= d i_1(q) + 2i_2(q) + i_3(q) \text{ and} \\ k_2(q) &= d i_3(q) + i_4(q) + 4i_5(q) \end{aligned} \quad (\text{B37})$$

in terms of the invariants $i_n(q)$ of the fourth-order ITF. We note for later convenience [48] that tracing additionally over the first index pair yields finally the scalar

$$\begin{aligned} s(q) &\equiv T_{\alpha\alpha\gamma\gamma}(\mathbf{q}) = d k_1(q) + k_2(q) \\ &= d^2 i_1(q) + 2d i_2(q) + 2d i_3(q) + i_4(q) + 4i_5(q). \end{aligned} \quad (\text{B38})$$

c. Contraction with a general constant tensor

Let us consider the inner product of an ITF (cf. Sec. B 4) with an arbitrary symmetric but not necessarily isotropic tensor. This case is important since a constant tensor in reciprocal space corresponds according to Eq. (A5) to an extremely localized SF in real space. We thus investigate the inner products

$$R_\alpha(\mathbf{q}) = \mathbf{G}_{\alpha\beta}(\mathbf{q})\tilde{S}_\beta \text{ and } R_{\alpha\beta}(\mathbf{q}) = \mathbf{G}_{\alpha\beta\gamma\delta}(\mathbf{q})\tilde{S}_{\gamma\delta} \quad (\text{B39})$$

where the GFs $\mathbf{G}_{\alpha\beta}(\mathbf{q})$ and $\mathbf{G}_{\alpha\beta\gamma\delta}(\mathbf{q})$ are ITFs. As emphasized elsewhere [15, 17, 18], the summation over repeated indices must be properly carried out. It is useful to diagonalize the second-order source tensor $\tilde{S}_{\alpha\beta}$ and to formulate the linear response in the corresponding eigenvector system. The RFs are then given by the sum

$$R_{\alpha\beta}(\mathbf{q}) = \mathbf{G}_{\alpha\beta 11}(\mathbf{q})\tilde{s}_1 + \dots + \mathbf{G}_{\alpha\beta dd}(\mathbf{q})\tilde{s}_d \quad (\text{B40})$$

with $\tilde{s}_1, \dots, \tilde{s}_d$ being the eigenvalues of the source tensor.

d. Isotropic constant source tensor

We assume now that not only the GFs but also the constant source terms are isotropic. Interestingly, following Eq. (B6) $\tilde{S}_\alpha = 0$ and, hence, $R_\alpha(\mathbf{q})$ must rigorously vanish while the second-order RF $R_{\alpha\beta}(\mathbf{q})$ is, of course, in general finite. Being isotropic it reads

$$R_{\alpha\beta}(\mathbf{q}) = k_1(q)\delta_{\alpha\beta} + k_2(q)\hat{q}_\alpha\hat{q}_\beta. \quad (\text{B41})$$

Using Eq. (B37) the two invariants may be written

$$\begin{aligned} k_1(q) &= [d i_1(q) + 2i_2(q) + i_3(q)]\tilde{s} \text{ and} \\ k_2(q) &= [d i_3(q) + i_4(q) + 4i_5(q)]\tilde{s} \end{aligned} \quad (\text{B42})$$

in terms of the invariants $i_n(q)$ of the GFs and the only invariant \tilde{s} of the source $\tilde{S}_{\alpha\beta} = \tilde{s}\delta_{\alpha\beta}$. As already emphasized elsewhere [17, 18], the ITF $R_{\alpha\beta}(\mathbf{q})$ depends for finite $k_2(q)$ on the wavevector components \hat{q}_α . Interestingly, the angular dependences of the GF and the RF are in general different. As may be seen from Eq. (B41), $R_{12}(\mathbf{q}) = k_2(q)\hat{q}_1\hat{q}_2$ while

$$\mathbf{G}_{1212}(\mathbf{q}) = i_2(q) + i_4(q)\hat{q}_1^2\hat{q}_2^2 + i_5(q)[\hat{q}_1^2 + \hat{q}_2^2] \quad (\text{B43})$$

according to Eq. (B19). We get in the (1, 2)-plane

$$R_{12}(\mathbf{q}) \propto \sin(2\theta) \quad (\text{B44})$$

while $\mathbf{G}_{1212}(\mathbf{q})$ is given by a q -dependent scalar plus a term proportional to $\cos(4\theta)$, i.e. the RF is *quadrupolar* while the GF is *octupolar* [24].

e. Anisotropic constant source tensor

In many physical situations, even for perfectly isotropic systems, the source is *not* isotropic. This may happen especially if the source for the perturbation is generated not by an external perturbation but by an intrinsic instantaneous fluctuation of the system, leading, e.g., to local plastic reorganizations of an elastic body. Let us focus on the second-order response $R_{\alpha\beta}(\mathbf{q})$. Albeit Eq. (B43) does not hold anymore we may still compute the field using Eq. (B40). Let us following the ‘‘shear-transformation-zone’’ model by Picard *et al.* [26] assume that only the eigenvalues \tilde{s}_1 and \tilde{s}_2 of $\tilde{S}_{\alpha\beta}$ are finite and, moreover, given by $\tilde{s}_1 = -\tilde{s}_2$. Hence,

$$R_{\alpha\beta}(\mathbf{q}) = \tilde{s}_1 [G_{\alpha\beta 11}(\mathbf{q}) - G_{\alpha\beta 22}(\mathbf{q})] \quad (\text{B45})$$

with $\mathbf{G}_{\alpha\beta\gamma\delta}(\mathbf{q})$ being given by Eq. (B19). Specifically, this implies $R_{12}(\mathbf{q}) \propto \hat{q}_1^3\hat{q}_2 - \hat{q}_1\hat{q}_2^3$ in any spatial dimension. We thus get in the 12-plane an octupolar field,

$$R_{12}(\mathbf{q}) \propto \sin(4\theta), \quad (\text{B46})$$

just as $G_{1212}(\mathbf{q}) \propto \cos(4\theta)$ but turned by a finite angle.

f. Contraction with \hat{q}_α

As mentioned in Appendix B 8 d, the vectorial response $R_\alpha(\mathbf{q})$ must vanish if $S_\alpha(\mathbf{q})$ is both isotropic and \mathbf{q} -independent. An observed finite RF indicates that the applied SF is either not (perfectly) isotropic or not (sufficiently) \mathbf{q} -independent. The latter case applies if the SF is due to identical dipolar distributions

$$S_\alpha(\mathbf{r}) = \partial_\alpha[\tilde{s}\mathcal{V}\delta(\mathbf{r})] \stackrel{\mathcal{F}}{\Leftrightarrow} S_\alpha(\mathbf{q}) = \tilde{s}iq_\alpha \quad (\text{B47})$$

in all directions α with \tilde{s} being a constant. Using Eq. (A6) and Eq. (A12) the RF is given by

$$R_\alpha(\mathbf{q}) = i\tilde{s}q_\beta\mathbf{G}_{\alpha\beta}(\mathbf{q}) = l_1(q)\hat{q}_\alpha \quad (\text{B48})$$

where in the final step the general identity Eq. (B14) for first-order ITFs was used. Using that $\mathbf{G}_{\alpha\beta}(\mathbf{q}) = k_1(q)\delta_{\alpha\beta} + k_2(q)\hat{q}_\alpha\hat{q}_\beta$ we get $l_1(q) = i\tilde{s}qk_L(q)$ for the invariant of the first-order ITF.

A second example of an inner product with \hat{q}_α leading to a lower order ITF is given by a second-order TF

$$T_{\alpha\beta}(\mathbf{q}) \equiv \hat{q}_\gamma\hat{q}_\delta T_{\alpha\gamma\beta\delta}(\mathbf{q}), \quad (\text{B49})$$

defined by taking twice the inner product of an ITF $T_{\alpha\beta\gamma\delta}(\mathbf{q})$ with \hat{q}_α . We use \mathcal{O}^{2-} for the linear operator turning according to Eq. (B49) a fourth-order ITF into a second-order ITF. Note that $T_{\alpha\beta}^\circ(\mathbf{q}) = T_{\alpha_1\beta_1}^\circ(\mathbf{q})$ implies

$$\begin{aligned} k_L(q) &\equiv T_{11}^\circ(\mathbf{q}) = T_{1111}^\circ(\mathbf{q}) \equiv i_L(q) \text{ and} \\ k_N(q) &\equiv T_{22}^\circ(\mathbf{q}) = T_{1212}^\circ(\mathbf{q}) \equiv i_G(q) \end{aligned} \quad (\text{B50})$$

for the invariants in NRC and using Eq. (B27)

$$k_1(q) = i_G(q) \text{ and } k_2(q) = i_L(q) - i_G(q) \quad (\text{B51})$$

for the invariants in ordinary coordinates.

Appendix C: Inverse Fourier Transformations

1. Introduction

We have formulated in Appendix II all properties in reciprocal space. Importantly, the FT of any ITF must also be an ITF, i.e.

$$T_{\alpha\dots}^*(\mathbf{r}) = T_{\alpha\dots}(\mathbf{r}^*) \stackrel{\mathcal{F}}{\Leftrightarrow} T_{\alpha\dots}^*(\mathbf{q}) = T_{\alpha\dots}(\mathbf{q}^*) \quad (\text{C1})$$

for the isotropy conditions in, respectively, real and in reciprocal space. (‘‘ \star ’’ marks again any orthogonal transformation), and ‘‘ $\alpha\dots$ ’’ stands for the full index list $\alpha_1\dots\alpha_o$.) This general relation holds due the linearity of the FT. If an ITF of a certain order and index symmetry is given in reciprocal space, the same holds in real space. Consistently with Eq. (C1), we state the corresponding ITFs in real space:

$$T_\alpha(\mathbf{r}) = \tilde{l}_1(r)\hat{r}_\alpha, \quad (\text{C2})$$

$$T_{\alpha\beta}(\mathbf{r}) = \tilde{k}_1(r)\delta_{\alpha\beta} + \tilde{k}_2(r)\hat{r}_\alpha\hat{r}_\beta, \quad (\text{C3})$$

$$\begin{aligned} T_{\alpha\beta\gamma}(\mathbf{r}) &= \tilde{j}_1(r)\hat{r}_\alpha\delta_{\beta\gamma} + \tilde{j}_2(r)\hat{r}_\beta\delta_{\alpha\gamma} \\ &+ \tilde{j}_3(r)\hat{r}_\gamma\delta_{\alpha\beta} + \tilde{j}_4(r)\hat{r}_\alpha\hat{r}_\beta\hat{r}_\gamma \text{ and} \end{aligned} \quad (\text{C4})$$

$$\begin{aligned} T_{\alpha\beta\gamma\delta}(\mathbf{r}) &= \tilde{i}_1(r)\delta_{\alpha\beta}\delta_{\gamma\delta} \\ &+ \tilde{i}_2(r)(\delta_{\alpha\gamma}\delta_{\beta\delta} + \delta_{\alpha\delta}\delta_{\beta\gamma}) \\ &+ \tilde{i}_3(r)(\hat{r}_\alpha\hat{r}_\beta\delta_{\gamma\delta} + \hat{r}_\gamma\hat{r}_\delta\delta_{\alpha\beta}) \\ &+ \tilde{i}_4(r)\hat{r}_\alpha\hat{r}_\beta\hat{r}_\gamma\hat{r}_\delta \\ &+ \tilde{i}_5(r)(\hat{r}_\alpha\hat{r}_\gamma\delta_{\beta\delta} + \hat{r}_\alpha\hat{r}_\delta\delta_{\beta\gamma} + \\ &\quad \hat{r}_\beta\hat{r}_\gamma\delta_{\alpha\delta} + \hat{r}_\beta\hat{r}_\delta\delta_{\alpha\gamma}) \end{aligned} \quad (\text{C5})$$

for $r > 0$. As for the ITFs in reciprocal space, the TF of order $o = 2$ is symmetric, the major and minor index symmetries hold for the TF of order $o = 4$ and TFs of even (odd) order are even (odd) with respect to $\mathbf{r} \leftrightarrow -\mathbf{r}$. We have used here a representation for $r > 0$ in terms of the components \hat{r}_α of the normalized vector $\hat{\mathbf{r}} = \mathbf{r}/r$ in real space. Using thus the same convenient reformulation as for the corresponding ITFs in reciprocal space, cf. Appendix B 4 c, all invariants for each ITF of order o have the same physical units. The components and the invariants of each TF in real and reciprocal space are, obviously, related by Eq. (13). The task is thus to get the invariants $\tilde{l}_n(r)$, $\tilde{k}_n(r)$, $\tilde{j}_n(r)$ and $\tilde{i}_n(r)$ in real space from the invariants $l_n(q)$, $k_n(q)$, $j_n(q)$ and $i_n(q)$ in reciprocal space and *visa versa*. We assume below for convenience that all invariants of a field of order o in reciprocal space are proportional to the *same* power law $s_\eta(q) = 1/Vq^\eta$ characterized by an exponent $\eta \geq 0$. We focus on the values $\eta = 0, 1$ and 2 . The calculation of the inverse FT is done in three steps:

- We first consider in Appendix C 2 the inverse FT of $f(\mathbf{q}) = s_\eta(q)Y(\hat{\mathbf{q}})$ with $Y(\hat{\mathbf{q}})$ being either a planar or a spherical harmonics. This yields $f(\mathbf{r}) = \tilde{f}(r)Y(\hat{\mathbf{r}})$ with the same function $Y(\cdot)$ as in reciprocal space and a scalar $\tilde{f}(r)$ depending on η .
- Using the known $\tilde{f}(r)$ we express \hat{q}_α , $\hat{q}_\alpha\hat{q}_\beta, \dots$ in terms of the $Y(\hat{\mathbf{q}})$ and, similarly \hat{r}_α , $\hat{r}_\alpha\hat{r}_\beta, \dots$ in terms of the $Y(\hat{\mathbf{r}})$. As shown in Appendix C 3, we thus obtain the inverse FT of all additive terms contributing to the generic ITFs in reciprocal space.
- We finally sum up in Appendix C 4 for all invariants in real space the different contributions stemming often from several invariants in reciprocal space.

2. Inverse FT of $f(\mathbf{q}) = f(q)Y(\hat{\mathbf{q}})$

a. Introduction

We determine here the inverse FT $f(\mathbf{r}) = \mathcal{F}^{-1}[f(\mathbf{q})]$ of the product $f(\mathbf{q}) = f(q)Y(\hat{\mathbf{q}})$ of a scalar function $f(q)$ and a function $Y(\hat{\mathbf{q}})$ depending only on the normalized direction $\hat{\mathbf{q}}$. In two dimensions $Y(\hat{\mathbf{q}}) = Y_l(\varphi_q)$ is given by the (non-normalized) “planar harmonics” $\cos(l\varphi_q)$ and $\sin(l\varphi_q)$ in terms of the polar angle φ_q and an integer l [17, 18]. In three dimensions we consider “spherical harmonics” $Y(\mathbf{q}) = Y_{lm}(\theta_q, \varphi_q)$ [32, 42, 49] in terms of the two polar angles θ_q and φ_q and the integers l and m with $-l \leq m \leq l$. The index q added to the angles indicates that the functions are taken in reciprocal space. Similarly, φ_r and θ_r indicate polar angles in real space. We show in Appendix C 2 b that

$$f(\mathbf{q}) = f(q)Y_l(\varphi_q) \xleftrightarrow{\mathcal{F}} f(\mathbf{r}) = \tilde{f}(r)Y_l(\varphi_r) \quad (\text{C6})$$

l	$d = 2$			$d = 3$		
	$\eta = 0$	$\eta = 1$	$\eta = 2$	$\eta = 0$	$\eta = 1$	$\eta = 2$
0	0	4	Eq. (C16)	0	$4/\pi$	2
1	$4i$	$4i$	$4i$	$8i/\pi$	$2i$	$4i/\pi$
2	-8	-4	-2	-6	$-8/\pi$	-1
3	$-12i$	$-4i$	$-4i/3$	$-32i/\pi$	$-3i$	$-8i/3\pi$
4	16	4	1	15	$32/3\pi$	$3/4$

TABLE I: Rescaled $\tilde{f}(r)/[8\pi r^{d-\eta}]$ according to Eq. (C15) for $d = 2$ and Eq. (C38) for $d = 3$ for different l and η . Only regular contributions for $r > 0$ are indicated. $l = 0$ corresponds to $\mathcal{F}^{-1}[f(\mathbf{q})]$ for a scalar function $f(\mathbf{q}) = s_\eta(q) = 1/Vq^\eta$. All entries for even (odd) l are real (imaginary). All entries for $d = 2$ and $\eta = 1$ stem from Eq. (C17).

for $d = 2$ and similarly in Appendix C 2 d that

$$f(\mathbf{q}) = f(q)Y_{lm}(\hat{\mathbf{q}}) \xleftrightarrow{\mathcal{F}} f(\mathbf{r}) = \tilde{f}(r)Y_{lm}(\hat{\mathbf{r}}) \quad (\text{C7})$$

for $d = 3$. In other words, the *same* function $Y(\cdot)$, with the *same* “quantum numbers” l and m , describes the angle dependence in real as in reciprocal space. Note that $\tilde{f}(r)$ may in general differ from $f(r) \equiv \mathcal{F}^{-1}[f(q)]$ (without the tilde). We investigate specifically the case

$$f(q) \equiv v(q)/V = s_\eta(q) \equiv 1/Vq^\eta. \quad (\text{C8})$$

Inverse FTs $f(\mathbf{r}) = s_\eta(r) \equiv \mathcal{F}^{-1}[s_\eta(q)]$, obtained below for a scalar function $f(\mathbf{q}) = s_\eta(q)$ are given in the third row ($l = 0$) of Table I for $d = 2$ and $d = 3$ for different η . We only indicate in this work regular (non-singular) contributions to the FT for $r > 0$ and possible but irrelevant singularities arising for small η are omitted.

b. Inverse FT for $d = 2$

Let us compute in $d = 2$ the inverse FT

$$f(\mathbf{r}) = \frac{1}{(2\pi)^2} \int d\mathbf{q} v(q)Y_l(\varphi_q) \exp(i\mathbf{q} \cdot \mathbf{r}) \quad (\text{C9})$$

for $Y_l(\varphi_q) = \cos(l\varphi_q)$ and $Y_l(\varphi_q) = \sin(l\varphi_q)$. We sort out in turn specific cases starting with the most simple ones. Let us note first that

$$Y_l(\varphi_q) = \sin(l\varphi_q) = 0 \text{ for } l = 0 \Rightarrow f(\mathbf{r}) = 0 \quad (\text{C10})$$

for all \mathbf{r} and $v(q)$. This trivial case is omitted below. Secondly, since $Y_l(\varphi_q) = \cos(l\varphi_q) = 1$ for $l = 0$ and assuming a constant $v(q)$, i.e. $\eta = 0$, Eq. (A4) implies

$$f(\mathbf{r}) = \delta(\mathbf{r}) + 0 \text{ for } l = \eta = 0, \quad (\text{C11})$$

i.e. $f(\mathbf{r})$ is strictly speaking a *distribution* [42] with a singularity at the origin and being zero elsewhere as emphasized by “0”. It is this value which is indicated in Table I for $d = 2$ and $l = \eta = 0$. We will find for small $\eta \leq 1/2$

(the bound being explained below) more cases like this where $f(\mathbf{r})$ is the sum of a singularity at the origin and a non-singular (regular) term for finite $r = |\mathbf{r}|$. Importantly, since we are only interested at distances $r > 0$ these singularities are irrelevant for the present study. We rewrite now Eq. (C9) as

$$f(\mathbf{r}) = \frac{1}{4\pi^2} \int_0^\infty dq qv(q) \int_0^{2\pi} d\varphi_q Y_l(\varphi_q) \times \exp[iq r \cos(\varphi_q - \varphi_r)] \quad (\text{C12})$$

with φ_r being the angle of $\hat{\mathbf{r}} = (\cos(\varphi_r), \sin(\varphi_r))$. Using $\varphi = \varphi_q - \varphi_r$ we have [45]

$$\begin{aligned} \cos(l\varphi + l\varphi_r) + \cos(-l\varphi + l\varphi_r) &= 2 \cos(l\varphi) \cos(l\varphi_r), \\ \sin(l\varphi + l\varphi_r) + \sin(-l\varphi + l\varphi_r) &= 2 \cos(l\varphi) \sin(l\varphi_r). \end{aligned}$$

For both $Y_l(x) = \cos(lx)$ and $Y_l(x) = \sin(lx)$ this leads to $f(\mathbf{r}) = \tilde{f}(r)Y_l(\varphi_r)$ with

$$\tilde{f}(r) = \frac{1}{2\pi^2} \int_0^\infty dq qv(q) \int_0^\pi d\varphi \cos(l\varphi) e^{iq r \cos(\varphi)} \quad (\text{C13})$$

confirming thus Eq. (C6). We focus below on $\tilde{f}(r)$. Results for several l and η are summarized in Table I. It is useful to rewrite Eq. (C13) in terms of integer Bessel functions $J_l(z)$ [45]. According Eq. (9.1.21) of Ref. [45]

$$J_l(z) = \frac{i^{-l}}{\pi} \int_0^\pi d\varphi \cos(l\varphi) \exp[iz \cos(\varphi)]. \quad (\text{C14})$$

This leads to

$$\tilde{f}(r) = \frac{i^l}{2\pi} \int_{q_{\min}}^{q_{\max}} dq qv(q) J_l(rq) \quad (\text{C15})$$

with $q_{\min} \rightarrow 0$ and $q_{\max} \rightarrow \infty$.

Let us next consider the specific case where $l = 0$ and $\eta = 2$. Since $J_0(x) \rightarrow 1$ for small x this leads to a logarithmic divergence at the lower integration bound q_{\min} of the above q -integral. As may be seen using Eq. (11.11.20) of Ref. [45] to leading order this yields

$$\tilde{f}(r) \approx \frac{1}{2\pi} (\ln(2) - \gamma - \ln(rq_{\min})) \quad (\text{C16})$$

with $\gamma = 0.577256$ being Euler's constant. This scalar function is elsewhere called $s_2(r)$. More straightforward is the case $\eta = 1$ for all l since $\int_0^\infty dx J_l(x) = 1$ for $l > -1$ according to Eq. (11.4.16) of Ref. [45]. Hence,

$$\tilde{f}(r) = \frac{i^l}{2\pi r} \text{ for } \eta = 1 \text{ and } l > -1. \quad (\text{C17})$$

Using that $J_1(x) = -J_0'(x)$ one sees using integration by parts that $\int dx x J_1(x) = \int dx J_0(x) = 1$. Whence,

$$\tilde{f}(r) = \frac{i}{2\pi r^2} \text{ for } \eta = 0 \text{ and } l = 1. \quad (\text{C18})$$

Note that Eq. (C18) just as Eq. (C17) hold without any additional singularity at the origin. We may also take advantage of the well-known recurrence relation [45]

$$\frac{x}{2l} (J_{l+1}(x) + J_{l-1}(x)) = J_l(x) \text{ for } l > 0. \quad (\text{C19})$$

Using $g_l^\eta(r) \equiv \tilde{f}(r, l, \eta)/i^l$ we get the recurrence relation

$$\frac{r}{2l} (g_{l+1}^\eta(r) + g_{l-1}^\eta(r)) = g_l^{\eta+1}(r) \text{ for } l > 0 \quad (\text{C20})$$

which even holds if singularities are included. Using this relation together with Eq. (C17) one obtains

$$\tilde{f}(r) = \frac{i^l}{2\pi l} \text{ for } \eta = 2 \text{ and } l > 0. \quad (\text{C21})$$

Using Eq. (C17), Eq. (C18) and Eq. (C20) we get

$$\tilde{f}(r) = \frac{i^l}{2\pi r^2} \text{ for } \eta = 0 \text{ and } l > 0 \quad (\text{C22})$$

in agreement with previous work [15, 17, 18]. Being zero for l , the latter result is actually also consistent with the non-singular term of Eq. (C11) and may thus be used for all $l \geq 0$. Note that additional singular contributions $\delta(r)/2\pi r$ arise for all $\eta = 0$ and even l as may be seen from the recurrence relation Eq. (C20) and the fact that all entries for $\eta = 1$ are analytic without singularity and that the same holds for $\eta = 0$ and $l = 1$.

It may be useful to note that Eq. (C22) for $\eta = 0$, Eq. (C17) for $\eta = 1$ and Eq. (C21) for $\eta = 2$ may also be obtained using the general integral relation for integer Bessel functions Eq. (11.4.16) of Ref. [45]

$$\int_0^\infty t^\mu J_\nu(t) dt = 2^\mu \frac{\Gamma\left(\frac{\nu+\mu+1}{2}\right)}{\Gamma\left(\frac{\nu-\mu+1}{2}\right)}. \quad (\text{C23})$$

Setting $\nu = l$ and $\mu = 1 - \eta$ implies

$$\tilde{f}(r) = \frac{i^l}{2\pi} 2^{1-\eta} \frac{\Gamma\left(\frac{l+2-\eta}{2}\right)}{\left(\frac{l+\eta}{2}\right)} \frac{1}{r^{2-\eta}} \text{ for } r > 0. \quad (\text{C24})$$

With the exception of Eq. (C16) for $l = 0$ and $\eta = 2$, this covers all other above-mentioned relations. Interestingly, Eq. (C23) is stated to hold (converge) only for $\mu + \nu > -1$ and $\mu < 1/2$ [45]. This implies the more restrictive condition $l + 2 > \eta > 1/2$. As already pointed out, a possible divergence for $\eta \leq 1/2$ however merely leads to an irrelevant $\delta(r)$ -singularity.

c. Spherical Bessel functions

For the FT in $d = 3$ presented in Sec. C2d it is useful to first remind several properties of spherical Bessel functions $j_l(x)$. The latter are related by [45]

$$j_l(x) = \sqrt{\frac{\pi}{2x}} J_{l+1/2}(x) \text{ with } l = 0, \pm 1, \pm 2, \dots \quad (\text{C25})$$

l	$\eta = 0$	$\eta = 1$	$\eta = 2$	$\eta = 3$
0	0	1	$\pi/2$	-
1	2	$\pi/2$	1	$\pi/4$
2	$3\pi/2$	2	$\pi/4$	$1/3$
3	8	$3\pi/4$	$2/3$	$\pi/16$
4	$15\pi/4$	$8/3$	$3\pi/16$	$2/15$
6	$105\pi/16$	$16/5$	$5\pi/32$	$8/105$
8	$315\pi/32$	$128/35$	$35\pi/256$	$32/315$

TABLE II: Non-singular contribution to the integral $\int_0^\infty dx x^{2-\eta} j_l(x)$ over spherical Bessel functions $j_l(x)$ for different l and exponents η . The values for $\eta = 2$ can be obtained, e.g., using Eq. (C29).

to Bessel function $J_\nu(x)$ of fractional order. Let us consider the infinite integral

$$\int_0^\infty dq q^{2-\eta} j_l(qr) = \frac{1}{r^{3-\eta}} \int_0^\infty dx x^{2-\eta} j_l(x) \quad (\text{C26})$$

for $r > 0$. (The integral boundaries are dropped below for clarity.) The non-singular contributions to the integral for several l and η are given in Table II. Naturally, the above integral is formally divergent at its upper bound for low η since all spherical Bessel functions $j_l(x)$ decay as $1/x$ in the large- x limit [45]. Nonetheless, as for the two-dimensional FT discussed in Sec. C 2 b, this a useful representation in the sense of distributions [42] since one can rewrite these integrals into a sum of a non-singular term (indicated in Table II) and a $\delta(r)$ -singularity (being irrelevant). For instance, using the identity

$$\int dq q^2 j_l(qr) j_l(qr') = \frac{\pi}{2r^2} \delta(r - r') \quad (\text{C27})$$

and by setting $l = 0$ and $r' = 0$ one obtains

$$\int dq q^2 j_0(qr) = \frac{\pi}{2r^2} \delta(r) + 0. \quad (\text{C28})$$

The non-singular contribution 0 for $r > 0$ of this case is indicated ($l = \eta = 0$) in the Table. Several other entries are given using the exact identities [45]

$$\int dx j_l(x) = \frac{\sqrt{\pi} \Gamma((l+1)/2)}{2 \Gamma(1+l/2)} \quad \text{and} \quad (\text{C29})$$

$$\int dx x^{-l} j_{l+1}(x) = \frac{1}{(2l+1)!!}, \quad (\text{C30})$$

e.g., the column of the Table for $\eta = 2$ stems from Eq. (C29). The remaining entries may be obtained using the recursion relation [45]

$$j_l(x) = \frac{x}{2l+1} (j_{l+1}(x) + j_{l-1}(x)) \quad (\text{C31})$$

holding for $l = 0, \pm 1, \pm 2, \dots$. This leads again to a recursion relation similar to Eq. (C20). For instance,

$$\begin{aligned} \int dq q^2 j_2(qr) &= \int dq q^2 j_0(qr) + \frac{3}{r} \int dq q j_1(qr) \\ &= \frac{\pi}{2r^2} \delta(r) + \frac{3\pi}{2r^3} \end{aligned} \quad (\text{C32})$$

corresponding to $l = 2$ and $\eta = 0$ in Table II. The above non-singular contribution for $l = \eta = 1$ is given by

$$\int dx x j_1(x) = - \int dx x \frac{d}{dx} j_0(x) = \frac{\pi}{2} \quad (\text{C33})$$

where the Rayleigh formula for spherical Bessel functions [45] was used in the first step and integration by parts and Eq. (C29) in the last step. In a similar way, we get all other non-singular contributions indicated in the Table. Interestingly, apart $l = \eta = 0$ all given entries in Table II can be directly obtained using the relation

$$\int dq q^{2-\eta} j_l(qr) = \sqrt{\pi} 2^{1-\eta} \frac{\Gamma\left(\frac{l-\eta+3}{2}\right)}{\Gamma\left(\frac{l+\eta}{2}\right)} \frac{1}{r^{3-\eta}}. \quad (\text{C34})$$

This relation follows directly from Eq. (C23) using Eq. (C25) and setting $\nu = l + 1/2$ and $\mu = 3/2 - \eta$. Note that only for $l + 3 > \eta > 1$ this relation converges rigorously *without* a $\delta(r)$ -singularity.

d. Inverse FT for $d = 3$

To compute the inverse FT of $f(\mathbf{q}) = f(q)Y_{lm}(\hat{\mathbf{q}})$ in $d = 3$ the plane wave expansion [49]

$$\exp(i\mathbf{q} \cdot \mathbf{r}) = 4\pi \sum_{l=0}^{\infty} i^l j_l(qr) \sum_{m=-l}^l Y_{lm}(\hat{\mathbf{q}}) Y_{lm}(\hat{\mathbf{r}}) \quad (\text{C35})$$

is used in terms of spherical Bessel functions $j_l(qr)$ and spherical harmonics $Y_{lm}(\hat{\mathbf{r}})$ and $Y_{lm}(\hat{\mathbf{q}})$ in real and reciprocal space. The ‘‘real form’’ of spherical harmonics [50] is used, e.g.,

$$Y_{0,0}(\hat{\mathbf{q}}) = \frac{1}{\sqrt{4\pi}} \quad \text{or} \quad Y_{1,-1}(\hat{\mathbf{q}}) = \sqrt{\frac{3}{4\pi}} \hat{q}_1 \quad (\text{C36})$$

and similarly for $Y_{lm}(\hat{\mathbf{r}})$ in real space. We also remind the orthogonality relation for spherical harmonics

$$\int d\hat{\mathbf{q}} Y_{lm}(\hat{\mathbf{q}}) Y_{l'm'}(\hat{\mathbf{q}}) = \delta_{ll'} \delta_{mm'} \quad (\text{C37})$$

with the integral carried out over the entire unit sphere. Let us consider the inverse FT of the (real) function $f(\mathbf{q}) = V^{-1} v(q) Y_{lm}(\hat{\mathbf{q}})$ with V being the volume and $v(q)$ a scalar function of the magnitude $q = |\mathbf{q}|$ of the wavevector \mathbf{q} . Using the orthogonality relation, Eq. (C37), one confirms Eq. (C7) and obtains

$$\tilde{f}(r) = \frac{i^l}{2\pi^2} \int dq q^2 v(q) j_l(qr). \quad (\text{C38})$$

η	$d = 2$	$d = 3$
0	4	$8/\pi$
1	4	2
2	4	$4/\pi$
3	4	1

TABLE III: Rescaled invariant $\check{l}_1(r)/[i8\pi r^{d-\eta}]$ as defined by $\mathcal{F}^{-1}[s_\eta(q)\hat{q}_\alpha] = \check{l}_1(r)\hat{r}_\alpha$. All $\check{l}_1(r)$ are imaginary.

For $v(q) = 1/q^\eta$ the q -integral is given by Eq. (C26), i.e. its non-singular contributions can be found in Table II. See the last three columns of Table I for the rescaled function $\check{f}(r)$ for $d = 3$ using units of $8\pi r^{d-\eta}$.

3. Inverse FT of additive terms of ITFs

a. Introduction

As already noted in Sec. B 4, generic ITFs in reciprocal space may be written as sums of terms or building blocks, such as $i_4(q)\hat{q}_\alpha\hat{q}_\beta\hat{q}_\gamma\hat{q}_\delta$ for Eq. (B19), being themselves ITFs. We investigate here the inverse FT of terms $s_\eta(q)\hat{q}_\alpha$, $s_\eta(q)\hat{q}_\alpha\hat{q}_\beta$, ... assuming $s_\eta(q) = 1/Vq^\eta$. Since the fields in real space must also be ITFs according to Eq. (C1) this implies the general structure

$$\mathcal{F}^{-1}[s_\eta(q)\hat{q}_\alpha] = \check{l}_1(r)\hat{r}_\alpha, \quad (\text{C39})$$

$$\mathcal{F}^{-1}[s_\eta(q)\hat{q}_\alpha\hat{q}_\beta] = \check{k}_1(r)\delta_{\alpha\beta} + \check{k}_2(r)\hat{r}_\alpha\hat{r}_\beta, \quad (\text{C40})$$

$$\begin{aligned} \mathcal{F}^{-1}[s_\eta(q)\hat{q}_\alpha\hat{q}_\beta\hat{q}_\gamma] &= \check{j}_1(r)[\delta_{\alpha\beta}\hat{r}_\gamma + \delta_{\beta\gamma}\hat{r}_\alpha + \delta_{\gamma\alpha}\hat{r}_\beta] \\ &+ \check{j}_4(r)\hat{r}_\alpha\hat{r}_\beta\hat{r}_\gamma \text{ and} \end{aligned} \quad (\text{C41})$$

$$\begin{aligned} \mathcal{F}^{-1}[s_\eta(q)\hat{q}_\alpha\hat{q}_\beta\hat{q}_\gamma\hat{q}_\delta] &= \check{i}_1(r)[\delta_{\alpha\beta}\delta_{\gamma\delta} + \delta_{\alpha\gamma}\delta_{\beta\delta} + \delta_{\alpha\delta}\delta_{\beta\gamma}] \\ &+ \check{i}_3(r)[\hat{r}_\alpha\hat{r}_\beta\delta_{\gamma\delta} + \hat{r}_\gamma\hat{r}_\delta\delta_{\alpha\beta} + \\ &\quad \hat{r}_\alpha\hat{r}_\gamma\delta_{\beta\delta} + \hat{r}_\alpha\hat{r}_\delta\delta_{\beta\gamma} + \\ &\quad \hat{r}_\beta\hat{r}_\gamma\delta_{\alpha\delta} + \hat{r}_\beta\hat{r}_\delta\delta_{\alpha\gamma}] \\ &+ \check{i}_4(r)\hat{r}_\alpha\hat{r}_\beta\hat{r}_\gamma\hat{r}_\delta \end{aligned} \quad (\text{C42})$$

with $\check{l}_n(r)$, $\check{k}_n(r)$, $\check{j}_n(r)$ and $\check{i}_n(r)$ being invariants computed below. We have used for Eq. (C41) and Eq. (C42) that these fields have *full index permutation symmetry* (in both spaces). As explained in Sec. B 4 d (for the corresponding fields in reciprocal space) this implies that $\check{j}_1(r) = \check{j}_2(r) = \check{j}_3(r)$, $\check{i}_1(r) = \check{i}_2(r)$ and $\check{i}_3(r) = \check{i}_5(r)$. Hence, the inverse FT Eq. (C41) must be characterized by only two invariants, $\check{j}_1(r)$ and $\check{j}_4(r)$, and Eq. (C42) by only three invariants, $\check{i}_1(r)$, $\check{i}_3(r)$ and $\check{i}_4(r)$.

b. Vector fields

Let us begin by computing the inverse FT of the isotropic vector field $s_\eta(q)\hat{q}_\alpha$ in $d = 2$ and $d = 3$ dimensions. Since the FT of a vector field is a vector

η	$d = 2$		$d = 3$	
	$\check{k}_1(r)$	$\check{k}_2(r)$	$\check{k}_1(r)$	$\check{k}_2(r)$
0	4	-8	2	-6
1	4	-4	$4/\pi$	$-8/\pi$
2	log. div.	-2	1	-1

TABLE IV: Invariants $\check{k}_1(r)$ and $\check{k}_2(r)$ for $r > 0$ obtained for $\mathcal{F}^{-1}[s_\eta(q)\hat{q}_\alpha\hat{q}_\beta] = \check{k}_1(r)\delta_{\alpha\beta} + \check{k}_2(r)\hat{r}_\alpha\hat{r}_\beta$. All invariants are given in units of $8\pi r^{d-\eta}$. As noted by “log. div.” a logarithmic divergence, cf. Eq. (C16) exists for $d = 2$ and $\eta = 2$.

field and since the FT of an isotropic field is an isotropic field, the most general form of the inverse FT must be given by Eq. (C39). To take advantage of the FT of $f(\mathbf{q}) = s_\eta(q)Y(\hat{\mathbf{q}})$ computed in Sec. C 2 we must express \hat{q}_α in terms of $Y(\hat{\mathbf{q}})$. In $d = 2$ we have $\hat{q}_1 = \cos(\varphi_q)$ and $\hat{q}_2 = \sin(\varphi_q)$ in reciprocal space and $\hat{r}_1 = \cos(\varphi_r)$ and $\hat{r}_2 = \sin(\varphi_r)$ in real space. $\check{l}_1(r)$ is thus given by Eq. (C15) for $l = 1$ as seen from Table I. In $d = 3$ one may use that the components \hat{q}_α are proportional to $Y_{lm}(\hat{\mathbf{q}})$ for $l = 1$, e.g., $\hat{q}_1 = \sqrt{4\pi/3}Y_{1,1}(\hat{\mathbf{q}})$ according to Eq. (C36), and similarly in real space. Using this one finds that $\check{l}_1(r) = \check{f}(r)$ is given by Eq. (C38) for $v(q) = 1/q^\eta$ and $l = 1$. Please see Table III for the relevant $\check{l}_1(r)$ for both spatial dimensions.

c. Second-order fields

The inverse FT of $s_\eta(q)\hat{q}_\alpha\hat{q}_\beta$ becomes a second-order ITF in real space, cf. Eq. (C40), in terms of two invariants $\check{k}_1(r)$ and $\check{k}_2(r)$. One useful relation to get these invariants is obtained by tracing over $\alpha = \beta$ and using that $\hat{q}_\alpha^2 = \hat{r}_\alpha^2 = 1$. This yields

$$d\check{k}_1(r) + \check{k}_2(r) = s_\eta(r) \quad (\text{C43})$$

with $s_\eta(r)$ being given in Table I. A second relation is obtained from the inverse FT for $\alpha = 1$ and $\beta = 2$, i.e.

$$\mathcal{F}^{-1}[\hat{q}_1\hat{q}_2/Vq^\eta] = \check{k}_2(r)\hat{r}_1\hat{r}_2. \quad (\text{C44})$$

We note that $\hat{q}_1\hat{q}_2 = \sin(2\varphi_q)/2$ in $d = 2$ and $\hat{q}_1\hat{q}_2 = \sqrt{4\pi/15}Y_{2,-2}(\hat{q})$ in $d = 3$ and similarly in real space. Using Table I for $l = 2$ yields $\check{k}_2(r)$. Finally, using Eq. (C43) one obtains $\check{k}_1(r) = (s_\eta(r) - \check{k}_2(r))/d$. Both invariants are given in Table IV.

d. Third-order fields

Since $s_\eta(q)\hat{q}_\alpha\hat{q}_\beta\hat{q}_\gamma$ is a third-order ITF with complete permutation symmetry of all indices, its inverse FT must take the generic form indicated in Eq. (C41) in terms of only two invariants $\check{j}_1(r)$ and $\check{j}_4(r)$. Two independent relations are thus needed to determine these invariants.

	$d = 2$		$d = 3$	
η	$\check{j}_1(r)$	$\check{j}_4(r)$	$\check{j}_1(r)$	$\check{j}_4(r)$
0	4	-12	$8/\pi$	$-32/\pi$
1	2	-4	1	-3
2	$4/3$	$-4/3$	$4/3\pi$	$-8/3\pi$

TABLE V: Invariants $\check{j}_1(r)$ and $\check{j}_4(r)$ with $r > 0$ for the inverse FT Eq. (C41) of $s_\eta(q)\hat{q}_\alpha\hat{q}_\beta\hat{q}_\gamma$. All invariants are given in units of $i8\pi r^{d-\eta}$.

	$d = 2$			$d = 3$		
η	$\check{i}_1(r)$	$\check{i}_3(r)$	$\check{i}_4(r)$	$\check{i}_1(r)$	$\check{i}_3(r)$	$\check{i}_4(r)$
0	2	-4	16	1	-3	15
1	$4/3$	$-4/3$	4	$4/3\pi$	$-8/3\pi$	$32/3\pi$
2	log	$-1/2$	1	$1/4$	$-1/4$	$3/4$

TABLE VI: Invariants $\check{i}_1(r) = \check{i}_2(r)$, $\check{i}_3(r) = \check{i}_5(r)$ and $\check{i}_4(r)$ for the inverse FT of the fourth-order ITF $s_\eta(q)\hat{q}_\alpha\hat{q}_\beta\hat{q}_\gamma\hat{q}_\delta$, cf. Eq. (C42). All invariants are given in units of $8\pi r^{d-\eta}$. The scalar function $s_2(r)$ for $d = 2$ and $\eta = 2$ is given by Eq. (C16).

One relation may be obtained by tracing over the last two indices $\beta = \gamma$ which reduces the third-order field to a vector field with

$$\check{l}_1(r)\hat{r}_\alpha = \mathcal{F}^{-1}[s_\eta(q)\hat{q}_\alpha] = [(d+2)\check{j}_1(r) + \check{j}_4(r)]\hat{r}_\alpha \quad (\text{C45})$$

for all \hat{r}_α , i.e. $\check{j}_1(r) = [\check{l}_1(r) - \check{j}_4(r)]/(d+2)$ with $\check{l}_1(r)$ being already discussed in Sec. C3b and summarized in Table III. The second relation is obtained for $d = 3$ using that for $\alpha = 1$, $\beta = 2$ and $\gamma = 3$ we have

$$\mathcal{F}^{-1}[\hat{q}_1\hat{q}_2\hat{q}_3/Vq^\eta] = \check{j}_4(r)\hat{r}_1\hat{r}_2\hat{r}_3, \quad (\text{C46})$$

and that $\hat{q}_1\hat{q}_2\hat{q}_3 = \sqrt{4\pi/105}Y_{3,-2}(\hat{\mathbf{q}})$ and similarly in real space. Taking advantage of Eq. (C38) or Table II for $l = 3$ one thus obtains $\check{j}_4(r)$ and then, using Eq. (C45) $\check{j}_1(r)$. The two-dimensional case is here slightly more complicated. One may use, e.g., the case $\alpha = \beta = \gamma = 1$ and that $\hat{q}_1^3 = \frac{1}{4}\cos(3\varphi_q) + \frac{3}{4}\cos(\varphi_q)$. Using then Table I for both $l = 1$ and $l = 3$ yields a second relation for $\check{j}_1(r)$ and $\check{j}_4(r)$ for each η . Using the general relation Eq. (C45) allows finally to determine both invariants. See Table V for the invariants $\check{j}_1(r)$ and $\check{j}_4(r)$.

e. Fourth-order fields

We turn finally to the inverse FT of the fourth-order ITF $s_\eta(q)\hat{q}_\alpha\hat{q}_\beta\hat{q}_\gamma\hat{q}_\delta$. As stated by Eq. (C42) the complete index symmetry implies that we have in real space a fourth-order ITF described by *three* invariants $\check{i}_1(r)$, $\check{i}_3(r)$ and $\check{i}_4(r)$. Three independent relations are thus needed. Two relations are immediately obtained by tracing over the last pair of indices $\gamma = \delta$ reducing the forth-order

n	$\check{i}_n(r)/4\pi r^2$	$\check{i}_n(r)/4\pi r^2$
1	5	$4\hat{i}_3 + 5\hat{i}_4$
2	-1	$-\hat{i}_4$
3	-6	$-4\hat{i}_3 - 6\hat{i}_4$
4	8	$8\hat{i}_4$
5	0	0

TABLE VII: Rescaled invariants $\check{i}_n(r)/4\pi r^2$ and $\check{i}_n(r)/4\pi r^2$ for $r > 0$, $d = 2$ and $\eta = 0$ using the ‘‘compact representation’’ obtained by means of the transformation Eq. (4). The results for $\eta = 0$ have already reported elsewhere [18].

fields to second-order fields. Using Eq. (B37) and again $\hat{q}_\gamma^2 = \hat{r}_\gamma^2 = 1$ this implies this implies

$$\begin{aligned} \mathcal{F}^{-1}[s_\eta(q)\hat{q}_\alpha\hat{q}_\beta] &= \check{k}_1(r)\delta_{\alpha\beta} + \check{k}_2(r)\hat{r}_\alpha\hat{r}_\beta \\ &= \left[(d+2)\check{i}_1(r) + \check{i}_3(r) \right] \delta_{\alpha\beta} \\ &\quad + \left[(d+4)\check{i}_3(r) + \check{i}_4(r) \right] \hat{r}_\alpha\hat{r}_\beta \end{aligned}$$

where Eq. (C42) was used in the second step. Since this must hold for any \hat{r}_α we have

$$\check{k}_1(r) = (d+2)\check{i}_1(r) + \check{i}_3(r) \quad \text{and} \quad (\text{C47})$$

$$\check{k}_2(r) = (d+4)\check{i}_3(r) + \check{i}_4(r). \quad (\text{C48})$$

The third relation is obtained by tracing additionally over the first pair of indices $\alpha = \beta$. In agreement with Eq. (B38) this yields the scalar relation

$$\begin{aligned} s_\eta(r) &= \mathcal{F}^{-1}[s_\eta(q)] \\ &= (d^2 + 2d)\check{i}_1(r) + (2d + 4)\check{i}_3(r) + \check{i}_4(r). \end{aligned} \quad (\text{C49})$$

Since $s_\eta(r)$, $\check{k}_1(r)$ and $\check{k}_2(r)$ are known (cf. Tables I and IV) these relations completely determine $\check{i}_1(r) = \check{i}_2(r)$, $\check{i}_3(r) = \check{i}_5(r)$ and $\check{i}_4(r)$ as indicated in Table VI.

For $d = 2$ these results correspond to the ‘‘extended representation’’ and not to the ‘‘compact representation’’ which we have used in previous work [17, 18] where we did focus on two-dimensional systems. Using Eq. (4) one may recast this as

$$\begin{aligned} \check{i}_1(r) &\rightarrow \check{i}_1(r) - 2\check{i}_5(r) \\ \check{i}_2(r) &\rightarrow \check{i}_2(r) + 1\check{i}_5(r) \\ \check{i}_3(r) &\rightarrow \check{i}_3(r) + 2\check{i}_5(r) \\ \check{i}_4(r) &\rightarrow \check{i}_4(r) \\ \check{i}_5(r) &\rightarrow 0 \end{aligned} \quad (\text{C50})$$

in terms of *four* invariants in agreement with Refs. [17, 18]. The values for $\eta = 0$ are stated in Table VII.

4. General isotropic tensor fields

The most general ITFs in real space consistent with the assumptions formulated in Appendix B1 have been

invariant	$d = 2$			$d = 3$		
	$\eta = 0$	$\eta = 1$	$\eta = 2$	$\eta = 0$	$\eta = 1$	$\eta = 2$
$s_\eta(r)$	0	2	log. div.	0	$\frac{4}{\pi}$	2
$\tilde{l}_1(r)/i$	$4\hat{l}_1$	$4\hat{l}_1$	$4\hat{l}_1$	$\frac{8}{\pi}\hat{l}_1$	$2\hat{l}_1$	$\frac{4}{\pi}\hat{l}_1$
$\tilde{k}_1(r)$	$4\hat{k}_2$	$4[\hat{k}_1 + \hat{k}_2]$	log. div.	$2\hat{k}_2$	$\frac{4}{\pi}[\hat{k}_1 + \hat{k}_2]$	$2\hat{k}_1 + \hat{k}_2$
$\tilde{k}_2(r)$	$-8\hat{k}_2$	$-4\hat{k}_2$	$-2\hat{k}_2$	$-6\hat{k}_2$	$-\frac{8}{\pi}\hat{k}_2$	$-\hat{k}_2$
$\tilde{j}_1(r)/i$	$4[\hat{j}_1 + \hat{j}_4]$	$2[2\hat{j}_1 + \hat{j}_4]$	$\frac{4}{3}[3\hat{j}_1 + \hat{j}_4]$	$\frac{4}{3}[\hat{j}_1 + \hat{j}_4]$	$1[2\hat{j}_1 + \hat{j}_4]$	$\frac{4}{3\pi}[3\hat{j}_1 + \hat{j}_4]$
$\tilde{j}_2(r)/i$	$4[\hat{j}_2 + \hat{j}_4]$	$2[2\hat{j}_2 + \hat{j}_4]$	$\frac{4}{3}[3\hat{j}_2 + \hat{j}_4]$	$\frac{4}{3}[\hat{j}_2 + \hat{j}_4]$	$1[2\hat{j}_2 + \hat{j}_4]$	$\frac{4}{3\pi}[3\hat{j}_2 + \hat{j}_4]$
$\tilde{j}_3(r)/i$	$4[\hat{j}_3 + \hat{j}_4]$	$2[2\hat{j}_3 + \hat{j}_4]$	$\frac{4}{3}[3\hat{j}_3 + \hat{j}_4]$	$\frac{4}{3}[\hat{j}_3 + \hat{j}_4]$	$1[2\hat{j}_3 + \hat{j}_4]$	$\frac{4}{3\pi}[3\hat{j}_3 + \hat{j}_4]$
$\tilde{j}_4(r)/i$	$-12\hat{j}_4$	$-4\hat{j}_4$	$-\frac{4}{3}\hat{j}_4$	$-\frac{32}{\pi}\hat{j}_4$	$-3\hat{j}_4$	$-\frac{8}{3\pi}\hat{j}_4$
$\tilde{i}_1(r)$	$2[4\hat{i}_3 + \hat{i}_4]$	$\frac{4}{3}[3\hat{i}_1 + 6\hat{i}_3 + \hat{i}_4]$	log. div.	$1[4\hat{i}_3 + \hat{i}_4]$	$\frac{4}{3\pi}[3\hat{i}_1 + 6\hat{i}_3 + \hat{i}_4]$	$\frac{1}{4}[8\hat{i}_1 + 8\hat{i}_3 + \hat{i}_4]$
$\tilde{i}_2(r)$	$2[4\hat{i}_5 + \hat{i}_4]$	$\frac{4}{3}[3\hat{i}_2 + 6\hat{i}_5 + \hat{i}_4]$	log. div.	$1[4\hat{i}_5 + \hat{i}_4]$	$\frac{4}{3\pi}[3\hat{i}_2 + 6\hat{i}_5 + \hat{i}_4]$	$\frac{1}{4}[8\hat{i}_1 + 8\hat{i}_5 + \hat{i}_4]$
$\tilde{i}_3(r)$	$-4[2\hat{i}_3 + \hat{i}_4]$	$-\frac{4}{3}[3\hat{i}_3 + \hat{i}_4]$	$-\frac{1}{2}[4\hat{i}_3 + \hat{i}_4]$	$-3[2\hat{i}_3 + \hat{i}_4]$	$-\frac{8}{3\pi}[3\hat{i}_3 + \hat{i}_4]$	$-\frac{1}{4}[4\hat{i}_3 + \hat{i}_4]$
$\tilde{i}_5(r)$	$-4[2\hat{i}_5 + \hat{i}_4]$	$-\frac{4}{3}[3\hat{i}_5 + \hat{i}_4]$	$-\frac{1}{2}[4\hat{i}_5 + \hat{i}_4]$	$-3[2\hat{i}_5 + \hat{i}_4]$	$-\frac{8}{3\pi}[3\hat{i}_5 + \hat{i}_4]$	$-\frac{1}{4}[4\hat{i}_5 + \hat{i}_4]$
$\tilde{i}_4(r)$	$16\hat{i}_4$	$1[4\hat{i}_4]$	\hat{i}_4	$15\hat{i}_4$	$\frac{8}{3\pi}[4\hat{i}_4]$	$\frac{3}{4}\hat{i}_4$

TABLE VIII: Invariants in real space for spatial dimensions $d = 2$ and $d = 3$ and power-law exponents $\eta = 0, 1$ and 2 . All invariants are given in units of $8\pi r^{d-\eta}$. Invariants of ITF of odd order o are imaginary as indicated in the first column. $\delta(r)$ -singularities are not indicated. Note that $s_\eta(r) = \mathcal{F}^{-1}[s_\eta(q)]$ and that $\eta = 0$ corresponds to constant invariants in reciprocal space. To simplify the comparison of different dimensions several entries have been factorized such that the brackets [...] for different d but same η are identical. For $d = 2$ the “extended representation” has been used, cf. Sec. B 4 e. “log. div.” in the fourth column marks the logarithmic divergence according to Eq. (C16), cf. Sec. C 2 b.

stated in Appendix C 1. Using the inverse FTs presented above in Appendix C 2 and Appendix C 3 all what remains to be done is to add up the different contributions. We emphasize that due to the dependence of the ITFs on \hat{r}_α (real space) and \hat{q}_α (reciprocal space) the invariants in real space $\tilde{l}_n(r)$, $\tilde{k}_n(r)$, $\tilde{j}_n(r)$ and $\tilde{i}_n(r)$ (marked by a tilde) differ in general from the (direct) inverse FTs $l_n(r)$, $k_n(r)$, $j_n(r)$ and $i_n(r)$ of the invariants $l_n(q)$, $k_n(q)$, $j_n(q)$ and $i_n(q)$ in reciprocal space, e.g., $k_n(r) \equiv \mathcal{F}^{-1}[k_n(q)] \neq \hat{k}_n(r)$. Note that the full index permutation symmetry holding for each additive term does not hold for their sums in general. This means that, e.g., $\tilde{j}_1(r) \neq \tilde{j}_2(r)$ or $\tilde{i}_3(r) \neq \tilde{i}_5(r)$ in general. All invariants of a field of order o in reciprocal space have a power law, i.e. $l_n(q) = \hat{l}_n s_\eta(q)$, $k_n(q) = \hat{k}_n s_\eta(q)$, $j_n(q) = \hat{j}_n s_\eta(q)$ and $i_n(q) = \hat{i}_n s_\eta(q)$ for all n with \hat{l}_n , \hat{k}_n , \hat{j}_n and \hat{i}_n being constants. Hence, $k_n(r) = \hat{k}_n s_\eta(r)$ or $i_n(r) = \hat{i}_n s_\eta(r)$. The invariants $\tilde{l}_n(r)$, $\tilde{k}_n(r)$, $\tilde{j}_n(r)$ and $\tilde{i}_n(r)$ can be expressed using the invariants $l_n(r)$, $k_n(r)$, $j_n(r)$ and $i_n(r)$ computed above for the individual building terms. Summing up the different contributions yields

$$\tilde{l}_1(r) = \hat{l}_1 \check{l}_1(r), \quad (\text{C51})$$

$$\tilde{k}_1(r) = k_1(r) + \hat{k}_2 \check{k}_1(r), \quad (\text{C52})$$

$$\tilde{k}_2(r) = \hat{k}_2 \check{k}_2(r), \quad (\text{C53})$$

$$\tilde{j}_1(r) = \hat{j}_1 \check{l}_1(r) + \hat{j}_4 \check{j}_1(r), \quad (\text{C54})$$

$$\tilde{j}_2(r) = \hat{j}_2 \check{l}_1(r) + \hat{j}_4 \check{j}_1(r), \quad (\text{C55})$$

$$\tilde{j}_3(r) = \hat{j}_3 \check{l}_1(r) + \hat{j}_4 \check{j}_1(r), \quad (\text{C56})$$

$$\tilde{j}_4(r) = \hat{j}_4 \check{j}_4(r), \quad (\text{C57})$$

$$\tilde{i}_1(r) = i_1(r) + 2\hat{i}_3 \check{k}_1(r) + \hat{i}_4 \check{i}_1(r), \quad (\text{C58})$$

$$\tilde{i}_2(r) = i_2(r) + 2\hat{i}_5 \check{k}_1(r) + \hat{i}_4 \check{i}_1(r), \quad (\text{C59})$$

$$\tilde{i}_3(r) = \hat{i}_3 \check{k}_2(r) + \hat{i}_4 \check{i}_3(r), \quad (\text{C60})$$

$$\tilde{i}_4(r) = \hat{i}_4 \check{i}_4(r) \text{ and} \quad (\text{C61})$$

$$\tilde{i}_5(r) = \hat{i}_5 \check{k}_2(r) + \hat{i}_4 \check{i}_3(r) \quad (\text{C62})$$

These results hold for any dimension d and any exponent η . Using the Tables I, III, IV, V and VI one finally gets the invariants in real space summarized in Table VIII.

As noted in Appendix B 4 e it is possible to rewrite the invariants of fourth-order isotropic fields in $d = 2$ more compactly in terms of four invariants using the transformation Eq. (4). This can be done (in any order) for both the invariants $\check{i}_1(r), \dots, \check{i}_5(r)$ of the building terms using Eq. (C50) and similarly for the composite invariants $\tilde{i}_1(r), \dots, \tilde{i}_5(r)$. The results for $\eta = 0$ stated in Table VII are consistent with Refs. [17, 18].

Appendix D: Linear displacement response

The displacements generated by a small force density $g_\alpha^{\text{ex}}(\mathbf{q})$ applied to a linear elastic body are given within linear response by

$$u_\alpha(\mathbf{q}) = \mathbf{G}_{\alpha\beta}(\mathbf{q}) g_\beta^{\text{ex}}(\mathbf{q}) \quad (\text{D1})$$

in reciprocal space in terms of the symmetric second-order GF TF $\mathbf{G}_{\alpha\beta}(\mathbf{q})$. For isotropic systems $\mathbf{G}_{\alpha\beta}(\mathbf{q})$ must be an ITF. Taking advantage of the FDT relation

$$\mathbf{G}_{\alpha\beta}(\mathbf{q}) = \beta V C_{\alpha\beta}(\mathbf{q}) \quad (\text{D2})$$

reminded in Sec. III F, the GFs are given by the CFs. We discuss below the displacement response for various imposed force density fields.

Let us first assume that the external perturbation is due to localized and well separated point forces, i.e. we have a force density $g_\alpha^{\text{ex}}(\mathbf{q}) = \sum_a f_\beta^a/V$ in reciprocal space. Using Eq. (36) the response in real space is thus

$$u_\alpha(\mathbf{r}) = \sum_a \beta c_{\alpha\beta}(\mathbf{r} - \mathbf{r}^a) f_\alpha^a. \quad (\text{D3})$$

Importantly, since $c_{\alpha\beta}(\mathbf{r}) \sim 1/\beta$ the GF $\mathbf{G}_{\alpha\beta}(\mathbf{r})$ does not depend explicitly on the temperature of the system. Note also that $u_\alpha(\mathbf{r})$ cannot be an ITF since the applied force in reciprocal space is a finite first-order tensor, i.e. according to Eq. (B6) *not* an isotropic tensor. One specific case may be worth noting for comparison. Let us consider following W. Thomson (1848) one point force $g_\alpha^{\text{ex}}(\mathbf{r}) = f_\alpha \delta(\mathbf{r})$ at the origin. Using Eq. (D3), Eq. (22) and Eq. (54) one directly obtains

$$u_\alpha(\mathbf{r}) = \frac{1}{8\pi r} \frac{1+\nu}{E(1-\nu)} [(3-4\nu)\delta_{\alpha\beta} + \hat{r}_\alpha \hat{r}_\beta] f_\beta \quad (\text{D4})$$

for $d = 3$ in agreement with Ref. [23].

Let us next impose force fields being the sum of dipoles created by pairs of close point forces of same magnitude but opposite sign. We first consider the case

$$g_\alpha^{\text{ex}}(\mathbf{r}) = f \delta_{\alpha\beta} [\delta(\mathbf{r} - h\mathbf{e}_\beta) - \delta(\mathbf{r} + h\mathbf{e}_\beta)], \quad (\text{D5})$$

i.e. identical dipoles along all d axes. Using Eq. (A8) for sufficiently small $p = 2h$ the source force density in reciprocal space is an ITF:

$$g_\alpha^{\text{ex}}(\mathbf{q}) = -i p q_\alpha \frac{f}{V}. \quad (\text{D6})$$

Since both $c_{\alpha\beta}(\mathbf{q})$ and the source are ITFs, the same applies due to the product theorem for the RF. Hence,

$$u_\alpha(\mathbf{q}) = l_1(q) \hat{q}_\alpha \overset{\mathcal{F}}{\leftrightarrow} u_\alpha(\mathbf{r}) = \tilde{l}_1(r) \hat{r}_\alpha \quad (\text{D7})$$

in agreement with Eq. (B14) and Eq. (C51). Using the results found in Sec. IV C 1 it is seen that

$$l_1(q) = -i \frac{pf}{VL(q)q} \quad (\text{D8})$$

only depends on the longitudinal modulus $L(q)$ and not on the shear modulus $G(q)$ (as expected due to the imposed isotropic pressure) decaying, moreover, inversely with q . Focusing on the continuum limit where $L(q) \approx \lambda + 2\mu$ and using Table III for $\eta = 1$ we finally get

$$\begin{aligned} \tilde{l}_1(r) &= \frac{pf}{\lambda + 2\mu} \frac{1}{2\pi r} \text{ for } d = 2 \text{ and} \\ \tilde{l}_1(r) &= \frac{pf}{\lambda + 2\mu} \frac{1}{4\pi r^2} \text{ for } d = 3. \end{aligned} \quad (\text{D9})$$

As a third and last case let us investigate a ‘‘shear-transformation zone’’ in the 12-plane (already mentioned in Appendix B 8 e) [26] where

$$\begin{aligned} g_\alpha^{\text{ex}}(\mathbf{r}) &= f_1 [\delta(\mathbf{r} - h\mathbf{e}_1) - \delta(\mathbf{r} + h\mathbf{e}_1)] \delta_{\alpha 1} \\ &+ f_2 [\delta(\mathbf{r} - h\mathbf{e}_2) - \delta(\mathbf{r} + h\mathbf{e}_2)] \delta_{\alpha 2}. \end{aligned} \quad (\text{D10})$$

We assume $f = f_1 = -f_2$, i.e. the two dipoles have opposite signs. While the GF is isotropic, this is not the case for the SF and the RF is thus not an ITF. Using

$$g_\alpha^{\text{ex}}(\mathbf{q}) = -i \frac{pf}{V} (\delta_{\alpha 1} q_1 - \delta_{\alpha 2} q_2) \quad (\text{D11})$$

and the known GF $\mathbf{G}_{\alpha\beta}(\mathbf{q}) = \beta c_{\alpha\beta}(\mathbf{q})$ one may, however, still write for $q\xi_{\text{cont}} \ll 1$ the inverse FT in terms of the invariants $\check{l}(r)$, $\check{j}_1(r)$ and $\check{j}_4(r)$ discussed in, respectively, Appendix C 3 b and Appendix C 3 d. This leads to

$$\begin{aligned} \frac{u_\alpha(\mathbf{r})}{ipf} &= \frac{1}{\mu} \check{l}(r) (\hat{r}_1 - \hat{r}_2) - \frac{\lambda + \mu}{\mu(\lambda + 2\mu)} \times \\ &\left[\check{j}_1(r) 2(\hat{r}_1 \delta_{\alpha 1} - \hat{r}_2 \delta_{\alpha 2}) + \check{j}_2(r) \hat{r}_\alpha (\hat{r}_1^2 - \hat{r}_2^2) \right]. \end{aligned} \quad (\text{D12})$$

The final results for $d = 2$ and $d = 3$ are then obtained using Table III and Table V for the exponent $\eta = 1$. More details on this important case will be given elsewhere.

The linear response due to a small SF was discussed in general terms in Appendix B 8 and more specifically for displacement TFs in the preceding paragraphs. Importantly, response TFs are mathematically defined in reciprocal space by a tensorial contraction of a GF by a SF. The RFs are thus not as for scalar fields simply proportional to the GF. Naturally, the RF contains both information from the GF, characterizing the system, and from the SF, characterizing the perturbation. While for an isotropic system the GF is an ITF, this is in general not the case for SF, e.g., for intrinsic spontaneous fluctuations, and the RF is in general not an ITF. Albeit being closely related, RFs and GFs differ in general.

We note finally that in a similar manner as for the displacements one may also obtain the strain response

$$\varepsilon_{\alpha\beta}(\mathbf{q}) = \mathbf{G}_{\alpha\beta\gamma\delta}(\mathbf{q}) \sigma_{\gamma\delta}^{\text{ex}}(\mathbf{q}) \quad (\text{D13})$$

caused by an imposed external stress $\sigma_{\alpha\beta}^{\text{ex}}(\mathbf{q})$. Using the definitions Eq. (7), Eq. (40) and Eq. (97) this may be also done directly starting from the displacement CFs using

$$\mathbf{G}_{\alpha\beta\gamma\delta}(\mathbf{q}) = q^2 \beta V \mathcal{O}^{2+} [c_{\alpha\beta}(\mathbf{q})]. \quad (\text{D14})$$

Appendix E: Relaxation times for strain CFs

As shown in Sec. V D, the ICFs $c_L(q, t)$ and $c_G(q, t)$ are related to the material functions $L(q, t)$ and $G(q, t)$ in Fourier-Laplace space by Eq. (102) using for overdamped systems the scalar $w(q, s) = q^2/\zeta s$ with ζ being the effective friction constant. We focus again on the simple limit for large t (small s). It was stated in Sec. V E that

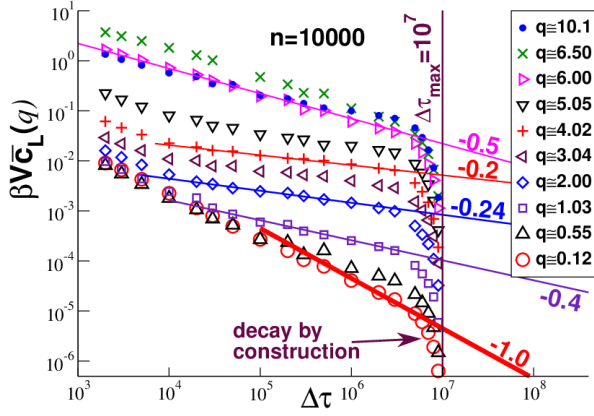


FIG. 13: Longitudinal ICF $\beta V \bar{c}_L(q, \Delta\tau)$ for pLJ systems for several q as a function of $\Delta\tau$. As indicated by the vertical line $\Delta\tau_{\max} = 10^7$ for $n = 10000$, i.e. the final strong decay of the data is expected due to the construction of the displacement field. The power-law slope with exponent -1 (bold solid line) expected for asymptotically large $\Delta\tau \ll \Delta\tau_{\max}$ is barely consistent with the smallest q indicated and much smaller effective exponents are visible for larger q (thin solid lines).

(not surprisingly) the ICFs must asymptotically decay exponentially for large t with relaxation times given by Eq. (103) in terms of the static generalized elastic moduli $L(q) \equiv \lim_{s \rightarrow 0} L(q, s)$ and $G(q) \equiv \lim_{s \rightarrow 0} G(q, s)$. These relations *assume* that the s -dependence of the material functions becomes irrelevant for $s \rightarrow 0$. While this leads indeed to useful relations for $q\xi_{\text{cont}} \ll 1$, higher order contributions may in general contribute. To see this let us consider the low- s expansion

$$L(q, s) = L(q) \left[1 + a_1 s + \frac{1}{2} a_2 s^2 + \dots \right] \quad (\text{E1})$$

with constants a_n depending *a priori* on q . Inserting this into the relation for the longitudinal ICF, cf. Eq. (102), we find to leading order

$$L(q) \beta V c_L(q, s) \simeq \frac{s}{s + 1/(\zeta/q^2 L(q) + a_1)}, \quad (\text{E2})$$

i.e. the linear term in Eq. (E1) cannot be neglected.

What is the physical meaning of a_1 ? We note first that according to Eq. (A15) this term corresponds in the time domain to a generalized longitudinal modulus

$$L(q, t) \approx L(q) [1 + a_1 \delta(t)] \quad (\text{E3})$$

with a_1 being an effective time scale characterizing the short-time behavior of $L(q, t)$. Let us introduce by

$$\begin{aligned} \eta_L(q, t) &\equiv \int_0^t dt [L(q, t) - L(q)] \\ \stackrel{\zeta}{\Leftrightarrow} \eta_L(q, s) &= [L(q, s) - L(q)]/s. \end{aligned} \quad (\text{E4})$$

a generalized viscosity associated to the longitudinal material function $L(q, t)$. Using the expansion Eq. (E1) and

the final value theorem of the LT, Eq. (A20), we get [46]

$$a_1 L(q) = \lim_{t \rightarrow \infty} \eta_L(q, t) = \lim_{s \rightarrow 0} \eta_L(q, s) = \eta_L(q), \quad (\text{E5})$$

i.e. a_1 characterizes the q -dependent longitudinal viscosity $\eta_L(q)$. Since a_1 is a time scale we call it from now $\tau_L^0(q)$. We introduce similarly $\tau_G^0(q)$ and $\eta_G(q)$ for the corresponding time scale and the generalized viscosity of the transverse ICF $\beta V c_G(q, s)$. The superscript “v” marks that these time scales characterize generalized viscosities. Using again Eq. (A16) one confirms that the above relations Eq. (105) are still applicable, however, in terms of the generalized relaxation times

$$\begin{aligned} \tau_L(q) &= (\zeta/q^2 + \eta_L(q))/L(q) \text{ and} \\ \tau_G(q) &= (\zeta/q^2 + \eta_G(q))/G(q). \end{aligned} \quad (\text{E6})$$

The additional phenomenological time scales

$$\tau_L^0(q) \equiv \eta_L(q)/L(q) \text{ and } \tau_G^0(q) \equiv \eta_G(q)/G(q), \quad (\text{E7})$$

characterizing the short-time behavior of both material functions, are expected to strongly increase for large q . One important reason is that $L(q)$ and $G(q)$ become extremely small for $q\xi_{\text{cont}} \gg 1$ as shown in Fig. 4.

Confirming the above statements, the dynamics for our two-dimensional overdamped model glass systems has been found to dramatically slow down for $q\xi_{\text{cont}} \gg 1$. We have thus unfortunately been unable to reach the predicted exponential decay for the possible production times $\Delta\tau_{\max}$. This is shown in Fig. 13 for the ICF $\bar{c}_L(q, \Delta\tau)$ of the t -averaged longitudinal strain fields. We plot here ICFs for several wavenumbers q as a function of the preaveraging time $\Delta\tau$ for our smaller systems with $n = 10000$ particles and a total production time $\Delta\tau_{\max} = 10^7$ (vertical line). The bold solid line indicates the power-law exponent -1 corresponding for $\bar{c}_L(q, \Delta\tau)$ to the exponential decay for $c_L(q, t)$. Apparently, much larger $\Delta\tau_{\max}$ are warranted to get a reasonable estimation of $\tau_L(q)$ and $\tau_G(q)$ for $q\xi_{\text{cont}} \gg 1$. We have thus been unable to measure in this limit $\tau_L(q)$ and $\tau_G(q)$ and thus the respective viscosity contributions $\tau_L^0(q)$ and $\tau_G^0(q)$.

- [1] P. M. Chaikin and T. C. Lubensky, *Principles of condensed matter physics* (Cambridge University Press, 1995).
- [2] J. S. Higgins and H. C. Benoît, *Polymers and Neutron Scattering* (Oxford University Press, Oxford, 1996).
- [3] J. P. Hansen and I. R. McDonald, *Theory of simple liquids* (Academic Press, New York, 2006), 3rd edition.
- [4] J. K. G. Dhont, *The Glass Transition: Relaxation dynamics in liquids and disordered materials* (Springer, Berlin-Heidelberg, 2001).
- [5] W. Götze, *Complex Dynamics of Glass-Forming Liquids: A Mode-Coupling Theory* (Oxford University Press, Oxford, 2009).
- [6] J. D. Ferry, *Viscoelastic properties of polymers* (John Wiley & Sons, New York, 1980).
- [7] M. Doi and S. F. Edwards, *The Theory of Polymer Dynamics* (Clarendon Press, Oxford, 1986).
- [8] M. Rubinstein and R. H. Colby, *Polymer Physics* (Oxford University Press, Oxford, 2003).
- [9] D. Forster, *Hydrodynamic Fluctuations, Broken Symmetry, and Correlation Functions* (Perseus Books, New York, 1995).
- [10] M. P. Allen and D. J. Tildesley, *Computer Simulation of Liquids, 2nd Edition* (Oxford University Press, Oxford, 2017).
- [11] A. Lemaitre, J. Chem. Phys. **143**, 164515 (2015).
- [12] A. Lemaitre, Phys. Rev. E **96**, 052101 (2017).
- [13] M. Maier, A. Zippelius, and M. Fuchs, Phys. Rev. Lett. **119**, 265701 (2017).
- [14] M. Maier, A. Zippelius, and M. Fuchs, J. Chem. Phys. **149**, 084502 (2018).
- [15] L. Klochko, J. Baschnagel, J. P. Wittmer, and A. N. Semenov, Soft Matter **14**, 6835 (2018).
- [16] L. Klochko, J. Baschnagel, J. Wittmer, H. Meyer, O. Benzerara, and A. N. Semenov, J. Chem. Phys. **156**, 164505 (2022).
- [17] J. Wittmer, A. Semenov, and J. Baschnagel, Phys. Rev. E **108**, 015002 (2023).
- [18] J. Wittmer, A. Semenov, and J. Baschnagel, Soft Matter **19**, 6140 (2023).
- [19] A. J. McConnell, *Applications of Tensor Analysis* (Hassell Street Press, 2021).
- [20] W. Schultz-Piszachich, *Mathematik 11: Tensoralgebra und -analysis* (Verlag Harri Deutsch, Thun und Frankfurt/Main, 1977).
- [21] E. B. Tadmor, R. E. Miller, and R. S. Elliot, *Continuum Mechanics and Thermodynamics* (Cambridge University Press, Cambridge, 2012).
- [22] We use carrets for the normalized components \hat{r}_α and \hat{q}_α of the field vectors in real and reciprocal space and often also to emphasize instantaneous observables.
- [23] L. D. Landau and E. M. Lifshitz, *Theory of Elasticity* (Pergamon Press, New York, 1959).
- [24] See the wikipedia entries on quadrupoles and multipolar expansion. For the (not normalized) basis functions $\cos(p\theta)$ or $\sin(p\theta)$ relevant for the 12-plane a monopole corresponds to $p = 0$, a dipole to $p = 1$, a quadrupole to $p = 2$ and an octupole to $p = 4$.
- [25] J. Eshelby, Proc. R. Soc. Lond. A **241**, 376 (1957).
- [26] G. Picard, A. Ajdari, F. Lequeux, and L. Bocquet, Eur. Phys. J. E **15**, 371 (2004).
- [27] F. Ebert, P. Dillmann, G. Maret, and P. Keim, Review of Scientific Instruments **80**, 083902 (2009).
- [28] C. Klix, F. Ebert, F. Weysser, M. Fuchs, G. Maret, and P. Keim, Phys. Rev. Lett. **109**, 178301 (2012).
- [29] C. L. Klix, G. Maret, and P. Keim, Phys. Rev. X **5**, 041033 (2015).
- [30] G. George, L. Klochko, A. Semenov, J. Baschnagel, and J. P. Wittmer, EPJE **44**, 13 (2021).
- [31] It is thus often justified to *extrapolate* the invariants obtained in the intermediate q -range for $q \rightarrow 0$ before computing analytically or numerically the inverse FTs.
- [32] W. Press, S. Teukolsky, W. Vetterling, and B. Flannery, *Numerical Recipes in FORTRAN: the art of scientific computing* (Cambridge University Press, Cambridge, 1992).
- [33] D. P. Landau and K. Binder, *A Guide to Monte Carlo Simulations in Statistical Physics* (Cambridge University Press, Cambridge, 2000).
- [34] A. Ninarello, L. Berthier, and D. Coslovich, Phys. Rev. X **7**, 021039 (2017).
- [35] D. R. Squire, A. C. Holt, and W. G. Hoover, Physica **42**, 388 (1969).
- [36] It is also possible to use instead the current particle position $r_\alpha^a(t)$ in the $\delta(\mathbf{r})$ -function to construct the displacement field in real space. Both operational definitions are equivalent for wavenumbers q smaller than the inverse typical (root-mean-squared) displacements [18].
- [37] See the Wikipedia entry on “Complex normal distributions” for details and further references.
- [38] See the Wikipedia entry on “Rayleigh distribution” for details and further references.
- [39] J. Rayleigh, Nature **72**, 318 (1905).
- [40] J. Maxwell, Phil. Mag. **19**, 19 (1860).
- [41] We define the friction coefficient ζ with respect to a force per volume, i.e. the dimension $[\zeta]$ of ζ differs from the one used elsewhere [7, 8]. In our notation we have $[\zeta] = [\eta_s]/\text{length}^2 = [\text{modulus}]/[\text{acceleration}]$.
- [42] W. A. Strauss, *Partial Differential Equations: An Introduction* (Wiley, New York, 2008), 2nd edition.
- [43] The wavevectors \mathbf{q} for finite real systems as in computational studies must obviously be discrete (“quantized”) and commensurate with the boundary conditions reflecting the size and shape of the system [17, 32, 42].
- [44] I. Rubinstein and L. Rubinstein, *Partial differential equations in classical mathematical physics* (Cambridge University Press, Cambridge, 1998).
- [45] M. Abramowitz and I. A. Stegun, *Handbook of Mathematical Functions* (Dover, New York, 1964).
- [46] Let $f(\mathbf{q}, s)$ be a function in Fourier-Laplace space with \mathbf{q} being the wavevector and s the Laplace variable. We often drop an argument if it vanishes, i.e. we write $f(s) \equiv f(\mathbf{q} = 0, s)$, $f(\mathbf{q}) \equiv f(\mathbf{q}, s = 0)$ and $f \equiv f(\mathbf{q} = 0, s = 0)$.
- [47] A. Lemaitre, J. Chem. Phys. **149**, 104107 (2018).
- [48] Using that $s(q) = 0$ implies that also its inverse FT $s(r)$ must vanish, one may, e.g., use Eq. (B38) to check the entries made in Table VIII.
- [49] J. D. Jackson, *Classical Electrodynamics* (Wiley, New York, 2007), 3rd edition.
- [50] See the wikipedia articles on “Spherical harmonics” and “Table of spherical harmonics” where a summary on “real spherical harmonics” is given.